2018-01-01

Investigating Early Age Behavior of Portland Cement Concrete in Arid Regions

Evan Wolf
University of Texas at El Paso, evan.wolf88@gmail.com

INVESTIGATING EARLY AGE BEHAVIOR OF PORTLAND CEMENT CONCRETE IN ARID REGIONS

EVAN LEE WOLF

Doctoral Program in Civil Engineering

APPROVED:

_____
Soheil Nazarian, Ph.D., Chair

_____
Cesar J. Carrasco, Ph.D.

_____
Calvin M. Stewart, Ph.D.

_____
Jeffrey Weidner, Ph.D.

_____
Charles H. Ambler, Ph.D.
Dean of the Graduate School

Dedication

To my wife, Teri Wolf, and kids, Holden and Sarah Wolf

INVESTIGATING EARLY AGE BEHAVIOR OF PORTLAND CEMENT CONCRETE IN ARID RIGIONS

by

EVAN LEE WOLF, B.S., M.S.

DISSERTATION

Presented to the Faculty of the Graduate School of

The University of Texas at El Paso

in Partial Fulfillment

of the Requirements

for the Degree of

DOCTOR OF PHILOSOPHY

Department of Civil Engineering

THE UNIVERSITY OF TEXAS AT EL PASO

August 2018

Acknowledgements

First and foremost, I would like to express my thanks and gratitude to my advisor Dr. Soheil Nazarian for his guidance and support throughout my time at the University of Texas at El Paso. Especially his technical knowledge and trust and confidence in me. I thank the committee members, Dr. Cesar Carrasco, Dr. Calvin Stewart, and Dr. Jeffrey Weidner for their assistance and guidance. Thank you to Dr. Shane Walker for his assistance in determining a simplified approach to model the heat transfer of the test specimens.

Thanks are also extended to Sergio Rocha for his advice, technical assistance, and time spent maintaining the testing system and temperate rooms. I appreciate the assistance provided by Ben Arras throughout the entire production and testing process as well as Dr. Prajwol Tamrakar for his support in developing and refining the necessary programs to efficiently analyze the collected data.

Great thanks to the Center for Transportation Infrastructure Systems (CTIS) for allowing me the use of their equipment for specimen production and testing. As well, I want to recognize Jobe Materials for donating the materials for this project. Specific thanks to John Cordova and Martin Alderette from Jobe for their insight and recommend adjustments to my experimental plan.

My deepest gratitude to my wife, Teri Wolf, and my kids, Holden and Sarah for their love, encouragement, and patience throughout the process. Their understanding, support, and home distractions kept me grounded in what is truly important.

Abstract

The early-age behavior and properties of portland cement concrete change rapidly over time as a result of the hydration process. Comprised of a series of chemical reactions, this process accelerates nonlinearly with the curing temperature. Gaining knowledge and understanding of the phases of the hydration process (i.e., dormant, setting, and hardening) plays an important role in the timely opening of roads, resuming of construction, and achieving long-term performance. Standard tests such as ASTM C403 arbitrarily define the time of initial and final setting of concrete. Despite decades of studies concerning setting times, actual predictions still span hours, while the quality of concrete is customarily evaluated by its compressive strength at 28-days. New technologies provide an accurate and detailed understanding of the hydration process. In this research, maturity concept, along with seismic and infrared technologies, were used to measure and evaluate portland cement concrete properties. The setting times and quality of early age concrete were evaluated using seismic and maturity tests. The thermal profiles of concrete specimens were observed during the first 48-hours to monitor the heat dissipation during the hydration process. The versatility of the approach was studied by conducting tests under varied environmental curing conditions on a reference mix as well varying the water-cement ratio, chemical admixtures, and gradation of coarse aggregates. Correlations of both the maturity and seismic modulus to conventional compressive strength test at 1-, 3- and 7-days are presented. Additionally, thermal profiles of concrete for different curing conditions and mixes are shown. Lastly, an approach for determining the initial and final sets is provided which, when coupled with the strength testing, validates the need for redefining sets based on measureable concrete properties.

Table of Contents

List of Tables

List of Figures

Chapter 1: Introduction

1.1 Problem Statement

Portland cement concrete is one of the most widely used construction materials due to its versatility and ability to be produced with different characteristics. Achieving these desired characteristics requires a knowledge of fresh concrete behavior as it contributes to the long-term characteristics of the fully cured concrete. This knowledge contributes to understanding the various processes that occur as fresh concrete hydration leads to setting and hardening. Understanding these processes is necessary to understand the strength development in concrete.

In today's fast-paced culture, finding ways to shorten the project timelines is always sought, whether for monetary benefit for the contractor and owner or convenience for the user. Shortening the timelines requires the ability to predict accurately when the concrete has sufficient strength to continue construction or open the structure for use. Continuing construction or allowing the use of the structure before the concrete has gained sufficient strength can have costly consequences.

The speed at which concrete develops strength depends on a number of variables related to environmental conditions and mix components. Changing conditions or components influences the speed of chemical reactions that causes strength development. This assortment of variables leaves an imperfect prediction of not only what the strength will be, but also when it is reached. Most strength predictions result from laboratory testing prior to final mix production, which are confirmed with destructive testing of specimens produced and stored under the same conditions or specimens cored from the in-place concrete. A significant amount of research has occurred that has led to far more robust concrete curing. However, robust prediction of strength development is still under study since waiting 28 days is impractical in today's society.

A number of variables, either mix-related or environmental-related, affect the rate of strength development. Mix-related variables broadly include type of aggregates, type of cement, use of chemical and mineral admixtures, and water-cement ratio. The rate of hydration during curing is affected by environmental variables (such as temperature and humidity) which influence the rate of strength development.

Because of the number of variables that influence strength development it is difficult to develop a single mix design for every project. Availability of mixture components varies by location and environmental conditions are beyond our control. However, understanding the different effects when designing a concrete mix and being able to impose a specific temperature and humidity, for a short time, can result in the desired strength development. Confirmation of desired strength still depends on 28-day compressive strength testing regardless of curing conditions imposed. Additionally, determining strength of concrete using destructive testing before final set is impossible due to its plastic nature.

To understand, predict, and model concrete characteristics at this early stage requires nondestructive testing approaches. The use of maturity testing and seismic technologies for characterizing the behavior of early age concrete has been studied previously (Nazarian et al. 1997; Medichetti 2002; Yuan et al. 2003, 2005; Yi et al. 2005; Nazarian et al. 2006; Yikici and Chen 2015; Benaicha et al. 2016; Collier et al. 2017). The seismic and maturity methods provide insight in the concrete behavior and relationship to strength using the standard tests. Those studies provided a better understanding of the relationships between temperature, modulus of elasticity, and strength development during the first hours after concrete pouring.

This study used both of these methods in an attempt to understand the early age strength development of concrete as different variables are adjusted. These experimental relationships can

eventually lead to models for predicting strength. In addition to these models an infrared camera was used to capture the thermal profile of the specimen during the hydration process. The increased understanding gained will enable concrete mix adjustments to fit the time and monetary requirements of the project.

1.2 Objective

The objective of this research is to develop a laboratory system based on nondestructive methods and thermal imaging to monitor the early age behavior of concrete that accounts for the environmental and mixture variations. Monitoring and data collection of temperature and seismic modulus of the concrete during early age can potentially provide measurements of the initial and final sets and the rate of hydration of mixes in a more rigorous manner.

This preliminary study will focus on the mixture variations using commonly specified admixtures in varying quantities as well as maximum aggregate size and gradation. Comparison of the results among different mixtures provides the opportunity to identify the compatibilities between the different admixtures to determine whether the inclusion of different admixtures at various levels enhances or hinders the strength development. Additionally, curing specimens at varying temperature and humidity provide greater understanding of the strength development under different environmental conditions.

1.3 Organization

A background on the parameters and processes that affect the strength development of portland cement concrete is presented in Chapter Two. In addition to explaining the hydration process and setting, that chapter discusses some of the most common supplementary cementitious materials (SCMs) and chemical admixtures used to yield concrete with desired characteristics.

Chapter Two also covers a literature review of studies related to maturation and strength development of portland cement concrete.

Chapter Three details the methodology followed in this research. The experimental design, preparation and testing of the mixes as well as environmental and mix related parameters evaluated.

The analysis of collected data is presented in Chapter Four. The effects of environmental and mix related parameters on concrete setting as well as strength and modulus growth are shown. Additionally, the relationships between strength, seismic modulus, and maturity are presented.

Results from developed methods are presented in Chapter Five. Approaches based on the seismic modulus to define the initial and final set in terms of time or maturity are described. Further, discussion of alternative maturity occurs along with presenting the thermal profiles of early age concrete.

Summary of the main points of this research, conclusions, and recommendations for further research are offered in Chapter Six.

Chapter 2: Literature Review

2.1 Early Age Portland Cement Concrete

Several processes occur during the early age of portland cement concrete (PCC) that can affect its properties. As a result of these processes concrete properties may change by orders of magnitude over a period of hours (Bertagnoli et al. 2009). Strength increases from an almost negligible value to several hundred or thousand pounds per square inch (psi). For this to happen the concrete must go through the hydration process causing the concrete to stiffen, set and ultimately harden. The hydration process is the main process that affects the occurrence of the other three while curing affects the rates that all of the processes occur. Definitions of stiffening, setting and hardening vary based on the source, but the meanings are the same. For this study, the following definitions will be used:

- *Stiffening* – the loss of consistency of the plastic cement paste (Mehta and Monteiro 2006).
- *Setting* – the process, due to chemical reactions, that results in a gradual development of rigidity of a cementitious mixture (ASTM C125 2015).
- *Hardening* – the gain of strength of a cementitious mixture as a result of hydration that occurs after final setting (ASTM C125 2015).

These three processes are controlled by the rate of hydration, which is controlled by the curing conditions applied. The concrete progresses from one process to the next as hydration continues, with the rate of hydration dictating the time for each process to occur. Although knowing each process is beneficial, the key one is the setting of the concrete, because this defines the end of stiffening and beginning of hardening.

2.1.1 Hydration

As water is added to a cement mixture, a chemical reaction occurs between the water and cement, initiating the hydration process. The process of hydration, and as a result the concrete strengthening, continues as long as moisture is present. The continuous strengthening of PCC can cease when there is not sufficient moisture in the system. Typically, this occurs when the relative humidity in the concrete drops below 80% (Mindess et al. 2003). During a series of chemical reactions, two key products are created, heat and the hydrates or bonding agents. The formation of the hydrate results from the reaction of water with the calcium silicates in the cement (Newman and Choo 2003a). Hydration is primarily a chemical reaction between water and cement, both individual particles and those attached to aggregates, and secondarily by diffusion and penetration of the hydrate already formed (Yi et al. 2005).

The hydration process is influenced by the mix, cement quantity, water-cement ratio, and ambient temperature. Variations in those factors affect the rate and duration of hydration. Mindess et al. (2003) reported that complete hydration occurred at a water-cement ratio of 0.42, indicating that primary hydration of all the cement particles was complete and any further hydration was of the already formed hydrate. As hydration progresses the concrete continues to develop strength as a result of the hydrates fixing to both the aggregates and one another forming a solid structure (Newman and Choo 2003b). The speed with which strength is developed depends on the rate of hydration. Increasing the temperature or using a cement with finer particles generally increases the rate of hydration (Lin and Meyer 2009). Two functions generally express the rate of hydration. The first is based on the rate of heat of hydration per unit mass of cement under specific hydration conditions and the second is thermal activity of each mineral compound in cement (Swaddiwudhipong et al. 2002).

The rate of hydration, *a*, at a specific time, *t*, is approximated as:

$$a(t) \approx \frac{Q(t)}{Q_{max}} \qquad \text{EQN 2.1}$$

where *Q(t)* is the amount of heat of hydration generated per unit mass of cement at time t and Q_{max} is the specific heat of hydration per unit mass of cement (cal/g). This method provides a linear relationship between the amount hydrated and heat generated. Use of thermal activity allows the calculation of an equivalent maturity for each compound, M_i

$$M_i(T,t) = \int_0^t exp\left\{\frac{-E_i(Q_i)}{R}\left[\frac{1}{T(t)} - \frac{1}{T_0}\right]\right\} d\tau \qquad \text{EQN 2.2}$$

where $E_i(Q_i)$ is the activation energy per mol of mineral compound *i* (cal/mol), *R* is the gas constant, T_0 is the reference temperature, and T(*t*) is the actual temperature of hydration at time t. When summed Equation 2.2 provides an exponential function in the form of

$$Q(t) = \sum\left(\int_0^M q_i dM_i\right) \qquad \text{EQN 2.3}$$

where q_i is the reference rate of hydration.

Neville (1996) and Glisic and Simon (2000) described the hydration as a three-stage process. Figures 2.1 and 2.2 summarize the process. The early stage, or Stage I, is the initial hydration that occurs after the addition of water. During this stage, there is a short period of rapid chemical dissolution causing a high evolution of heat, followed by a one- to two-hour dormant period. During Stage II, or the middle stage, the setting of PCC occurs. In that stage, growing layers of hydration products in the PCC begin to contact one another forming a solid structure. The evolution of heat continues to increase from the end of the dormant period until it peaks at the point where all of the primary reactions between water and cement have occurred. The late stage, or Stage III, is the longest stage when diffusion controls the renewal of reaction. This stage continues as long as water and hydration products are available to react. As long as this stage continues, the concrete continues to harden as the pores in the system continue to shrink as

hydration products grow and fill the spaces. The process continues to produce heat, but the high point is at the beginning of this stage and decreases as hydration continues.

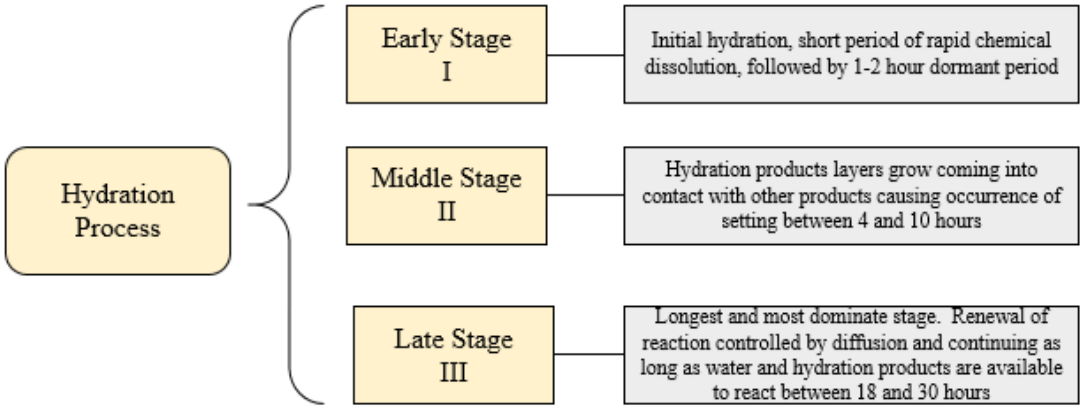

Figure 2.1 Phases in Hydration Process

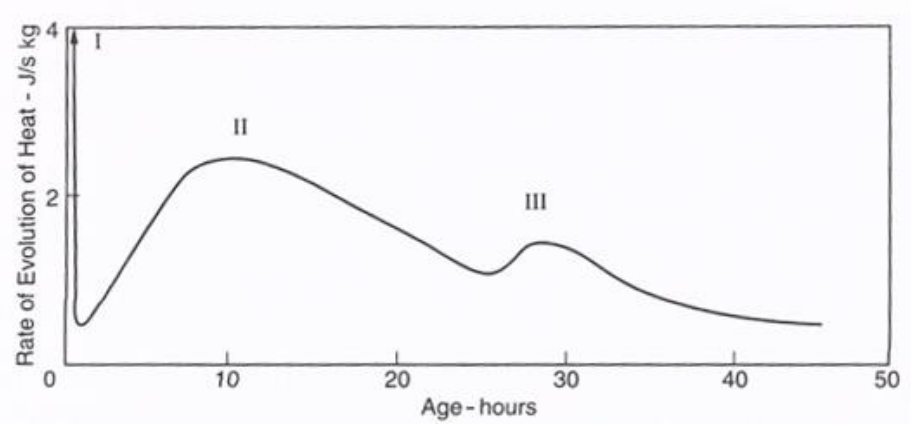

Figure 2.2 Three-Stage Heat Evolution of Portland Cement (Neville 1996)

As seen in Figure 2.3, Mindess et al. (2003) depicted the rate of heat evolution in a similar manner to Neville (1996), but in five stages. They further explained the relevance of each stage to the concrete properties. They described Neville's early stage as the initial hydrolysis and induction period. The induction or dormant period determines the initial set of the concrete. The acceleration period most closely relates to the middle stage since this phase is a chemically controlled reaction and sees the formation of hydration creating bonds. This formation determines the final set as well as the rate of initial hardening. The late stage is the combination of what

Mindess et al. labeled as the deceleration and steady state stages. Both stages experience diffusion-controlled reactions, which occur at a slower rate and produce less heat. Deceleration is the stage that the rate of early strength gain is determined while steady state determines the long-term strength gain.

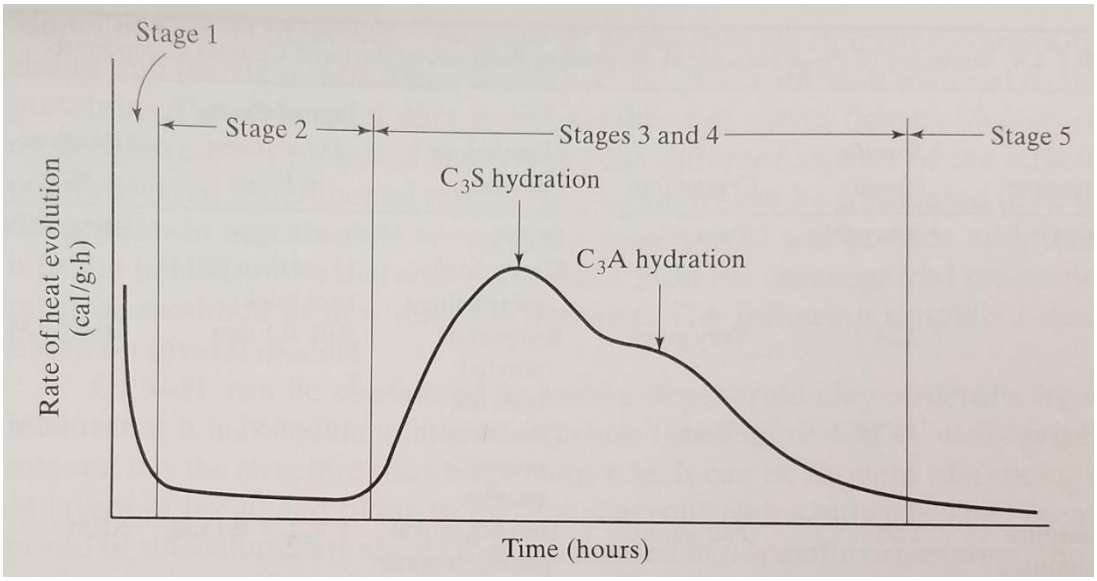

Figure 2.3 Five-Stage Heat Evolution of Portland Cement (Mindess et al. 2003)

2.1.2 Setting and Hardening

Concrete setting is characterized into two distinct phases, as determined by the penetration resistance of cement paste obtained with the Vicat apparatus (ASTM C403 2016). Another method uses a penetrometer to determine penetration resistance of cement mortar (ASTM C403 2016). Although both methods are the standard for determining concrete set time, they are destructive methods that either damage the placed concrete or require making test specimens. Gams and Trtnik (2013) suggested the use of longitudinal waves as a nondestructive alternative approach for determining setting times. Two advantages of their approach were the method is testable on in-situ concrete and it is unaffected by the presence of fine and coarse aggregates. They found that the ratio between maximum amplitudes at different dominant frequencies could provide accurate determination of the setting times.

The initial set, which typically occurs between two and four hours from mixing, is defined as the time when the paste stiffens to a point where it is no longer workable. While the final set, or time when the concrete has hardened to a point it can sustain a load, occurs between five and eight hours (Mindess et al. 2003; Mehta and Monteiro 2006). Variables such as the composition of the cement, water-cement ratio, temperature, and use of admixtures influence the time it takes for concrete to set. Cements with finer particles set faster since their higher surface area causes faster reaction between the water and cement. Bentz (2008) stated that higher water-cement ratio caused a greater amount of reaction, but slowed down the setting time. The extra water in the system slows the rate that the hydrates encounter each other and form a mutual bond. Increases in temperature typically decrease the setting times while the addition of admixtures can either increase or decrease the time based on the type of admixture used.

Figure 2.4 depicts the hardening of cement paste as cement progresses after the addition of water until hardening. Concrete hardening occurs subsequent to setting and is the phase where the mechanical properties develop, specifically strength. Figure 2.5 illustrates the typical strength gain over time as well as where setting occurs in relation to limits of handling and hardening Although the final set typically occurs after around eight hours, it still takes one to two days for concrete to achieve appreciable strength (Mehta and Monteiro 2006). As hardening progresses hydrates continue to form which reduces the pores in the system causing strength gain. During the dormant stage there is no mutual contact resulting in negligible strength. Once the initial set occurs, the cement paste begins to come into contact and bond with other hydration products and reduce the pores as it reaches final set and moves into hardening.

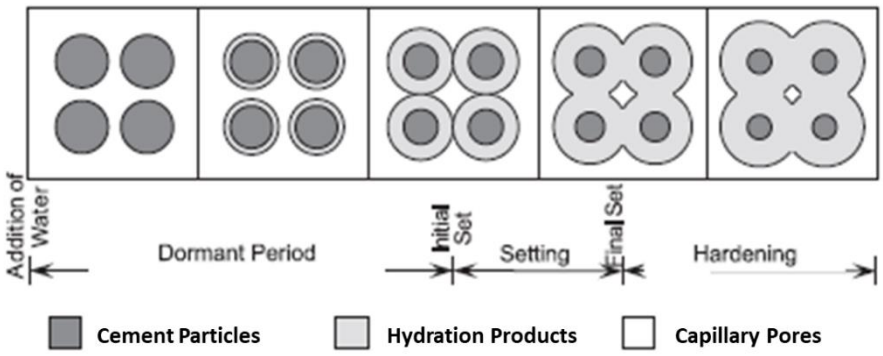

Figure 2.4 Hardening of Cement Paste (Glisic and Simon 2000)

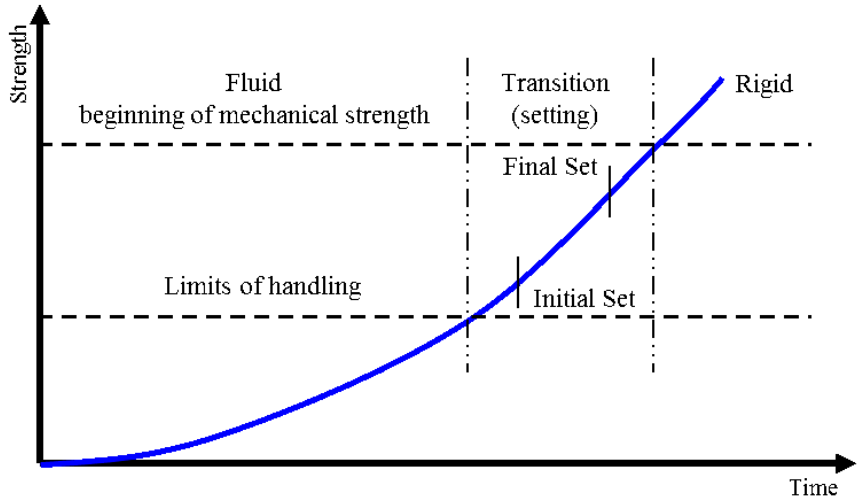

Figure 2.5 Process of Setting and Hardening (adapted from Mindess et al. 2003)

2.1.3 Curing

To promote proper curing, the temperature and the movement of moisture have to be controlled (Neville 1996). Mehta and Monteiro (2006) further stated that controlling the temperature and preventing moisture loss must occur for sufficient time for the concrete to reach a desired strength. It is during this process that PCC develops its hardened properties. Employment of various lab and field methods during curing enables control of the temperature and moisture. Decisions into which methods are used depends on time, cost, and ambient conditions. Table 2.1 provides further discussion of these effects. In general, higher temperatures and prolonged exposure to moisture result in increased strength development at early stages.

Table 2.1 Concrete Curing

Source	Discussion
Neville (1996)	• Standard curing temperature ranges between 64 and 70 degrees Fahrenheit. • Higher temperatures at curing increases hydration reactions by reducing the dormant period, thus promoting early strength • High pressure steam curing has resulted in 28 day strength at 24 hours
Mehta and Monteiro (2006)	• The longer moist curing occurs, the higher strength of concrete will be • Higher temperature promotes faster hydration and thus faster strength development
Mindess et al. (2003)	• Higher curing temperature causes higher early strength, but lower ultimate strength • Sealed concrete gains strength slower than continuously moist cured • To reach 70% specified strength 7 days moist curing should be prescribed
Yi et al. (2005)	• Increasing initial curing temperature increases early strength, but decreased long-term strength • Changes in curing temperatures influence the diffusion and penetration of hydrates affecting strength development; generally, as temperature increases diffusion and penetration increases.

2.2 Strength Estimation and Development

Concrete strength develops over time based on various factors. Regardless of these factors, the 28-day strength determines the concrete strength rating. At this point, strength development is far slower and the measured strength provides a higher confidence. However, the practicality of waiting 28 days to verify the concrete strength is in doubt. Project managers, contractors, and owners alike desire to complete projects rapidly, and a 28-day wait period presents an obstacle to this desire. As such, being able to estimate the 28-day strength with confidence at earlier stages is highly desirable. Estimating the final strength with a high degree of certainty requires a thorough understanding of the early age behavior. Being able to estimate the strength based on testing of the in-situ concrete is ideal as it best represents the actual conditions. Testing to determine the strength, without causing damage to the concrete is necessary. Two such methods are the maturity test, which relates the time and temperature of the concrete to the strength while the other uses seismic waves to determine the elastic modulus. In the laboratory, the Free-Free Resonant Column

(FFRC) is used while field-testing uses the Portable Seismic Property Analyzer (PSPA). Since this research focuses on lab testing, the FFRC testing is discussed in detail below.

2.2.1 Free-Free Resonant Column Method

The Free-Free Resonant Column (FFRC) test method utilizes wave propagation principles to determine the modulus and Poisson's ratio by measuring the resonant frequencies of a cylindrical specimen. Based on the recorded resonant frequencies and dimensions of the specimen, the modulus is calculated.

Components of the FFRC apparatus include a data acquisition system, an accelerometer, and an instrument hammer, as shown in Figure 2.6. Generation of compressive waves occurs by the impact from the instrumented hammer. These waves propagate through the specimen and are recorded by the accelerometer to determine the resonant frequencies. Shown in a frequency versus amplitude graph two peak frequencies appear; the lower peak represents the shear frequency (f_s) while the higher is the longitudinal frequency (f_L). These frequencies correspond to the shear wave and compression wave, respectively as seen in the middle output plot of Figure 2.6.

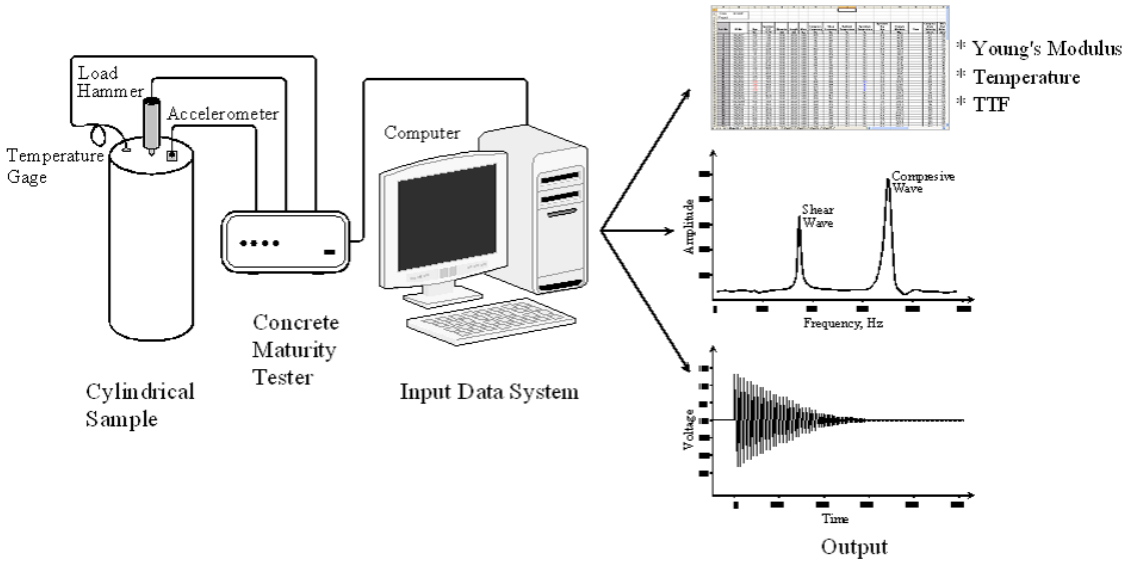

Figure 2.6 Free-Free Resonant Column Test Layout Apparatus

With the known mass (M), length (L), and cross sectional area of the specimen (A_s) of the specimen, the density (ρ) is calculated from;

$$\rho = \frac{M}{LA_s} \quad \text{EQN 2.4}$$

Young's modulus (E) is estimated by the following equation:

$$E = \rho(2f_L L)^2 \quad \text{EQN 2.5}$$

Poisson's ratio (v) is estimated from:

$$\upsilon = \frac{(0.5\lambda - 1)}{(\lambda - 1)} \quad \text{EQN 2.6}$$

where

$$\lambda = \left[\frac{f_L}{f_s}\right]^2 C_{L/D} \quad \text{EQN 2.7}$$

$C_{L/D}$ is a correction factor when the length-to-diameter ratio is not 2.

Nazarian et al. (1997) found strong correlations between the moduli found using the FFRC method and both the compressive and tensile strengths of the specimens. Medichetti (2002) showed that the relationship between the compressive strength and Young's modulus appeared to be independent of the concrete mixture for the same aggregate source. Nazarian et al. (2006) later confirmed that the laboratory calibration curve between the seismic modulus and compressive strength can be developed with confidence. This allows the FFRC apparatus to be a useful tool to assess the concrete strength during the hardening process.

2.2.2 Maturity

Since time and temperature both affect the hydration process and thus the strength development of concrete, developing a function that is defined as the product of these factors is the basis of the maturity method as shown in Equation 2.8 (ASTM C1074 2011):

$$M(t) = \sum(T_\alpha - T_0)\Delta t \quad \text{EQN 2.8}$$

where T_α = average concrete temperature, T_0 = datum temperature, and Δt = time interval. Use of the maturity function aids in determining an equivalent age at a reference temperature which takes effects from both time and temperature into account. Mehta and Monteiro (2006) presented the following equation, to determine the equivalent age, t_e, based on temperature during a time interval:

$$t_e = \frac{\sum(T_\alpha - T_0)\Delta t}{(T_r - T_0)} \qquad \text{EQN 2.9}$$

where T_r = reference temperature.

Medichetti (2002) studied the strengths, Young's modulus, and maturity parameters of several slabs and cores. She reported good correlations among compressive strength, flexural strength, and seismic modulus with maturity values as judged by the coefficients of determination, R^2 around 0.90 (see Figure 2.7). Tensile strength had a less strong correlation as evidence by and R^2 value of 0.81 seen in Figure 2.7c. Overall, a good correlation between the maturity values and Young's modulus was found, as seen by an R^2 of 0.94 (see Figure 2.7d).

2.3 Imaging

Infrared imaging provides a nondestructive method for the evaluation of subsurface defects in concrete structures. This methods are commonly used to identify cracks and delamination as well as locate steel reinforcement (Pla-Rucki and Eberhard 1995). The principle behind infrared imaging is that subsurface anomalies cause localized difference at the object's surface due to varying rates of heat transfer (Weil 1991; Büyüköztürk 1998). Although all three modes of heat transfer (i.e. radiation, conduction, and convection) affect the surface temperature of the material, radiation serves as the measurement used for infrared imaging. The infrared detector measures the emitted infrared radiation which is then converted to a visual image based on the Stefan Boltzmann

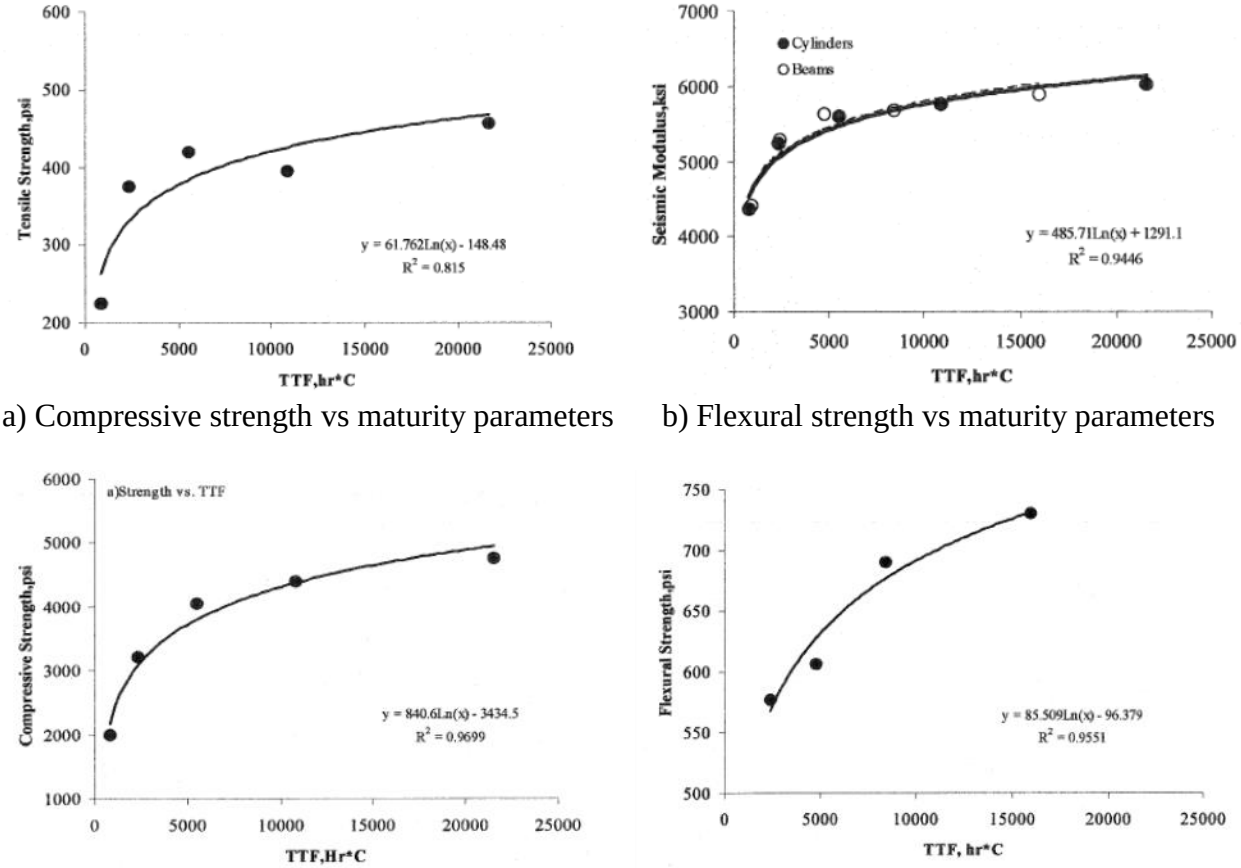

a) Compressive strength vs maturity parameters b) Flexural strength vs maturity parameters

c) Tensile strength vs maturity parameter d) Seismic modulus vs maturity parameters

Figure 2.7 Correlations Determined by Medichetti (2002)

law (Maser and Roddis 1990; Clark et al. 2003). Radiation is calculated from:

$$E_r = \epsilon\sigma T^4 \qquad \text{EQN 2.10}$$

where E_r = radiation emissive power, T = temperature, ϵ = emissivity, and σ = Stefan-Boltzmann constant.

Hiasa et al. (2014) noted that the ambient temperature surrounding the specimen during infrared imaging creates thermal noise, affecting the temperature reading. Weil (1991) reported that the surface conditions and subsurface configuration also affected the readings during infrared imaging. Although these shortcomings are the result of conduction and convection, they are more prominent during field-testing where environmental conditions are not controlled and the potential of anomalies in the large sections of concrete is higher than in cylindrical lab specimens.

Use of infrared imaging on early age concrete is limited. One study that used infrared imaging on early age concrete was completed by Azenha et al. (2011). That study sought to verify the feasibility of applying thermography to early age concrete during hydration and to validate a model to predict temperature development. The research not only validated their model, but also showed that the temperatures measured by the internal thermocouples were correlated with those measured with the infrared devices. A drawback found during the study was the need for visual contact with the specimen, as formwork would prevent temperature measurement or degrade the confidence of the results.

2.3 Concrete Mix Design

Three considerations drive the concrete mixture design. The first and most important is a hardened concrete with a desired compressive strength. Design of concrete based on a specified compressive strength is the dominant method regardless of the intended use. American Concrete Institute (ACI) Committee 211 (Kosmatka et al. 2002) indicated that the absolute volume method provides the most accurate proportioning for gaining a desired compressive strength. The flexural strength of PCC is calculated from the compressive strength by the generally accepted conversion factor of 7.5 to 10 times the square root of the compressive strength in psi (Kosmatka et al. 2002).

The second factor considered is setting time. Having a concrete that sets rapidly allows for continued construction and faster opening of the project, which is highly desired by all parties for either monetary benefit or convenience. Producing a faster or slower setting time is typically accomplished through adjusting the amount of fines or chemical admixtures. Increasing fines, increases the rate of hydration, which accelerates the setting time.

Workability of the concrete, which is the third consideration of the mix design, is associated with the water-to-cement ratio. The rapid hydration of concrete can occur with a low

water-to-cement ratio; however, the lower the ratio is the more problematic the workability will become. A decrease in workability typically yields a faster setting but is much more labor intensive to pour and provides less time for finishing.

Since compressive strength is the primary factor driving concrete mix design, an understanding of the effects caused by the different components of PCC is necessary. Characteristics of the primary components of PCC contribute to strength development, typically by providing increased surface area for hydration to occur or a textured surface for the hydration products to bond with.

2.3.1 Mixture Variables and Strength Development

Aggregate, cement, and water serve as the three core components needed for producing concrete. The cement-aggregate ratio, water-cement ratio, and sand-coarse aggregate ratio are three of the four controllable variables in mixture design. Variability in these components can either help or hinder the strength development of concrete. Understanding their impact on strength, as well as cost, can influence the type and quantity of these components used in the mixture.

Aggregate

The particle gradation, shape, texture, strength and stiffness of the aggregate impact the concrete strength (Neville 1996). The properties of the aggregates used have small effect on the strength development but do influence the strength. The type of aggregate used in concrete mixtures is the most uncertain of the core components in terms of composition because of variability from location to location. Typically, locally sourced aggregates are used for convenience and economic reasons.

The particle gradation of the aggregates determines the voids content in the mixture and as a result, the amount of cement needed to create the bond between the particles. Higher voids yield a lower strength PCC while increase in the cement content causes increased cost. The shape and texture of the aggregates determine the level of bonding between the cement paste and aggregate particles. Rougher, angular surface particles provide increased bonding with the cement paste while smooth, spherical particles increase the workability (Neville 1996; Mindess et al. 2003). An increased bond between the cement paste and aggregate particles provides higher strength because of improved ability to transfer stress throughout the concrete. Aggregate strength and stiffness contribute to the overall strength of the concrete when this increased bond occurs as the particle can carry stress based on its strength. However, if a weak bond occurs or the particle has low strength, the load-induced stress causes failure at the weaker point.

Portland Cement

The type and amount of portland cement in a concrete mixture is typically the greatest contributor of cost of the core components. Each chemical component of cement plays a role in the strength development. Typical chemical components include tricalcium silicate (C_3S), dicalcium silicate (C_2S), tricalcium aluminate (C_3A), tetracalcium aluminoferrite (C_4AF), and calcium sulfate dihydrate (CSH_2) in addition to other minor impurities (Mindess et al. 2003). The quantities of these compounds and the fineness of the cement determine cement classification as is seen in Table 2.2. Each type of cement is desirable for certain purposes. Type I is typically associated with general construction; whereas Type III is best when rapid strength development is desired. When controlling heat of hydration Types II or IV are used while Type V is suited for sulfate resistance.

C_3S is the chemical compound that contributes the most to strength of concrete especially rapid initial strength (Newman and Choo 2003b). C_2S normally contributes to the long-term strength of concrete (Newman and Choo 2003b; Caldarone 2009).

Table 2.2 Typical Chemical Composition and Properties of Portland Cements
(Mindess et al. 2003)

Component	Type I	Type II	Type III	Type IV	Type V
C_3S	55	55	55	42	55
C_2S	18	19	17	32	22
C_3A	10	6	10	4	4
C_4AF	8	11	8	15	12
CSH_2	6	5	6	4	4
Fineness (m^2/kg)	365	375	550	340	380
1 Day Strength (psi)	2200	2000	3500	600	1750

Aside from the chemical compounds in cement, the fineness of the cement plays a significant role in the hydration and strength development of concrete. Finer cements provide an increased surface area which results in a higher rate of hydration and increased strength development (Mindess et al. 2003; Lin and Meyer 2009). As seen in Table 2.2, Types I and III portland cements have nearly identical chemical compositions, but Type III is 50% finer and yields a one day strength almost 60% higher than Type I. Neville (1996) states that cement containing 95% of particles between 3 and 30 microns is best for rapid hydration and strength development while Mindess et al. (2003) stated particles below 3 microns had the greatest influence on 1-day strength. Alexander (1972) stated that hydration during the first two days occurred mainly with the fines and the outermost layers of coarser particles. This hydration of the fines improves the early strength development and shortens the setting time.

Water-Cement Ratio/Water Content

Water serves two primary roles in the production of concrete. First, it initiates and maintains the hydration process. Once the there is no more moisture the hydration process ceases

thus ending strength development. The water-cement ratio ultimately determines the degree of hydration of the mixture, with amount of water necessary typically being below normal water-cement ratio. The reason water-cement ratios are usually higher than the amount need for full hydration is to increase the workability. Although this has less to do with strength development, it is extremely important in the placing of concrete. However, higher water content typically yields more pore space in the mixture, which means lower strength and durability (Newman and Choo 2003b). Bentz (2008) indicated that the higher water content yielded greater hydration, but increases the setting time. Thus, a balance is necessary between gaining the desired strength and the workability of the concrete during placement. Understanding the inverse relationship between strength and the water-cement ratio enables one to make the necessary adjustments to other controlled variables to get the desired strength with needed workability (Mehta and Monteiro 2006). According to Mindess et al. (2003), the typical water-cement ratios used for high-strength concrete varies from 0.22 to 0.50. This wide range indicates the adjustment of either the cement-aggregate ratio or sand-coarse aggregate ratio; but more than likely the inclusion of the fourth controllable ratio, the use of admixtures.

2.4 Admixtures

The use of admixtures in PCC influences the processes that occur in early age concrete, thus affecting the characteristics of the hardening concrete. Mineral admixtures, also called supplementary cementitious materials (SCMs), generally serve as additional cementing material or as a replacement for a portion of the cement. The properties of mineral admixtures also influence concrete characteristics as well as aid in limiting deterioration of the concrete at later stages of its life. Chemical admixtures, on the other hand, generally influence the early age process of concrete to affect setting time, rate of hydration, or the amount of entrained air.

2.4.1 Mineral Admixtures

Commonly used mineral admixtures or SCMs are either naturally occurring or by-products from other industries. Their use typically benefits concrete by increasing the resistance to chemical attack and/or adding cementitious effect allowing for either replacement of portland cement or addition of cementitious material to improve strength. Strength improvements result from the effects the SCMs have on the hydration process caused by the chemical composition, particle size distribution, particle shape, and reactivity (Neville 1996). The ability to replace portland cement with a SCM, especially those that are by-products, helps conserve resources while reducing waste from other industries.

Table 2.3 lists the source and common material traits of each SCM. The most common SCMs include ground granulated blast furnace slag (GGBFS), fly ash, (FA), silica fume (SF), and natural materials. All but the natural materials are by-products of other industries and require their own classification based on processes and controls used by each specific source, while natural materials are products from volcanic rock and minerals.

Table 2.3 Common Mineral Admixtures (Adapted from Neville (1996); Mindess et al. (2003); Newman and Choo (2003a); Mehta and Monteiro (2006); and Parande et al. (2009))

Name	Source	Material traits
GGBFS	By-product of iron blast furnace	• Chemically same oxides as cement, but different proportions • Physical structure and composition vary based on manufacturing processes and cooling method used
FA	Waste product of coal burning electric plants	• Spherical with very high fineness • Classification based on type of coal using ASTM C 618-94a
SF	By product of alloy manufacturing, produced by electric arc-furnace	• Extremely fine particles • Composition varies based on type of alloy produced and furnace used • Expensive • Most commonly associated with high early strength
Metakaolin	Kaolin clay	• Higher purity due to controlled refining process • Comparable effects as SF, but lower cost

Table 2.4 explains the effects of common SCMs on the concrete as well as their typical content ranges used. Natural materials used as mineral admixtures are typically categorized as volcanic glasses, volcanic tuffs, calcined clays or shales, or diatomaceous earth. Regardless of

Table 2.4 SCM Effects on Concrete (Adapted from Popovics (1982); Payá et al. (1995); Neville (1996); Ding and Li (2002); Langan et al. (2002); Papadakis and Tsimas (2002); Targan et al. (2002); Mindess et al. (2003); Newman and Choo (2003a; c); Ganesh Babu and Dinakar (2006); Mehta and Monteiro (2006); and Caldarone (2009))

Name	Effects	Range
GGBFS	• Resistant to chemical attack • Controls early development of heat of hydration, thus low rate of strength gain, but improved long-term strength • Increased workability • Increased sensitivity to changes in water content • Retardation effect on setting up to 1 hour • Reduced heat evolution	35-65%
FA	• Reduces water demand up to 15% with no change in workability • Delays initial setting by about 1 hour • Hydration process more sensitive to temperature than pure Portland cement concrete • Reduces early strength, especially at low temperatures • Increases curing time at cold temperatures • Low strength development • Reduce heat generation • Strength enhance when particles smaller than 10 microns	20-50%
SF	• High fineness improves packing near aggregate • Higher modulus of elasticity • Requires increased mixing time to ensure uniform dispersion • Accelerates hydration if GGBFS is in the mix, also sensitive to water-cement ratio • Increased water requirement • Increased rate of strength development	3-15%
Metakaolin	• Very rapid hydration process • Increased strength • Increased rate of strength gain • Improved workability • Higher early strength due to filler effect	5-20%

which category the material belongs to, the presence of pozzolans made the use of natural materials as mineral admixtures ideal because of the benefits from the pozzolanic reaction; slow rate of heat

of liberation, reaction consumes lime, and efficiency at filling capillary spaces (Mehta and Monteiro 2006). However, their use is less prevalent than GGBS, FA, and SF due to economic and environmental reasons. For that reason, and the diversity of potential natural minerals, there is little literature on the various types of natural minerals. One natural mineral studied outside the United States is metakaolin, which is produced by thermal activation of kaolin clay and is considered comparable to silica fume. Although first studied in the 1990's, metakaolin is not widely used in industry due to limited and sometimes contradictory results. Badogiannis et al. (2002); Ding and Li (2002); Babu and Apparao (2003); Ganesh Babu and Dinakar (2006); Parande et al. (2009); Ismael and Ghanim (2015) evaluated the use of metakaolin as an admixture in concrete, with conclusions that its use increased concrete strength due to filler effect and reactivity, with 15 to 20% replacement being optimal.

2.4.2 Chemical Admixtures

The main characteristic of chemical admixtures according to Neville (1996) are that the chemical product, typically added in quantities of less than 5% mass of cement, achieves a specific modification of normal concrete properties. Properties affected include setting time, rate of strength development, and workability to name a few. Regardless of the desired property modification, the effectiveness depends on the amount added to the mix and the other constituents. Selection of chemical admixtures depends on the desired effect sought at the location of the project. Table 2.5 list the different types of chemical admixtures approved for use by TxDOT along with the desired effect and known advantages and disadvantages.

Table 2.5 TxDOT Approved Chemical Admixtures (Adapted from(Neville 1996; Mehta and Monteiro 2006;Caldarone 2009; Construction Division - Materials & Pavements 2016;))

Name	Desired Effect	Advantages	Disadvantages
Water Reducing	Reduce water content while maintaining workability	• Reduce water content by 5-10% • Improves hydration causing higher rate of early strength • Reduce required amount of cement	
Retarding	Retard the setting of concrete	• Prolongs time to transport, place, and compact concrete in hot weather • Increased strength beyond 7 days	Severely reduces early strength Incorrect quantities can inhibit setting and hardening
Accelerating	Accelerate setting and early strength development	• Allows placement at low temperatures. (35-40 F) • Allows early finishing • Allows structure to be placed in service earlier	At high temps can cause shrinkage cracking Degrades long-term strength development
Water-Reducing, Retarding	Reduce the quantity of mixing water required to achieve given consistency of concrete and retard the concrete setting	• Reduces water content and prolongs time to transport, place, and compact concrete	
High-Range Water Reducing (HRWR) or Superplasticizers	Reduce the quantity of mixing water by 12% or greater	• Better hydration • Rapid placing • Extreme high strength at lower water content with normal workability • Reduce water content 25-35%; increase 24 hr. strength 50-75%	
High-Range Water Reducing and Retarding or Superplasticizer and Retarding	Reduce the quantity of mixing water by 12% or greater and retard setting		
Air Entraining	Increase air content in the concrete	• Increased resistance to freeze-thaw • Improved workability	Increased porosity decreases strength

2.5 Alkali Silica Reaction

Although not the focus of this project, the author felt it necessary to conduct a rudimentary understanding of the causes and preventative measures for alkali silica reaction (ASR) because of worldwide recognition of ASR as a distress mechanism in concrete. This understanding ensures established preventive measures drive mix selection in this project, as there is little benefit to early strength if service life is reduced due to ASR. Symptoms often associated with ASR include map cracking, expansion, discoloration, pop-outs, and gel exudations (Fournier et al. 2010; Thomas et al. 2013). Although primarily aesthetic, these symptoms can be concerning to the populace and have an effect on other properties of the concrete. According to Giannini et al. (2013), ASR caused little effect on the load bearing capacity, but did cause a decrease in the mechanical properties. The amount of change as mentioned by Fournier et al. (2010) is identified in Table 2.6.

Table 2.6 Effect on Mechanical Properties Due to ASR (Adapted from Fournier et al. (2010))

Property	Effect
Compressive Strength	up to 60% reduction
Splitting Strength	up to 60% reduction
Elastic Modulus	up to 60% reduction
Direct Tensile Strength	up to 80% reduction

Defined as a chemical reaction between the alkalis in the concrete and silica from aggregates that produces a gel, ASR requires moisture to occur (Kreitman 2011; Giannini et al. 2013; Thomas et al. 2013; Nixon et al. 2016). This gel causes the symptoms discussed above. For the reaction to occur all three components (alkali, silica, and moisture) must be present. Alkali sources include Portland cement, aggregates, chemical admixtures, and supplementary cementitious materials (SCMs). The alkali content of the cement was originally thought to be the controlling source, but more recently, the content of the concrete was found to be more important (Thomas et al. 2013). Silica contributions by aggregates vary by type while the reactivity varies by the chemical structure of the aggregate (Thomas et al. 2013). The initial reaction typically

occurs when the internal relative humidity of the concrete is over 80% (Fournier et al. 2010). Reaction gel expansion causing cracks enables migration of water from external to the structure inward, thus allowing the reaction to continue.

With only three components necessary for ASR to occur, prevention focuses on removing or reducing one of the components or adding a chemical admixture to prevent the reaction. Use of non-reactive aggregates is not always feasible due to cost limits in cases where a source is not near or difficult to access. Limiting moisture generally occurs by treating the concrete after construction to prevent external migration of water, but addition of some admixtures or SCMs are effective in limiting the initial reaction. Use of low-alkali cement is the longest used approach to lowering the alkaline content; however, increased importance on the alkali content in concrete is more dominate, with recommendation being below 3 kg/m^3 (Thomas et al. 2013). Aside from low-alkali cement, the other, more efficient option is to include SCMs in the mix. The addition of SCMs replaces a percentage of the cement used in the mix. Additionally, SCMs such as slag and silica fume limit water permeability while fly ash reduces alkali availability, thus limiting components necessary for ASR to occur (Kreitman 2011). The amount of SCMs required depends on several factors when determining the concrete mixture. Thomas et al. (2012) and Thomas et al. (2013) provide several tables with general guidelines for the common types of SCMs. With the positive effects of adding a single SCM to the mixture, the combination of SCMs to create ternary blends with accumulative effects; however, conditions apply. Table 2.7 summarizes the general guidelines with regard to mix design to prevent ASR occurrence.

Table 2.7 Summary of Mix Design Guidelines

Guidelines		Notes	Reference
Alkali Limit	1.8 to 3.0 kg./m^3 3.0 to 5.0 lb./yd^3	Level dependent on prevention level required	Thomas et al. (2013)
	Alkali content of concrete = cement content of concrete x alkali content of cement (Thomas et al. 2012)		
Low-calcium fly ash	20 to 30%		Thomas et al. (2013)
Moderate calcium fly ash	25 to 35%		
High Calcium fly ash	40 to 60%		
Silica fume	8 to 15%		
Slag	35 to 65%		
Ternary blend	$\frac{fa}{FA}+\frac{sg}{SG}+\frac{sf}{SF}\geq 1$	See below	Thomas et al. (2012)

fa – fly ash to be used in combination
sg – slag to be used in combination
sf – silica fume to be used in combination

FA – minimum fly ash used on its own
SG – minimum slag used on its own
SF – minimum silica fume used on its own

2.6 Summary

The hydration of concrete is the controlling factor of both early age and long term concrete strength development. Although the time of setting and onset of hardening is useful when working with concrete, understanding how hydration can affect them is important. Adjustment of several variables provides a concrete with a fast set and hardening. Either the mix design can be adjusted, curing conditions can be changed, or both.

When looking at the mix design selection of the aggregate in terms of gradation, shape, texture, and size all affect the strength. Rough, angular aggregate of smaller size that is well graded is preferred for high strength concrete. Portland cement with a higher fineness increased the rate of hydration due to the increased surface area available to react with water and bond with other particles and aggregate. A higher water-cement ratio can increase the rate of hydration, but the extra, unreacted, water can prevent the hydrate products from bonding causing larger pores and lower strength. Addition of admixtures, whether mineral or chemical, also affects the rate of hydration and strength development. Mineral admixtures provide an increased amount of fines in

the mixture to speed hydration as well as cementing ability depending on which type is used. While the use of chemical admixtures such as accelerators and water reducers can increase the rate of hydration, resulting in a faster set as well as an equivalent workability with a reduced water-cement ratio. The increase in curing temperature, prolonging of moisture on the concrete, or both for longer periods encourages continued rapid hydration in the concrete causing increased strength development. Once the relative humidity of the concrete drops below 80%, hydration stops. The longer temperature and humidity are controlled the longer hydration occurs, but in order to open pavements to further use the curing conditions must be shortened.

The 28-day strength determines the classification of final strength, but waiting 28 days is not practical. Therefore, methods have been developed to measure the concrete at early ages and estimate the 28-day strength. The maturity method estimates the strength based on a time-temperature factor. This corresponds to understanding the rate of hydration of the concrete. Use of the Free-Free Resonant Column to measure the frequency of seismic waves determines the modulus and thus relates it to the concrete strength. Potential of ASR, in the long term, for concrete is less of a concern when mineral admixtures are used in the mix. As such, no further discussion of ASR is necessary based on the reference mix used throughout this research, further discussed in the next chapter.

Chapter 3: Methodology

3.1 Introduction

To achieve the objective of this research, both environmental parameters and mix related parameters were adjusted. Six different environmental conditions were simulated by varying the temperature and humidity during curing of a reference mix. The mix parameters primarily related to the quantities of chemical admixtures and coarse aggregates. The assessment of the rate of hydration and strength development occurred by monitoring the temperature and seismic modulus of the specimens nondestructively. The correlations of the temperature and seismic modulus to strength were established by conducting compressive strength tests at one, three, and seven days. The evolution of heat throughout the specimen over the first 48 hours from the time of water to cement contact was monitored using infrared imagery.

The concept and procedures for this research follow ASTM and TxDOT standards. Testing procedures used included cylinder preparation, determination of set, compressive testing, maturity, and seismic modulus. The ASTM and TxDOT methods are similar with a few minor exceptions. TxDOT does not have a procedure for free-free resonance test and uses a different datum temperature for determining maturity. ASTM C1074 states to use a datum of 32°F when the curing temperature is between 32°F and 104°F whereas Tex-426-A states to use a datum temperature of 14°F (TxDOT Designation: Tex-426-A 2010; ASTM C1074 2011). Since all other procedures follow the ASTM methods, this research used the datum temperature prescribed by ASTM C1074.

3.2 Experimental Design

Laboratory tests were carried out to measure the strength, maturity, set, and seismic modulus. Additionally, thermal imaging techniques were used to monitor the specimen for 48 hours. Standard 6-inch by 12-inch cylindrical specimens were used throughout this study.

Figure 3.1 graphically depicts a summary of the activities for this project. The mix-related parameters considered the presence and quantity of several chemical admixtures, change in coarse aggregate gradation as well as the water-to-cement ratio.

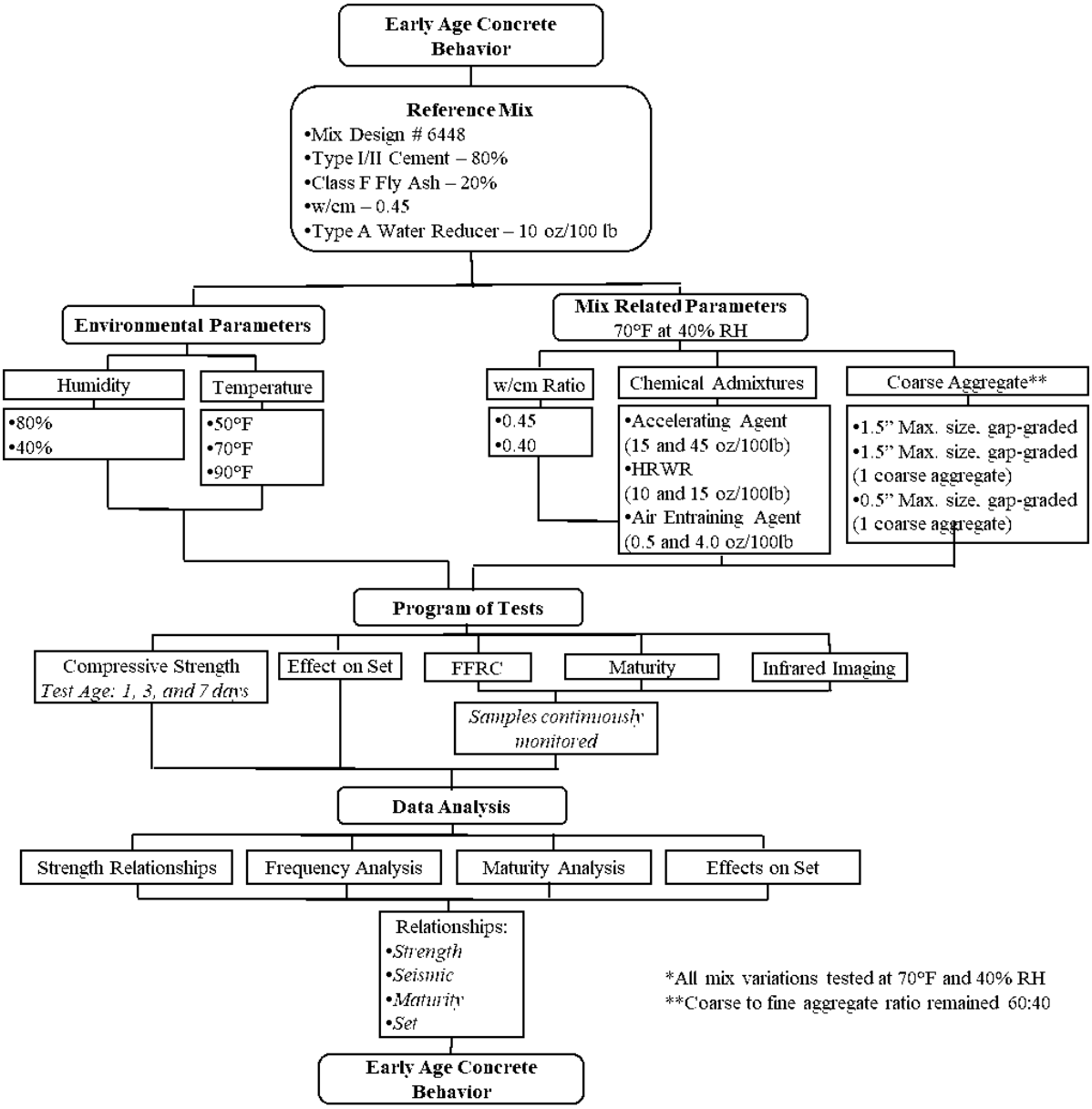

Figure 3.1 Project Work Plan

Twelve different mixes beyond the reference mix were used for this purpose. A detailed description of the reference mix is found in Tables 3.1 and 3.2 while Table 3.3 outlines the mix proportions for the twelve remaining mixes tested. For each mix tested, 12 cylinders were

prepared. Of the cylinders, three were placed in an environmental chamber and cured under standard curing conditions (70°F and 100% humidity) while the remaining nine were placed in a temperature control room at the specified temperature and humidity. Three cylinders had thermocouples inserted during preparation. Aside from collecting internal temperature data, these cylinders were used to collect seismic data, and infrared imaging. Imaging occurred for 48 hours while temperature and seismic data was collected for seven days. The computer used for monitoring of temperature and seismic response also controlled the ambient temperature in the room by use of a thermocouple placed in the room and heating/ cooling occurring based on the readings. FFRC and compressive strength testing occurred on three cylinders from the temperature room and one cylinder from the environmental chamber at one-, three- and seven-days.

Table 3.1 Reference Mix

Mix Component	Type/Class/Grade	Producer/Source	% or Dosage
Portland Cement	Type I/II	GCC Rio Grande/Samalayuca	80
Fly Ash	F	Salt River Materials/Escalante	20
Water Reducer	A	Euclid Chemical Eucon X-15	10
Coarse Aggregate 1	3	Jobe Materials, L.P./Avispa	13
Coarse Aggregate 2	5 (67)	Jobe Materials, L.P./Avispa	42
Intermediate Aggregate		Jobe Materials, L.P./Avispa	5
Fine Aggregate		Jobe Materials, L.P./Dyer	40
w/cm	0.45		

Table 3.2 Aggregate Gradation

Sieve Size	Sieve Size (in)	Coarse Agg. 1 % Passing	Coarse Agg. 2 % Passing	Intermediate Agg. % Passing	Fine Agg. % Passing
2 ½ in	2.500	100	100	100	100
2 in	2.000	100	100	100	100
1 ½ in	1.500	76	100	100	100
1 in	1.000	17	100	100	100
¾ in	0.750	2	96	100	100
½ in	0.500	1	62	98	99
3/8 in	0.375		35	65	95
No. 4	0.187		3	4	93
No. 8	0.093		1	1	86
No. 16	0.047			1	71
No. 30	0.024				56
No. 50	0.012				22
No. 100	0.006				2
No. 200	0.003				0.3

Table 3.3 Test Mix Proportions

Batch	Cement	Fly Ash	Water Reducer	Accelerating Agent	High Range Water-Reducer	Air-Entraining Agent	Coarse Agg. #1	Coarse Agg. #2	Intermediate Agg.	Fine Agg.	w/cm ratio
	%		oz./100 lbs. cement				%				
Reference	80	20	10	-	-	-	13	42	5	40	0.45
0.40 w-c	80	20	10	-	-	-	13	42	5	40	0.40
15 oz. AA	80	20	10	15	-	-	13	42	5	40	0.45
45 oz. AA	80	20	10	45	-	-	13	42	5	40	0.45
45 oz. AA; 0.40 w-c	80	20	10	45	-	-	13	42	5	40	0.40
10 oz. HRWR	80	20	10	-	10	-	13	42	5	40	0.45
15 oz. HRWR	80	20	10	-	15	-	13	42	5	40	0.45
10 oz. HRWR; 0.40 w-c	80	20	10	-	10	-	13	42	5	40	0.40
0.5 oz. AE	80	20	10	-	-	0.5	13	42	5	40	0.45
4 oz. AE	80	20	10	-	-	4	13	42	5	40	0.45
0.5 oz. AE; 0.40 w-c	80	20	10	-	-	-0.5	13	42	5	40	0.40
Large Agg.	80	20	10	-	-	-	60	-	-	40	0.45
Small Agg.	80	20	10	-	-	-	-	-	60	40	0.45

In addition, three mortar mix cylinders were prepared to check the sets using the penetration resistance method. These specimens were also placed in the temperature control room where the nine concrete cylinders were maintained.

The construction of a frame was necessary to hold the impact hammers, accelerometers, and thermocouples as well as controlled the cylinder spacing needed for thermal imaging. Figure 3.2 is a picture of the complete frame during monitoring of three specimens. The frame consisted of a plywood board with a 2 in. x 4 in. board on the left and right side to hold a threaded rod. Cylinders were placed on top of a 1-in. piece of hard foam to limit interference during collection of seismic data. Figure 3.3 depicts the close up of the seismic and temperature monitoring of a

single cylinder. Impact hammers were connected to a turnbuckle hanging from the rod and adjusted left or right as necessary to provide impact at the center of the specimen. The turnbuckle provided means of vertical adjustment to ensure proper impact occurred. Monitoring of the specimens occurred continuously for seven days with data recorded at specified intervals. Further explanation of each test is found in the following sections.

Figure 3.2 Specimen Testing Frame

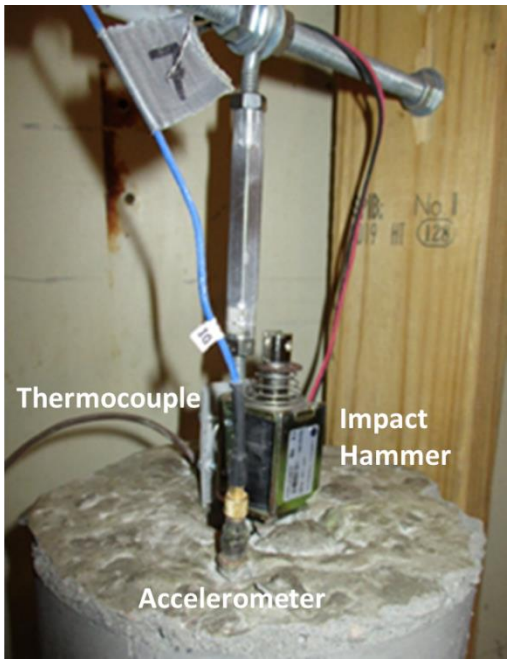

Figure 3.3 Seismic Modulus and Internal Temperature Monitoring

Figure 3.4 is a schematic of the monitoring, with seismic and temperature data collected by a stand-alone computer system. Output from the system consisted of ambient temperature as well as the specimen temperature, compression wave frequency, and shear wave frequency of each cylinder. The data acquisition system provided modulus values as early as 90 min. from the initial water-cement contact during mixing.

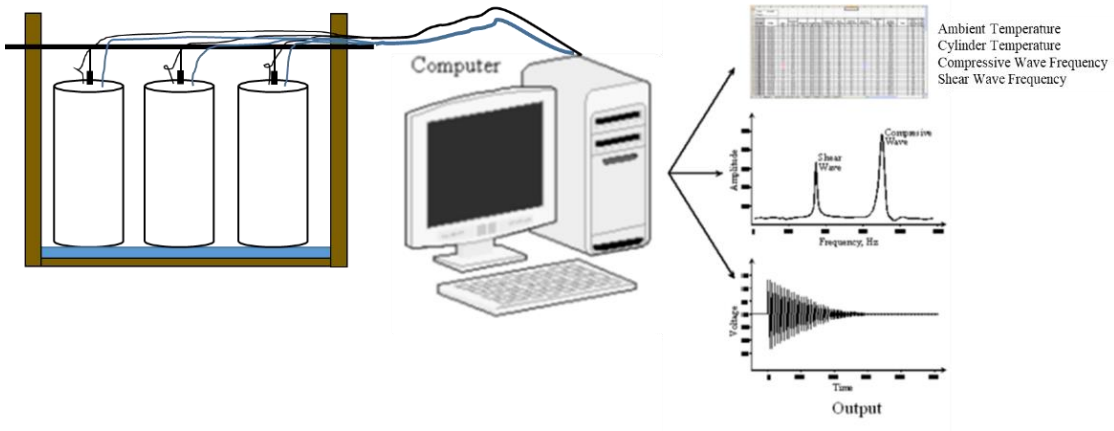

Figure 3.4 Seven-Day Monitoring Schematic

3.2.1 Reference Mix

TxDOT specifications, which provided the basis for the selection of the reference mix, mandate a compressive strength of 3,200 psi for traffic opening and 4,000 psi as the 28-day strength (TxDOT 2014). The maximum time to achieve 3,200 psi for opening is seven days, but can be as early as 48 hrs or even 24 hrs for high early strength concrete. With these requirements, approximately 15 high early strength (HES) and Class P mixes tested by TxDOT El Paso District Laboratory were reviewed. The final selection depended on the mixes that had the fewest number of admixtures as part of the mix. The mix parameters that remained unchanged during the research were the aggregates source, type of concrete, amount of water reducer, and amount of fly ash.

The mixture comprised of three different coarse aggregates and one fine aggregate from a local supplier. Table 3.3 shows the aggregate gradations. The absorption of Coarse Aggregate #1

and #2 were 0.5%, the intermediate aggregate was 0.6%, and the fine had an absorption of 0.7%. The type I/II portland cement and Class F fly ash used adhered to ASTM C150 and ASTM C618, respectively. To minimize the potential variability of aggregate properties during quarrying operations, the entire supply of required materials for the completion of this study were stockpiled at the beginning of the project.

Eucon X-15, a mid-range water-reducer, produced by Euclid Chemical was used in the reference mix. The mix contained a dosage of 10 fluid ounces per 100 pounds of cementing material. These dosages remained constant for all other mixes evaluated.

The inclusion and amount of chemical admixtures (i.e., accelerating agent, high range water reducer, and air-entraining agent) were varied in subsequent mixtures, as was the water-cement ratio. To study the impact of the gradation, the proportions of the materials from different bins were varied. The amount of fly ash, type of cement, and coarse-to-fine aggregate ratio remained constant throughout the research.

3.2.2 Specimen Preparation

The specimens were cast in 6 in. by 12 in. cylindrical molds in compliance with ASTM C470. Prior to mixing, all aggregates were oven dried to prevent the presence of excess moisture in the mixture from any of the aggregates. Once dried, the aggregates were cooled to room temperature prior to mixing. Mixing and consolidation of each mix followed the procedure listed in ASTM C192. All cylinders were cured for seven days at a specific nominal temperature and humidity. Three cylinders of every mix underwent standard curing at 70°F and 100% humidity to allow the comparison of their FFRC moduli and compressive strengths with those of the reference mix at standard curing. Demolding of all specimens occurred 24 hours after casting.

3.2.3 Environmental Related Parameters

All tests were carried out in an environmental chamber where the humidity and temperature could be controlled. Environmental factors that affect the concrete strength development include the humidity and temperature. Average daily humidity across Texas ranges from a high of nearly 80% on the Gulf coast to a low of about 40% around El Paso. Based on this information, the curing of specimens occurred at 80% and 40% nominal humidity levels at three different temperatures as discussed below. The use of these two humidity levels allowed for a comparison of strength development near the extremes experienced in Texas.

The specimens were cured at three different nominal temperatures of 50°F, 70°F and 90°F. The 50°F temperature is above the minimum temperature restriction for placing concrete (TxDOT 2014). The 90°F temperature served as the high-end temperature while 70°F was the medium range temperature. These three temperature ranges were used only with the reference mix at both 80% and 40% humidity.

3.2.4 Mix Related Parameters

The mix related parameters evaluated were the water-cement ratio, three chemical admixtures (accelerating agent, high-range water-reducer, and air entraining agent) and changes to maximum coarse aggregate size and gradation. A discussion of each of these components and their individual impact are presented below. Curing conditions for all mixes occurred at 70°F and 40% humidity. This correlates to the average temperature and humidity experienced in El Paso.

Water-Cement Ratio

The w/c ratio influences the strength development and the workability of fresh concrete. Higher w/c ratios generally indicate the need for increased workability but strength generally decreases as seen in Figure 3.5. To evaluate the impact of w/c ratio, the reference mix (w/c = 0.45)

and a mix with w/c ratio of 0.40 were considered. A mix with higher w/c ratio than the reference was not considered since the reference mix contained a water reducer. In these experiments, the cement content was maintained constant while the water content varied for the two w/c ratios. Experiments with lower w/c ratio were also carried out for mixes with chemical admixtures as discussed below.

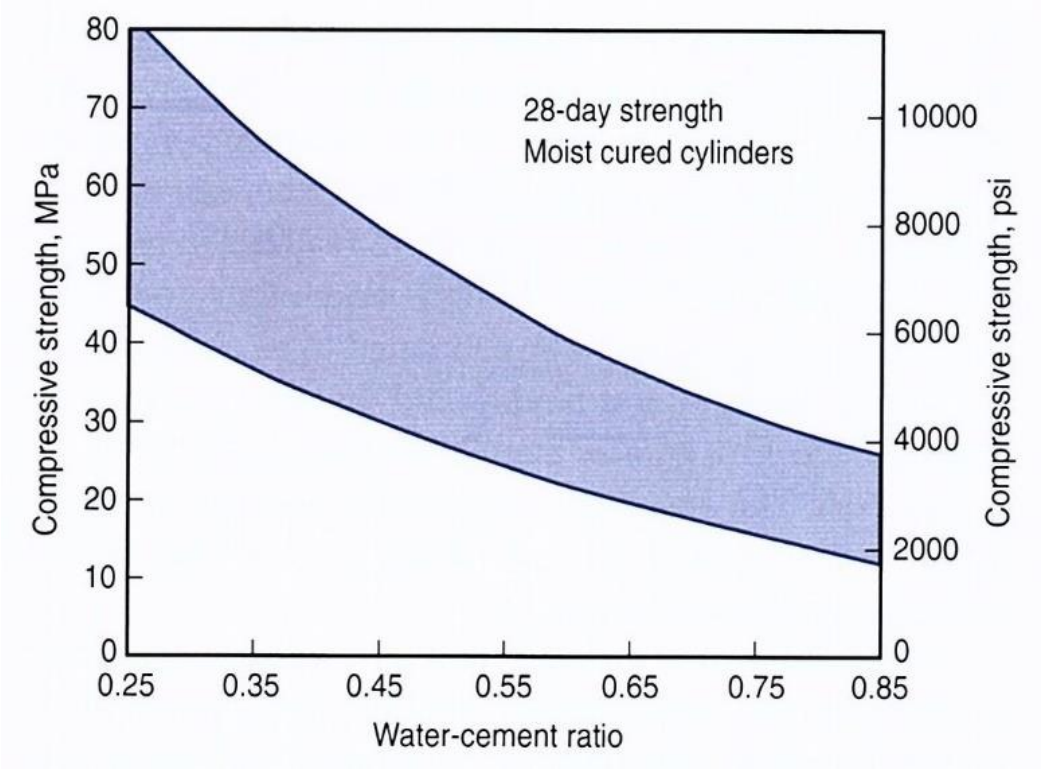

Figure 3.5 Strength to Water-Cement Ratio Relationships (Kosmatka et al. 2002)

Chemical Admixtures

According to ASTM C125 (2015), an admixture is defined as a material other than water, aggregates, cementitious material, and fiber reinforcement that is used as an ingredient of a mixture to modify its freshly mixed, setting, or hardened properties and that is added to the mix before or during its mixing. A discussion of chemical admixtures used for this research and the concrete properties modified by their inclusion in the mix follows.

Accelerating Agent

The accelerating agent used in this research was Accelguard ACN 200 produced by Euclid Chemical to decrease the time to the initial set. The low and high dosages used were 15 and 45 oz. per 100 lbs. of cementitious material, which fell within the manufacturer's recommended values.

High-range Water-Reducer

To evaluate the extent to which using a high-range water-reducer affects the early strength, a low and high dosages of 10 and 15 oz. per 100 lbs. of cementitious material of Eucon SP produced by Euclid Chemical were added to the mix. These ranges again fell within the manufactured recommend range.

Air Entraining Agent

To evaluate the extent of the impact of air-entraining agent on the strength, two dosages within the prescribed range were selected. The evaluation occurred at dosages of 0.5 and 4 oz. per 100 lbs. of cementitious material of Eucon AEA-92 produced by Euclid Chemical.

Coarse Aggregate

Changes in the coarse aggregate proportion was simulated by eliminating two of the coarse aggregates used while maintaining a coarse to fine aggregate ratio of 60:40 as shown in Figure 3.6. The overall reference mix is gap-graded with a maximum aggregate size of 1.5 in. Use of strictly Coarse Aggregate #1 results in a more extreme gap-graded mix with the same maximum aggregate size. Conversely, including just the intermediate aggregate yields a gap-graded mix as well, but with a maximum aggregate size of 0.5 in. TxDOT specifications classifies Coarse Aggregate #1 as a Grade 3; therefore, allowing both the reference mix and the mix with strictly this aggregate to meet the requirements for use in Class P concrete (TxDOT 2014). Use of the intermediate

aggregate, Grade 6, meets requirements of Class P concrete with a caveat. TxDOT specifications caveat states, "other grades of coarse aggregate maybe used in non-structural concrete classes when allowed by the Engineer."

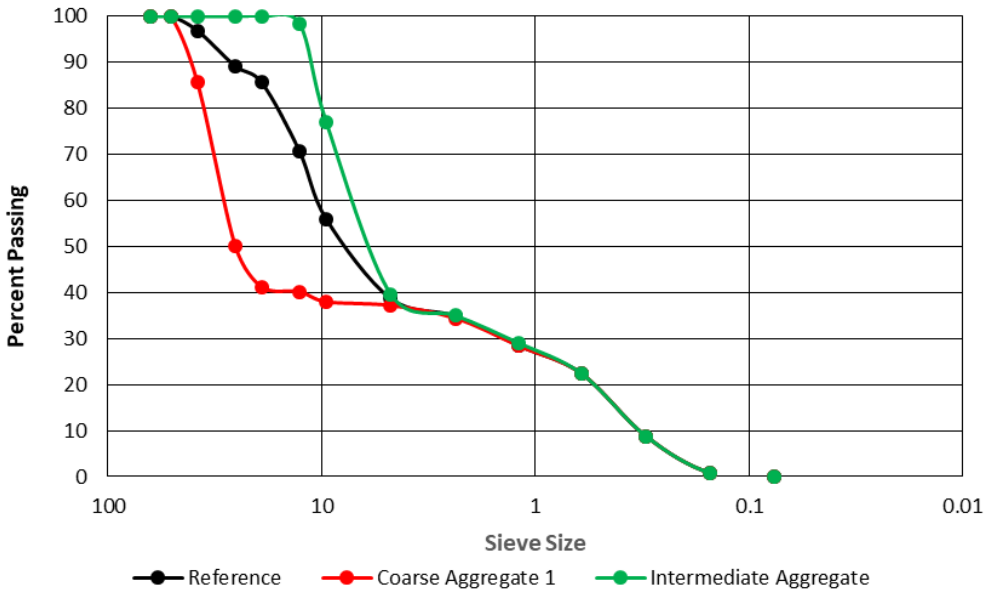

Figure 3.6 Coarse Aggregate Gradation

3.3 Methods for Assessing Strength

Table 3.4 presents the destructive or nondestructive methods used in this research to assess the strength or stiffness of PCC. Destructive methods use techniques to assess the properties of a test specimen with damage occurring to the specimen. These methods provide a direct measurement of the specimen strength. On the other hand, nondestructive methods obtain information about the internal conditions or properties of a test specimen without causing damage to the specimen.

Table 3.4 Tests to Assess Concrete Properties

Method	Concrete Test	Test Standard
Set	Set by Penetration Test	ASTM C403
Destructive	Compressive Strength Test	ASTM C39
Nondestructive	Maturity Test	ASTM C1074
	Seismic Test (FFRC)	ASTM C215

3.3.1 Compressive Strength Test

Performance of the standard compression test in accordance with ASTM C39 occurred on all 6 in. diameter by 12 in. length specimens. Testing occurred at one, three and seven days for all mixes, with four specimens tested per day as outlined in ASTM C39. Tested specimens include three specimens from the desired temperature and humidity with the fourth specimen under standard curing. An Instron universal testing machine allowed the cylindrical specimens to be loaded in uniaxial compression at a load rate of 30 psi/sec until failure (see Figure 3.3). This load rate conforms to the recommended load rate of 35 ± 7 psi/sec stated in ASTM C39.

Figure 3.7 Compressive Strength Test

3.3.2 Maturity Test

The internal temperatures of three separate specimens were monitored for seven days using thermocouples at measurements frequencies shown in Table 3.5.

Table 3.5 Recording Intervals

Time from Mixing, hr.	Frequency of measurement per hour
0-12	12
12-24	4
24-48	2
48-168	1

The method outlined in ASTM C1074 was used to convert the recorded temperature time histories into time-temperature factors (TTF). In addition to the standard method of calculating TTF, an alternative approach was tested in which the datum temperature used was the instantaneous temperature of the environmental chamber. The rationale behind this approach was to delineate the heat of hydration from ambient temperature. The maturity values obtained with the new datum, which are referred to as alternative TTFs for the remainder of this document, are compared with the traditional one in Figure 3.8 over the seven-day monitoring period of the reference mix cured at 90°F and 40% humidity. The alternative TTF provides some insight in the original heat equilibrium between the specimen and ambient temperature followed by rapid increase in the alternative TTF during the setting period followed by a rapid decrease occurring at the time of mold removal and the eventual stabilization of the alternative TTF. This behavior will be discussed later in this report.

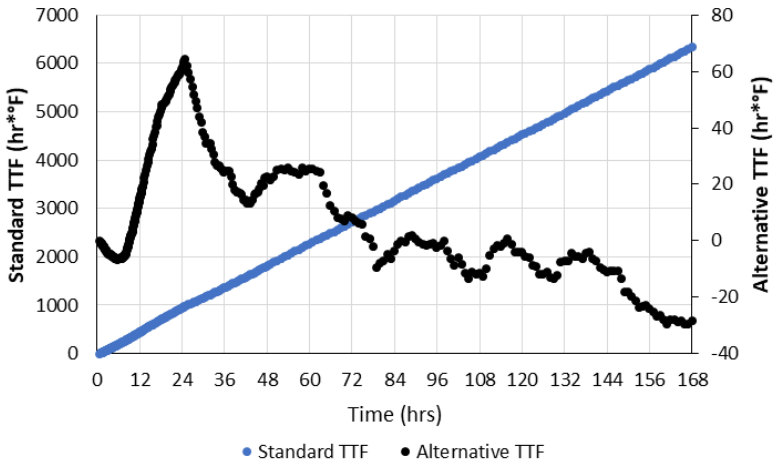

Figure 3.8 Comparison of Maturity Calculation Approaches

3.3.3 Free-Free Resonant Column

The progressions of the seismic moduli of three specimens were monitored with a fully-automated free-free resonant column method that complied with ASTM C215 (2014). The seismic moduli were measured simultaneous with the internal temperatures over a seven-day period.

Based on difficulties found by Lara (2008) concerning transmission of seismic energy with an impact hammer on fresh concrete, accelerometers were attached to the head of a nail that was placed in the concrete offset from the point of impact. Additionally, point of impact occurred on large aggregates present on the surface of the specimen.

As a way to verify the seismic modulus from the automated system, a manual (traditional) FFRC test was carried out on each specimen prior to the one, three, and seven day compressive strength testing. The manual and automatic moduli were within 3% of one another.

3.4 Infrared Imaging

The infrared imaging was used to produce a thermal profile of monitored specimens at distinct points during the first 48 hours after production. Although there are ASTM test methods for use of infrared imaging systems, none of them apply to early age concrete. Rather the methods apply to other applications such as detecting delamination in bridge decks (ASTM C4788) or inspecting insulation (ASTM C1060). A trial-and-error approach was followed to establish a consistent method. An Infrared Cameras Inc. model T2I system was used to collect thermal images of three specimens placed at a distance of approximately 5 ft. The specimens were spaced about 1 in. apart to obtain concurrent images of the three specimens with limited background interference as seen in Figure 3.9. The device was calibrated prior to the start of data collection for every mix and curing condition. Data collection occurred at five-minute intervals for a 48-hour period. It was difficult to isolate the thermal images from each individual specimen beyond 24 hours, since

the specimens' temperatures were similar to the ambient temperature regardless of the environmental chamber's temperature.

Figure 3.9 Set-up for Thermal Imaging of Cylinders

Figure 3.10 shows a raw image collected during testing. A rectangular frame was placed around each of the three cylinders. The digital temperature data for each vertical and horizontal pixel of each specimen was exported into an excel worksheet developed for analyzing the data. The ambient temperature was first subtracted from the temperature measured at each pixel. This data was then imaged based on the criteria included in Table 3.6. Images captured at the start of curing, initial set, final set, 24, 36, and 48 hrs after curing were of particular interest since they provided a better understanding of how the heat of hydration dissipated at critical times. An example of such data is presented in Figure 3.11.

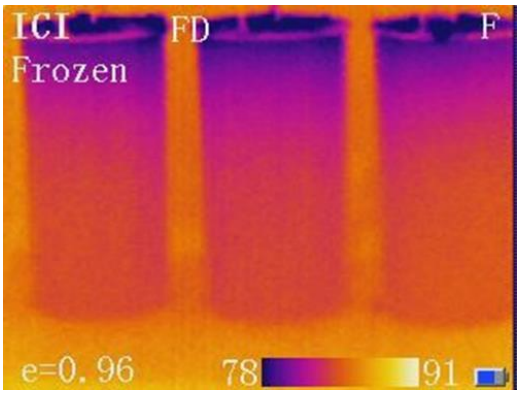

Figure 3.10 Thermal Image of Cylinders

Table 3.6 Infrared Imaging Value and Color Assignment

Normalized Temperature	Assigned Value	Meaning	Color
> 10° above ambient	2	Hot	Red
4<ambient<10	1	Warm	Yellow
-4<ambient<4	0	Neutral	White
< -4° below ambient	-1	Cold	Blue

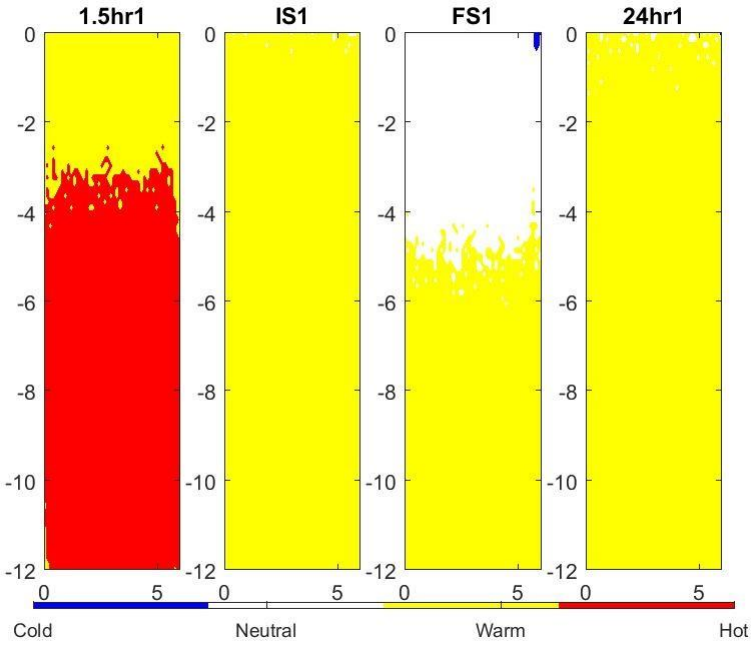

Figure 3.11 Example Thermal Profile of Single Cylinder

3.5 Determination of Set

The initial and final sets for each mix were estimated as per ASTM C403 using a Humboldt ACME Penetrometer (Figure 3.12). Rather than sieving the concrete mix, the mortar mix was prepared by including all components of the mix except the two large coarse aggregates and the intermediate aggregate. The primary reason for this activity was to limit the amount of material wasted. Mortar specimens experienced the same curing conditions as the specimens in the environmental chamber. Using these points coupled with the creation of thermal profiles provided a better understanding of the heat of hydration throughout the specimen.

Figure 3.12 Penetrometer

3.6 Modulus Based Approach for Determining Setting Times

The variation of seismic modulus with time may allow the identification of the dormant, setting, and hardening stages of concrete. Figure 3.13a shows the variation in seismic modulus with time while Figure 3.13b shows the variation of seismic modulus with maturity of the reference mix cured at 70°F and 40% humidity. Regardless of the abscissa, three different phases (i.e., dormant, setting and hardening) are visible. For both figures, the recorded data and best-fit curves are shown. The best-fit curves are based on the first 72 hours of recorded data, as discussed further in the following sections.

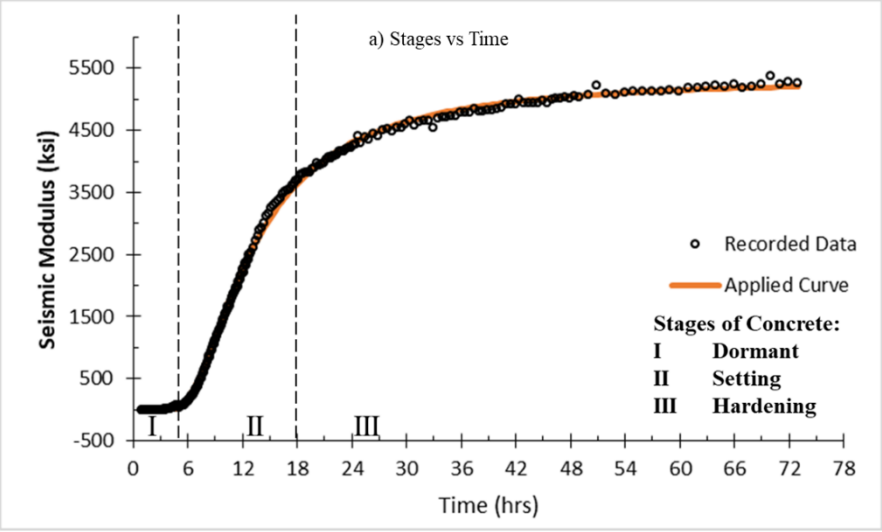

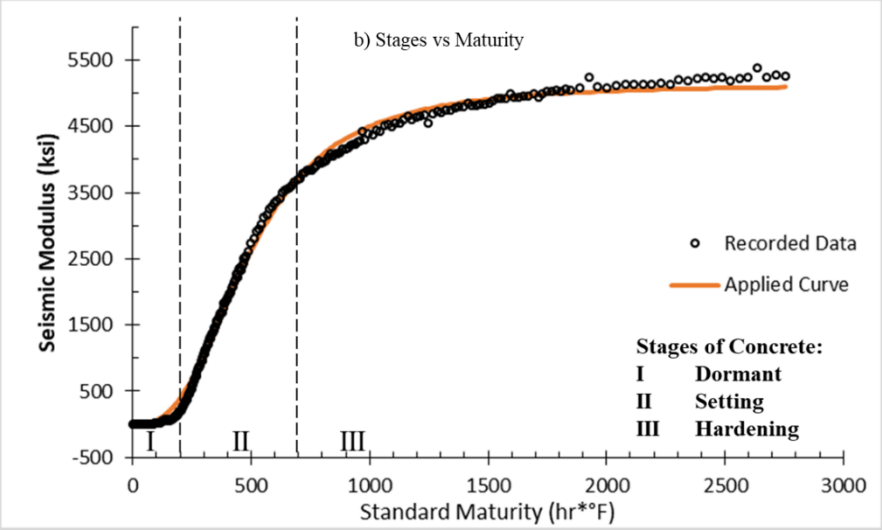

Figure 3.13 Basic Stages of Concrete Hydration

3.6.1 Determining Set from a Time-Based Modulus Growth

The equation that best represented the modulus growth over time was found to be

$$modulus = e^{\left(a-\left(\frac{b}{(time)^2}\right)\right)} \qquad \text{EQN 3.1}$$

where *a* and *b* are coefficients that are obtained through curve fitting. Variable *a* is related to the long-term modulus while variable *b* controls how fast the modulus becomes asymptotic to the long-term modulus. The best fit curve as per Eq. 3.1 represents the recorded data well for the first

72 hrs. Three zones can be observed in Figure 3.13. Table 3.7 describes the interpretation of the three approximated segments.

Table 3.7 Stages of Hydration from Variation in Modulus with Time

Stage	Model Name	Description
Dormant	y_1	Near horizontal model, early-age
Setting	y_2	Steep gain model
Hardening	y_3	Near horizontal model, long-term

Figure 3.14a shows the best fit curve shown in Figure 3.13a can be approximated with three lines. The intersections between the two adjacent lines were considered as alternative definitions of times of initial and final set based on the modulus development. The intersection of models y_1 and y_2 defines the initial set time (IS = 5.8 hrs). While the intersection of models y_2 and y_3 defines the final set time (FS = 18.0 hrs). For this mix, the proposed modulus-based initial set time was within 15 minutes of the set time from the standard penetration resistance approach; while the proposed and standard final sets differed by 60 minutes. The differences between the standard and proposed methods can be attributed to several factors. For example, the traditional set time is based on the mortar portion of the mix whereas the proposed method is based on the actual mix.

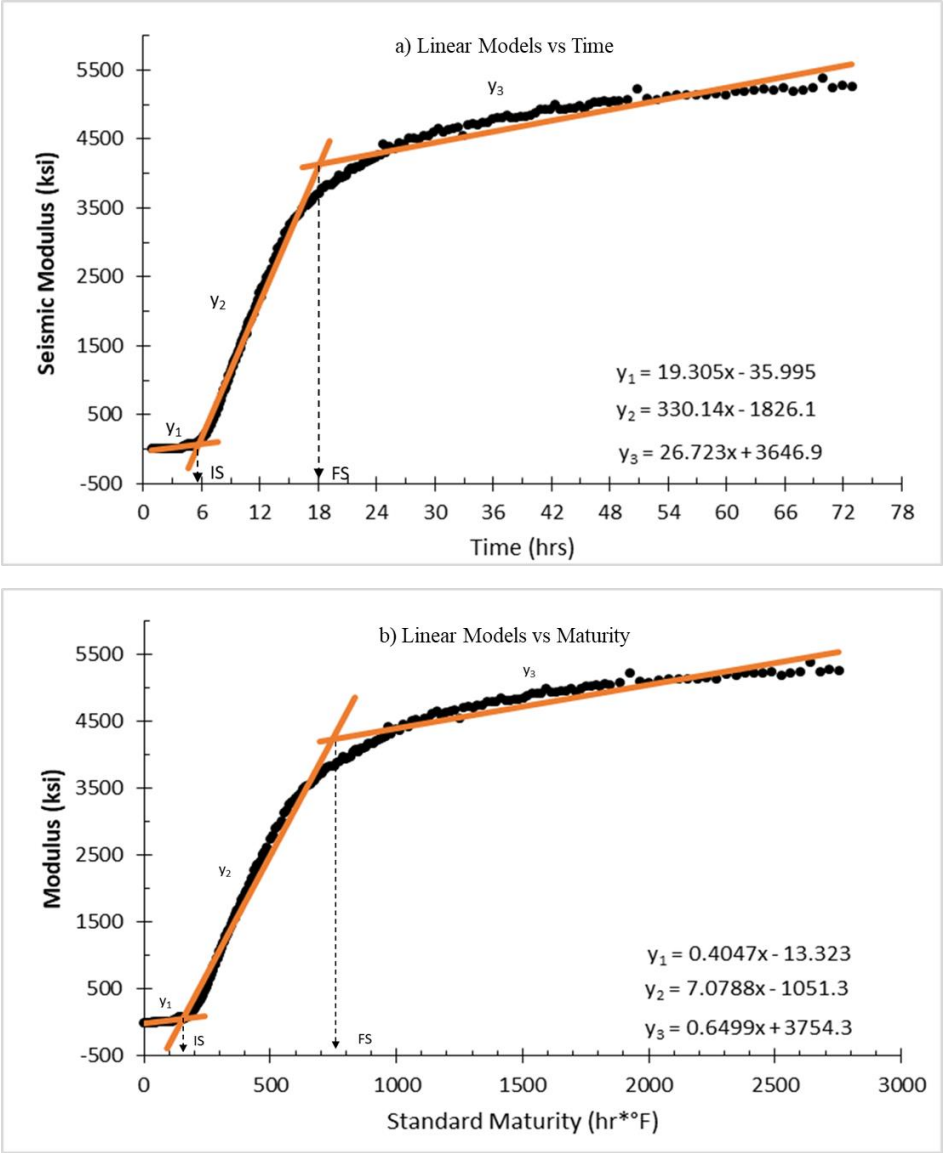

Figure 3.14 Linear Models Used to Determine Alternative Initial and Final Sets

3.6.2 Determining Set from a Standard Maturity-Based Modulus Growth

Changing the abscissa from time to maturity does not significantly change the shape of the modulus growth as seen in Figures 3.13a and 3.13b. However, it does change the equation that can model the growth, largely due to the change in scale. Because of this scale change, an equation with more than two coefficients is needed to model the modulus behavior. In this case, the most appropriate equation found is:

$$modulus = \frac{c}{1+\left(\frac{d}{TTF}\right)^{f}} \quad \text{EQN 3.2}$$

where *c,* corresponds to the long-term modulus while variables *d* and *f,* define the early-age modulus and growth. As seen in Figure 3.13b, this equation represents the recorded data well up to a standard maturity of 2,000 hr.*°F.

Figure 3.14b shows the three stages of the concrete. In this case, the initial set is at a standard maturity of 156 hr.*°F or approximately 5.1 hrs; while the final set occurs at a standard maturity of 748 hr.*°F or approximately 19.1 hrs.

3.7 Summary

This chapter outlines the methodology for evaluating early age behavior of portland cement concrete. An experiment design to study the effects of both environmental conditions and mix parameters on the strength and modulus development of one mix was developed. Six environmental variations based on the average high and low temperatures and humidity were considered to model the extreme weather conditions experienced across Texas. Mix parameters included reduction of w/c ratio, addition of admixtures approved for use by TxDOT, and change in maximum aggregate size and gradation. The quantity of admixtures occurred at the high and low range of manufacturer recommended dosages.

The continuous monitoring allows for a detailed evaluation of the modulus growth with time and maturity. These comparisons provide the opportunity to identify trends that may be useful in calculating or monitoring what stage of hydration the concrete is undergoing. The potential for considering an alternate datum for calculating the concrete maturity is also studied. This alternative datum may yield more detailed information about the concrete strength gain than the standard maturity will, since it is more sensitive to environmental factors.

Even though the penetration resistance test to determine set has been effectively used for decades, it does not consider the concrete properties as a whole. A method to determine the initial and final set based on modulus development is discussed. Determination is possible using either time or maturity as the x-axis parameter. The test matrix carried out can be used to evaluate the effectiveness of considering the concrete mix as opposed to the mortar.

Chapter 4: Results and Analysis

4.1 Introduction

As discussed in Chapter 3, testing each mix yielded times of initial and final set, internal temperature with time, compression wave frequency with time, shear wave frequency with time, compressive strength at 1 day, 3 days and 7 days of curing, and infrared images of the specimens with time for the first 48 hours. From this information, the time-temperature factors, seismic moduli, Poisson's ratios, and thermal profiles were obtained. The impact of the environmental-related and mix-related parameters on the estimated parameters are discussed here. All environmental tests were carried out using the reference mix while all mix variations were tested at 70°F and 40% humidity.

Figure 4.1 contains a visual comparison of the seismic moduli obtained from the automated and manual FFRC tests. The results from the two tests are quite comparable except for the 1-day testing, where the two moduli differ by about 11%. The differences in 1-day moduli are attributed to the small differences in testing times in the early age while the modulus growth is rather accelerated as well as dimensional differences between the specimens. Given the closeness of the automatic and manual moduli for all mixes, only the continuous monitoring results are shown for the remainder of this document, except when the results from the standard-cured specimens that were maintained in a curing chamber (instead of the environmental chamber) are reported. In addition to a strong correspondence to the manual FFRC test, the automated system yielded similar results across the three monitored specimens. Across the eighteen mixes, the average standard deviation of the recorded moduli among the three specimens was less than 270 ksi. A lower standard deviation was achieved when occasional misaligned specimens were eliminated.

Figure 4.2 demonstrates the variations of the internal temperatures for three different ambient curing temperatures measured with the embedded thermocouples. For the first four to six hours, the internal temperatures are either increasing or decreasing toward the ambient temperature based on the ambient setting and the conditions that the specimens were prepared in. Ignoring the first six hours of data where the specimens were rapidly equilibrating to the environmental chamber temperature, the maximum thermocouple reading for every mix, which was about 110% of the ambient temperature setting, typically occurred between 12 and 18 hours from mixing.

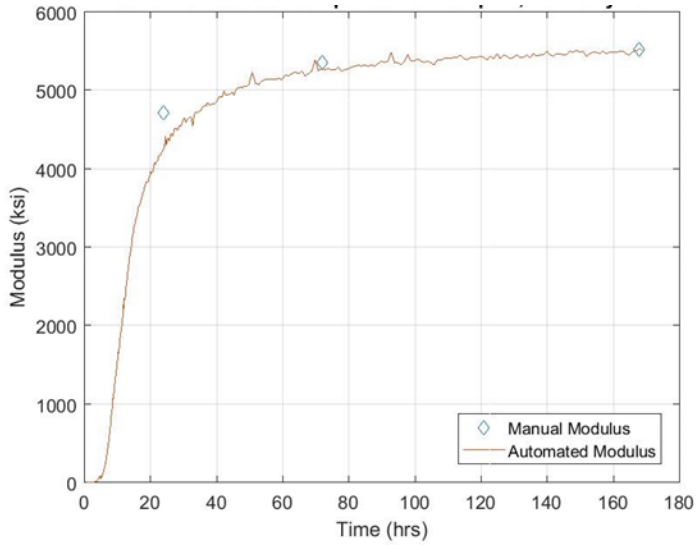

Figure 4.1 Comparison of Seismic Moduli from Automatic and Manual FFRC Tests

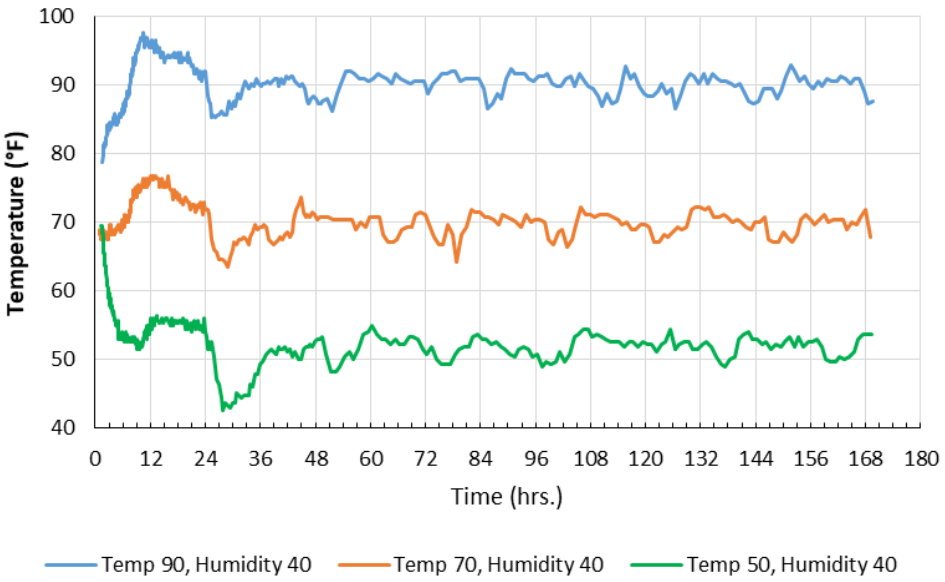

Figure 4.2 Internal Temperature Trends

The second common observation was the similarity of the timing of the peaks and valleys of the generalized hydration plots reported by Neville (1996) and Mindess et al. (2003) in Chapter 2. Within a few hours of one another, all concrete mixes go through an approximate nine-hour period without heat production starting from when the mix is between 25 and 28 hours old. These points correspond to the period where hydration changes from C3S to C3A. After that period, the specimens are generally at the same temperature as the ambient temperature.

The variation in internal temperature is compared with the variation in alternative maturity with time in Figure 4.3. Unlike the standard TTF, the alternative TTF trend seen in Figure 4.3 provides the opportunity to understand better the impact of the ambient temperature on the curing of concrete.

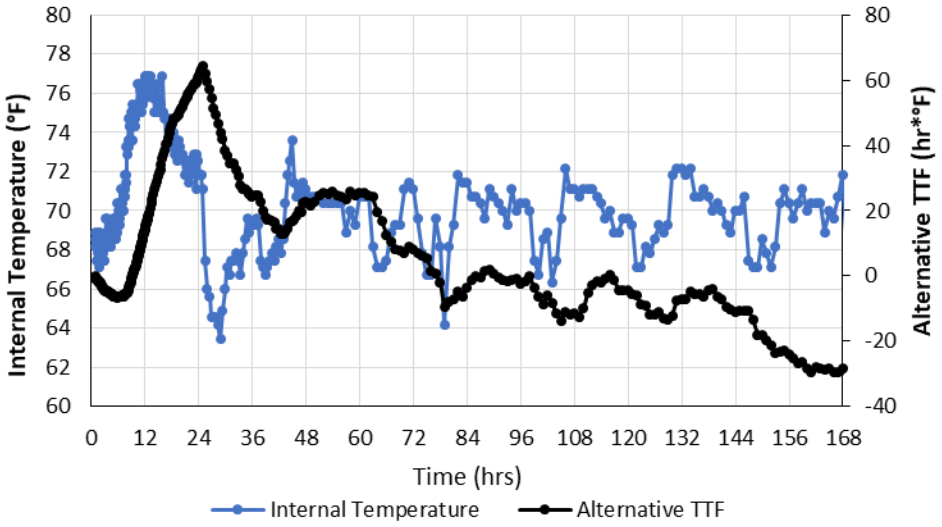

Figure 4.3 Internal Temperature and Corresponding Alternative TTF of Reference Mix Cured at 70°F and 40% Humidity

Figure 4.4 depicts the variations of the alternative TTF with time for the three internal temperature time histories shown in Figure 4.2. The primary trends observed across the three curing temperatures are a peak around 24 hrs and a generally linear behavior beyond 60 hrs. The initial drop of alternative TTF readings observed at the higher temperature curing cause lower readings than those recorded at the 50°F curing.

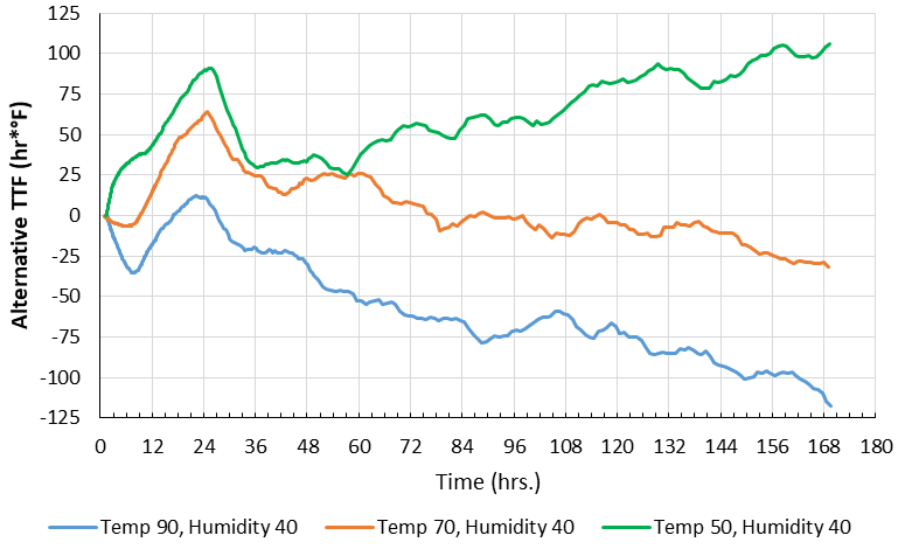

Figure 4.4 Corresponding Alternative TTF Trends

4.2 Modulus-Strength Relationships

Figure 4.5 depicts the variations in compressive strength with seismic modulus for the reference mix cured at 70°F and 40% humidity. The equation that best explains the modulus-strength relationship was an exponential equation of the basic form of

$$strength = je^{k*modulus} \quad \text{EQN 4.1}$$

where *j* and *k* are the coefficients defining the intercept and shape of the curve.

Table 4.1 summarizes the modulus-strength relationship for each mix tested. A larger variance was observed in the *j*-coefficients while the *k*-coefficients were more similar across the mixes. The average value of the *k*-coefficients was 8.5×10^{-4} with a standard deviation of 2.1×10^{-4}. This indicates the strength development in a fairly uniform manner as modulus increases during the first seven days. Overall a high confidence was found for each mix as seen by the R^2 values. Lower R^2 values generally occurred in the mixes that experienced a drop or little gain in strength between three and seven days.

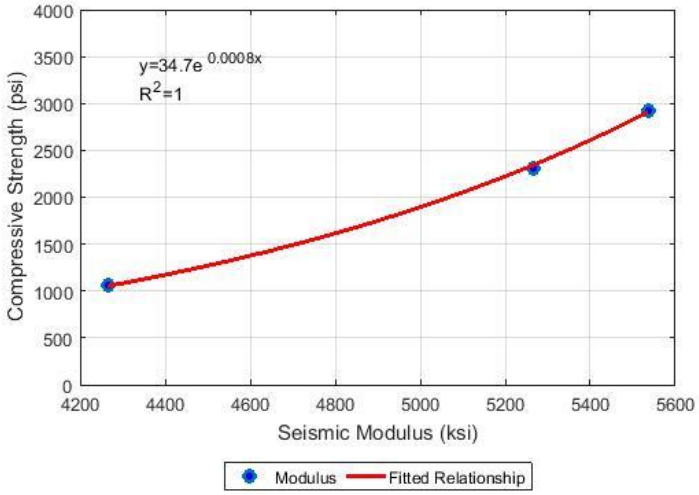

Figure 4.5 Modulus-Strength Relationship of Reference Mix Cured at 70°F and 40% Humidity

Table 4.1 Modulus-Strength Relationship Coefficients and R^2 Values

Mix	*j*	*k* (x10^{-4})	R^2
Temp 50 Humidity 40	1.4	13.7	1.00
Temp 50 Humidity 80	30.1	8.31	1.00
Temp 70 Humidity 40	34.7	8.00	1.00
Temp 70 Humidity 80	28.9	7.95	0.96
Temp 90 Humidity 40	30.2	8.12	0.97
Temp 90 Humidity 80	85.1	6.08	0.94
0.40 w-c	85.0	6.00	0.96
15 oz. AA	34.3	8.12	0.97
45 oz. AA	10.3	10.6	1.00
45 oz. AA; 0.40 w-c	20.3	8.60	0.99
10 oz. HRWR	13.1	9.07	0.94
15 oz. HRWR	15.4	9.40	0.99
10 oz. HRWR; 0.40 w-c	41.5	7.15	1.00
0.5 oz. AE	27.3	8.57	0.99
4 oz. AE	16.1	12.7	0.95
0.5 oz. AE; 0.40 w-c	103.0	5.55	0.86
Large Agg.	45.2	6.54	0.99
Small Agg.	40.3	7.91	1.00

No significant trends are observed amongst the *j*- or *k*-coefficients with regard to environmental conditions or mix changes. The mix change that saw the greatest similarities in both coefficients involved the addition of a high-range water reducer, while the 70°F curing showed a very similar *k*-coefficient between the two humidity conditions. The 0.5 oz AE; 0.40 w-c mix resulted in a much larger *j*-coefficient and much lower *k*-coefficient compared to all other mixes. This mix also had the lowest confidence as seen by the R^2 value.

4.3 Standard Maturity-Strength Relationships

The results and fitted trend line for the reference mix cured at 70F and 40% humidity are shown in Figure 4.6. A logarithmic equation was found to best model the standard maturity-strength relationship. The equation was of the basic form of

$$strength = \mathrm{m}\ln(TTF) - n \qquad \text{EQN 4.2}$$

where *m* and *n* serve as coefficients controlling the rate of growth and y-intercept , respectively.

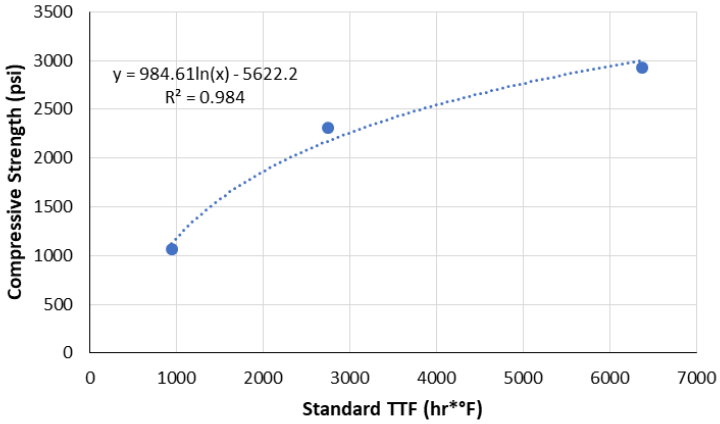

Figure 4.6 Standard Maturity-Strength Relationship for Reference Mix Cured at 70°F and 40% Humidity

Table 4.2 lists the standard maturity-strength relationship and associated R^2 value for every mix tested. Most mixes show a good relationship between standard maturity and strength. The growth factor (*m*-coefficient) observed in Table 4.2 are generally greater than 1,100 for low temperature (50°F) curing, less than 650 for high temperature (90°F) curing and in between the two for 70°F curing. The mix with the reduced water-cement ratio, mixes with accelerating agent, and the mix with the large coarse aggregates generally exhibited lower *m*-coefficients. The two mixes with the lowest *m*-coefficients were the mix with the high dosage of air entertainer and the mix with low dosage of air entertainer combined with a low-water cement ratio. These mixes also had the lowest R^2 value.

Table 4.2 Standard Maturity-Strength Relationship Coefficients and R^2 Values

Mix	*m*	*n*	R^2
Temp 50 Humidity 40	1188.3	7266.4	1.00
Temp 50 Humidity 80	1230.7	7178.2	1.00
Temp 70 Humidity 40	984.6	5622.2	0.98
Temp 70 Humidity 80	1008.7	5821.7	1.00
Temp 90 Humidity 40	619.6	2782.9	0.99
Temp 90 Humidity 80	590.7	2554.0	0.81
0.40 w-c	719.0	3448.9	0.87
15 oz. AA	892.6	4945.5	0.97
45 oz. AA	903.9	5204.8	0.93
45 oz. AA; 0.40 w-c	830.7	4366.9	0.85
10 oz. HRWR	1155.8	6859.2	0.96
15 oz. HRWR	907.0	5318.4	0.94
10 oz. HRWR; 0.40 w-c	901.0	4640.6	0.94
0.5 oz. AE	1005.1	5880.3	0.91
4 oz. AE	375.9	2194.6	0.81
0.5 oz. AE; 0.40 w-c	638.5	2868	0.66
Large Agg.	718.3	3689.5	0.95
Small Agg.	1136.1	6483.5	0.95

4.4 Impact of Environmental Parameters

The reference mix was tested under different combinations of three temperatures and a high and low humidity to document their effects on the concrete times of set as well as strength and modulus development. Additionally, the impact of the time of mold removal was briefly investigated to document its impact on strength and modulus development.

4.4.1 Impact of Temperature

The variations in penetration-based times of set with temperature under humidity conditions of 80% and 40% are shown in Figure 4.7. Regardless of the level of humidity, times of set occurred earlier at higher temperature. It took twice as long for the specimens cured at 50°F to transition from the initial set to final set as compared to specimens cured at 70°F and 90°F.

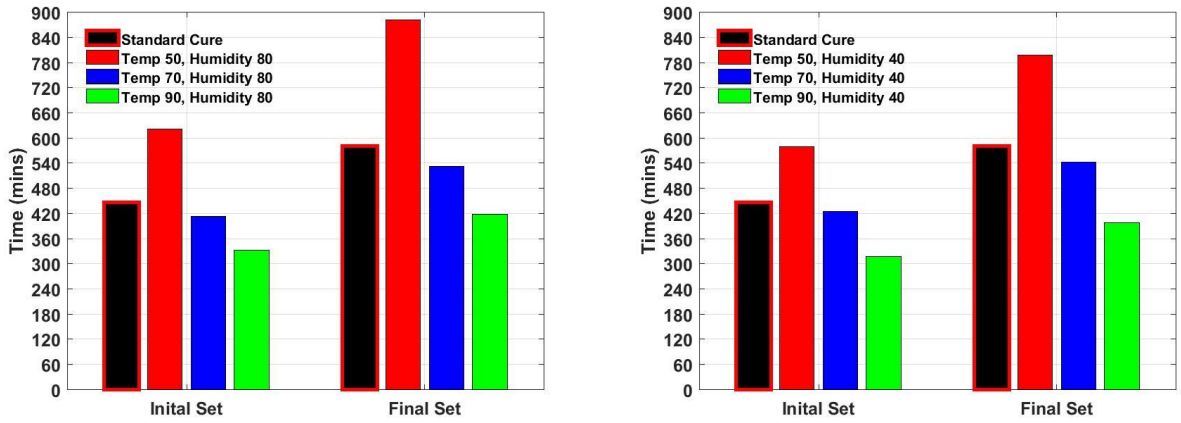

Figure 4.7 Temperature Impact on Set at High and Low Humidity

Figure 4.8 summarizes the variations in modulus with time for the low and high humidity curing conditions. For a given humidity level, the moduli appear to converge to a similar values and would likely yield similar 28-day results. Increased curing temperature caused more rapid increase in modulus of the specimens while the specimens cured at lower temperatures exhibited a slower rate of modulus growth. The specimens exposed to the high and mid-range curing temperatures generally become asymptotic to their long-term moduli between 40 and 60 hours; whereas the specimens cured at 50°F required about 80 hours to reach to that level.

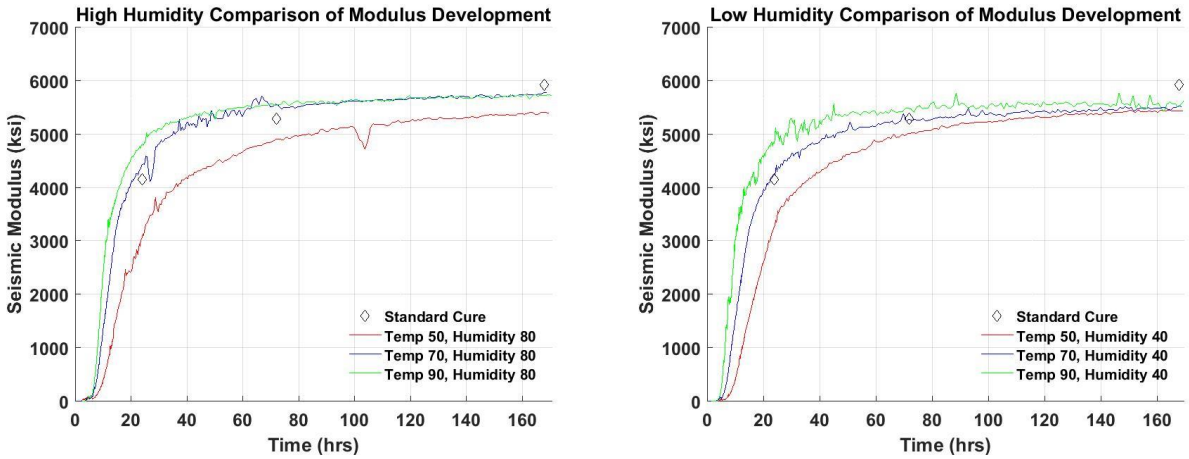

Figure 4.8 Temperature Impact on Modulus Development at High and Low Humidity

Figure 4.9 shows the variations in compressive strength with time. The results obtained are consistent with the previous research reviewed in Chapter 2. Changing the curing temperature

from 70°F to 90°F yielded more proportional changes in the properties than observed when the curing temperature was changed from 70°F to 50°F. High temperature curing resulted in a high one-day strength following by a less than 50% gain at three-days. By seven days there was little strength gain recorded, indicating a rapid initial strength gain that rapidly decreases beyond three days. Low temperature curing on the other hand resulted in a very low one-day strength following by rapid gain to the achieved three-day strength. Although the strength gain from three-to seven days was less rapid, it was still a larger rate of gain than see at high temperature curing. Therefore, unlike the early rapid growth seen at 90°F, the low temperature curing went through an initial slower rate of growth followed by a consistent rate of growth to reach the three- and seven-day strengths.

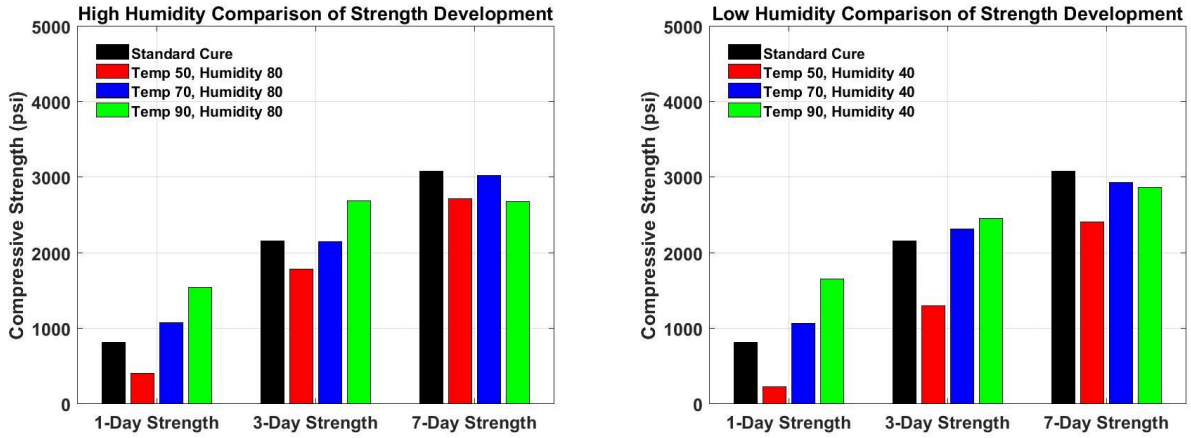

Figure 4.9 Temperature Impact on Strength at High and Low Humidity

4.4.2 Impact of Humidity

The impact of humidity during curing was analyzed across the three curing temperatures at a low, 40%, and high, 80% humidity. Results indicated there is still and impact from humidity on set, strength, and modulus; however this impact is not as great as that caused by temperature. Referring back to Figure 4.7, the low humidity specimens show faster times of initial and final set when compare to the high humidity specimens cured at the same temperature. For the 70°F and

90°F curing, times of initial and final set where within 20 minutes of each other for both humidity conditions. The low temperature curing; however, reached initial set almost 45 minutes faster at low humidity and over an hour faster for final set.

Figure 4.10 shows the variations in the internal temperature of the specimens cured at the same temperature but different levels of humidity. The impact of the humidity on the internal temperature is rather small as compared to the impact of curing temperature discussed in the previous section. However, the impact of the humidity on the strength and to lesser extent on modulus is more pronounced as discussed below. By 36 hours, the trend has minor fluctuations and averages to the ambient temperature reading. This indicates that minimal heat is generated from the concrete and temperature changes primarily result from changes in the environment. Further findings are discussed below to expand on humidity impacts at each tested temperature.

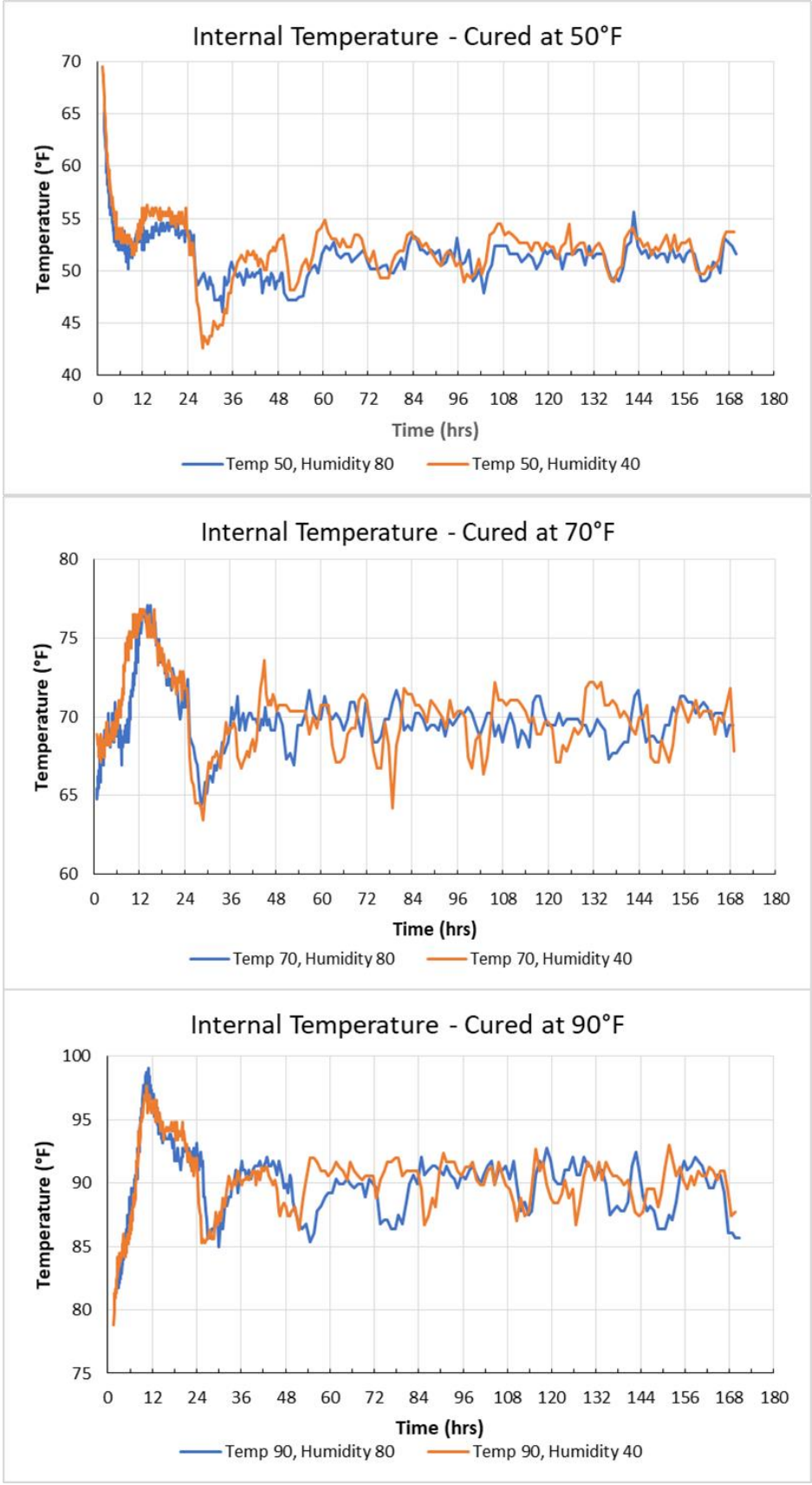

Figure 4.10 Internal Temperature Comparisons

Figure 4.11 depicts the variations in strength and modulus with time for the specimens cured at 50°F. The specimens cured at 40% humidity yield lower compressive strengths for the first seven days as compared to the specimens cured at 80% humidity. However, the increase in modulus with time seems to be almost independent of the humidity. Reviewing the times of initial and final set previously depicted in Figure 4.7, the low humidity curing conditions saw both initial and final set occur nearly an hour earlier than the high humidity curing.

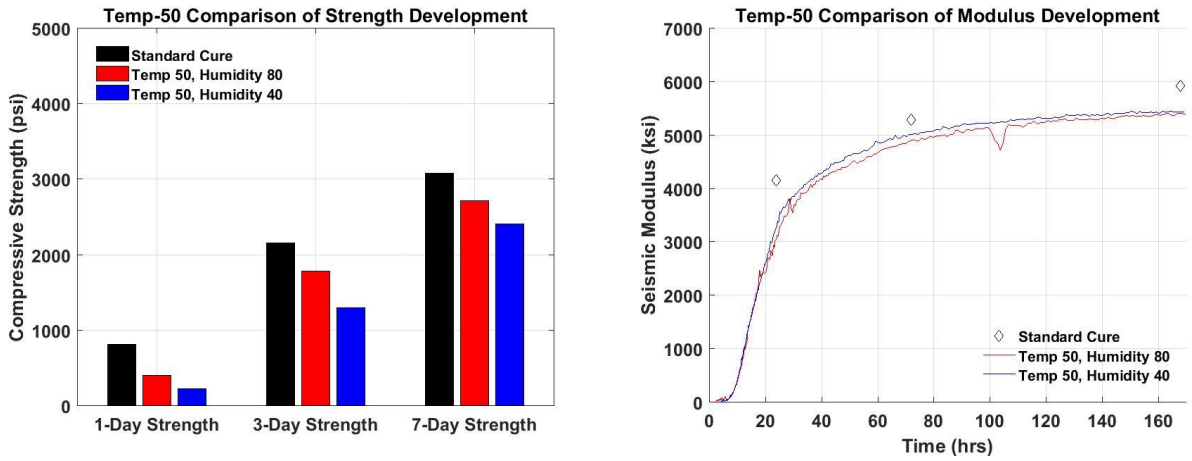

Figure 4.11 Strength and Modulus Development at 50°F Curing

As shown in Figure 4.12, the specimens cured at 70°F at two humidity conditions exhibited similar strengths and moduli for all three testing periods. As shown in Figure 4.7, the initial and final sets across the three humidity conditions were within 60 minutes of one another, with the specimens cured at 40% and 80% humidity exhibiting sets that are 15 minutes of each other.

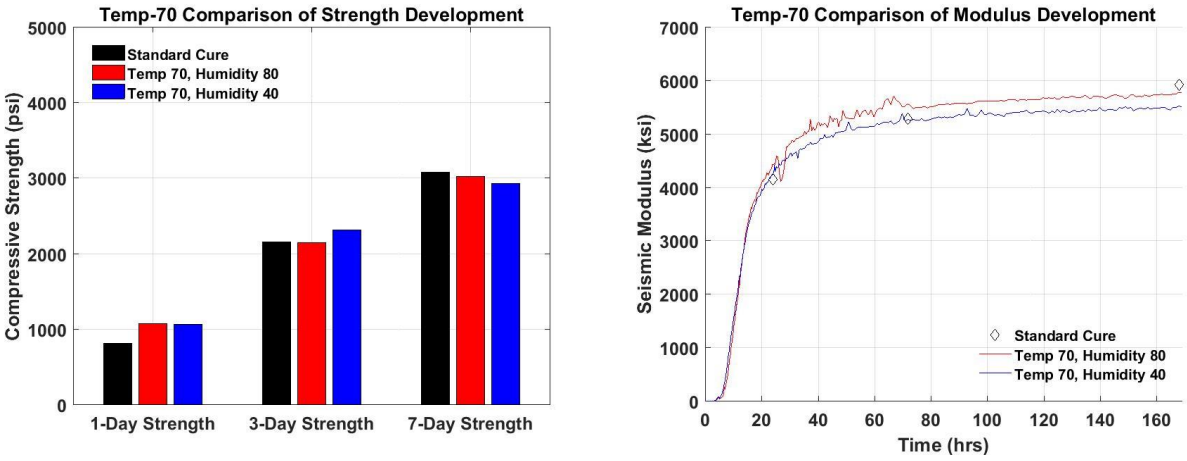

Figure 4.12 Strength and Modulus Development at 70°F Curing

The humidity had little impact on the sets, strength and modulus gains when the specimens were cured at high temperature (90˚F). As shown in Figure 4.7, the times of set were within 20 minutes of one another. As shown in Figure 4.13, the humidity had also minimal effect on modulus development and marginal effect on strength development. One significant findings is the significant gain in strength and modulus for the specimens cured at 90˚F relative to those cured under standard curing conditions of 70˚F and 100% humidity. This trend reverses after 7 days when the strength and modulus of the standard cured specimens are greater than those cured at higher temperature.

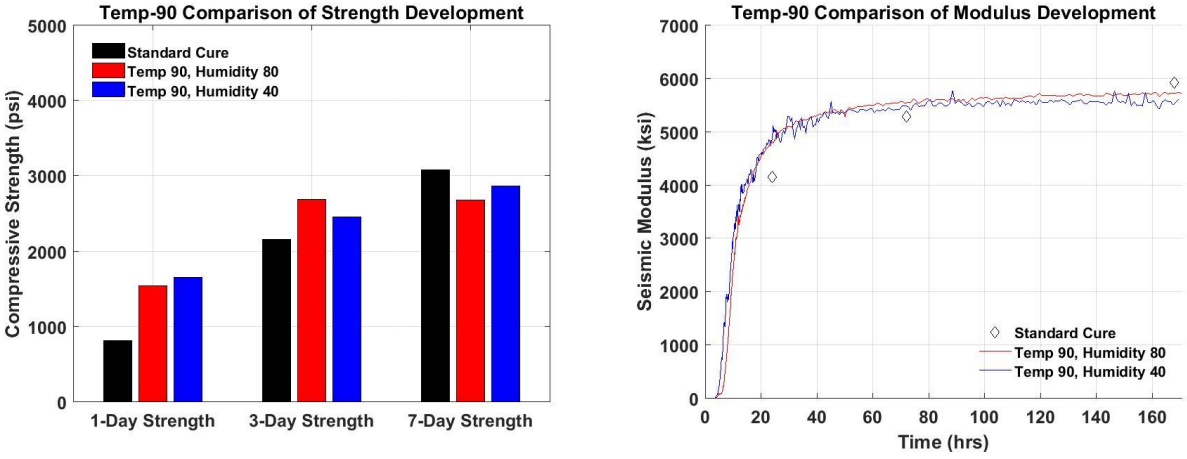

Figure 4.13 Strength and Modulus Development at 90°F Curing

In summary, the one-day strengths for the specimens cured at high humidity at the two higher temperatures were essentially the same or slightly greater than the strengths at the lower humidity. This pattern was not seen at the low temperature scenarios due to the ambient temperature slowing the hydration process. Therefore, the impact of humidity plays a larger role at lower curing temperatures, but still not to the same extent as curing temperature.

4.4.3 Mold Removal

A brief investigation was carried out to observe the impact of the removal of the mold after 24 hours on the properties of the concrete. The variations in the internal temperatures of two specimens (one demolded after 24 hrs and the other maintained in the mold for seven days) from the reference mix and under the same the same curing conditions are shown in Figure 4.14. The temperatures for the first six hours change rapidly in order to reach equilibrium. The temperature patterns from the two specimens are similar between 6 hrs and 24 hrs. At the nominal time of 24 hrs, the demolded specimen experiences a drastic drop of the temperature, despite the fact that the specimen was demolded in the environmental chamber with a nominal temperature of 70°F. This pattern was observed for all the demolded specimens as previously shown in Figure 4.10. However, that pattern is not evident for the specimens contained in the mold. When the mold is removed the entire surface area of the specimen is able to transfer heat and moisture that may result in the cooling of the specimen beyond the ambient temperature.

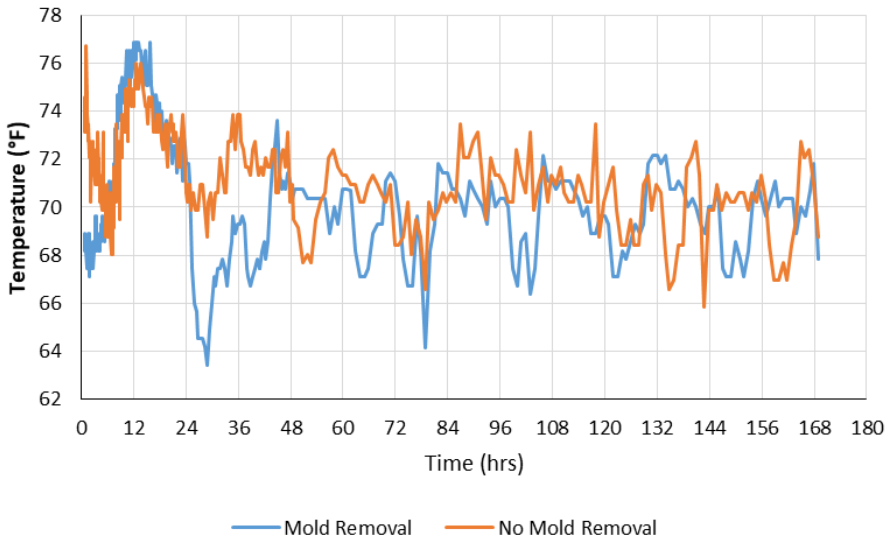

Figure 4.14 Impact of Mold on Internal Temperature of Specimens Cured at 70˚F and 40% Humidity

This loss of heat moisture slows the hydration resulting in lower strength and seismic modulus at seven days. Removal of the mold yielded an average seven-day strength of 2,925 psi while leaving the mold on for the full seven days resulted in an average strength of 3,370 psi. Figure 4.15 depicts the modulus development for both conditions. Modulus development is similar for the first 20 hrs of monitoring, with increases growth observed in the specimens that remained in the mold. Removal of the mold resulted in a seven-day modulus reduction of nearly 650 ksi.

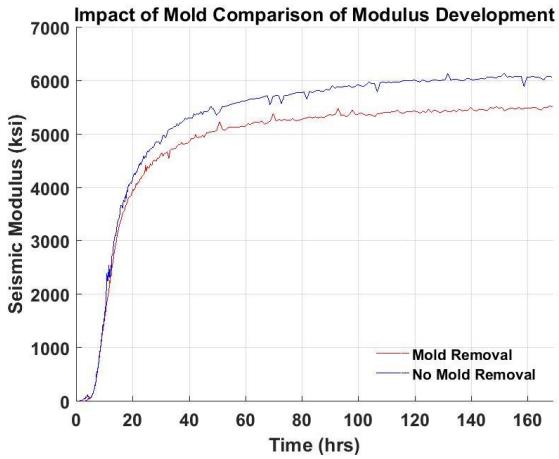

Figure 4.15 Impact of Mold on Modulus Development of Specimens Cured at 70˚F and 40% Humidity

4.5 Mix Related Parameters

The following sections discuss the effects of perturbing the water-cement ratio, accelerating agent, high-range water reducer, air entraining agent, and gradation of the coarse aggregate on the early age characteristics of a mix. Since all mixes were cured at 70°F and 40% humidity, their characteristics were compared to the reference mix that was cured under the same conditions. In addition to the cylinders cured under those environmental conditions, three cylinders from each mix were prepared and cured under the standard curing conditions for comparison purposes.

Appendix A contains detailed information about the variation in internal temperature with time. The trends observed for different mixes are similar to the trends observed for the reference mix cured at 70°F as discussed in the previous section. For that reason no further discussion on that topic is included.

4.5.1 Impact of w/c Ratio

As shown in Figure 4.16, reducing the water-to-cement ratio from the reference value of 0.45 to 0.40 reduced the time of initial set from 7.1 hrs to 6.2 hrs; while the time to final set decreased from 9.0 hrs to 8.1 hrs.

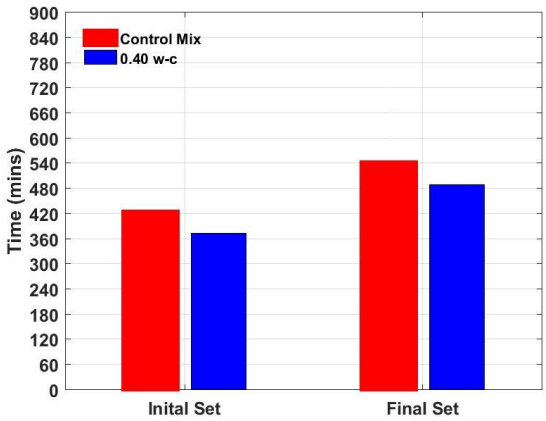

Figure 4.16 Impact of Set Caused by Change in Water-Cement Ratio

The changes in strength and modulus with time caused by reducing the water-cement ratio are depicted in Figure 4.17. As compared to the standard mix, the mix with less water exhibited higher strength for the first three days, and slightly lower strength after seven days. Reduced water yielded an average one-day strength approximately 300 psi greater than the reference mix and an average three-day strength nearly 250 psi greater. However, the modulus of the reference mix was consistently less than the modulus of the mix with less water throughout the seven days of testing.

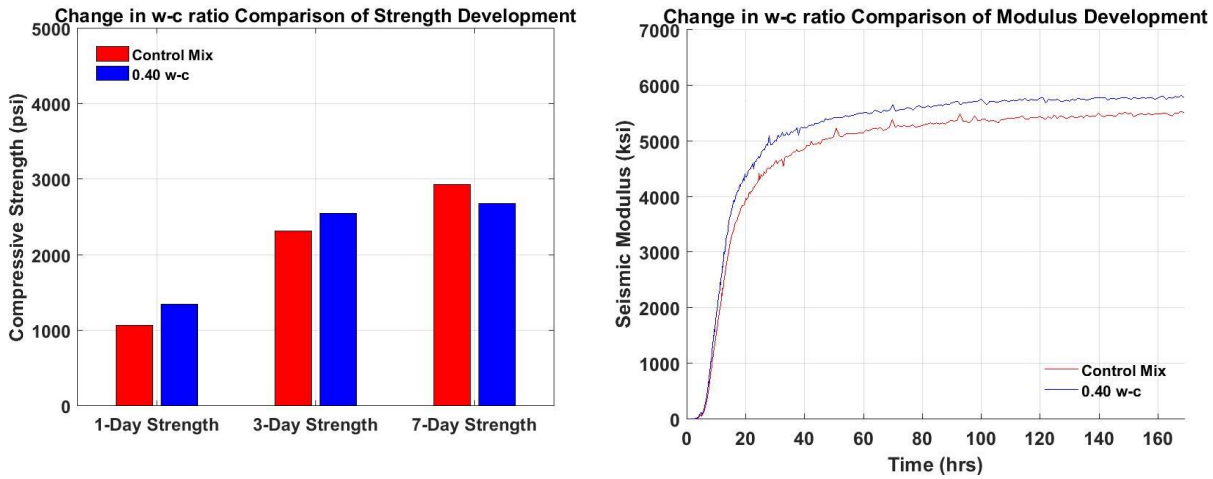

Figure 4.17 Strength and Modulus Development for Change in Water-Cement Ratio

As seen in Figure 4.18, consistent increase in strength and modulus due to decrease in water-to-cement ratio was observed for specimens cured under standard curing. One-day strength was almost 500 psi greater while three- and seven-days specimens were 1,700 psi to 1,800 psi stronger than the reference mix. Similarly, the modulus determined from the FFRC tests on the specimens with lower water-cement ratio was 1,000 ksi greater than those from the standard mix after one and three days and 700 ksi after seven days.

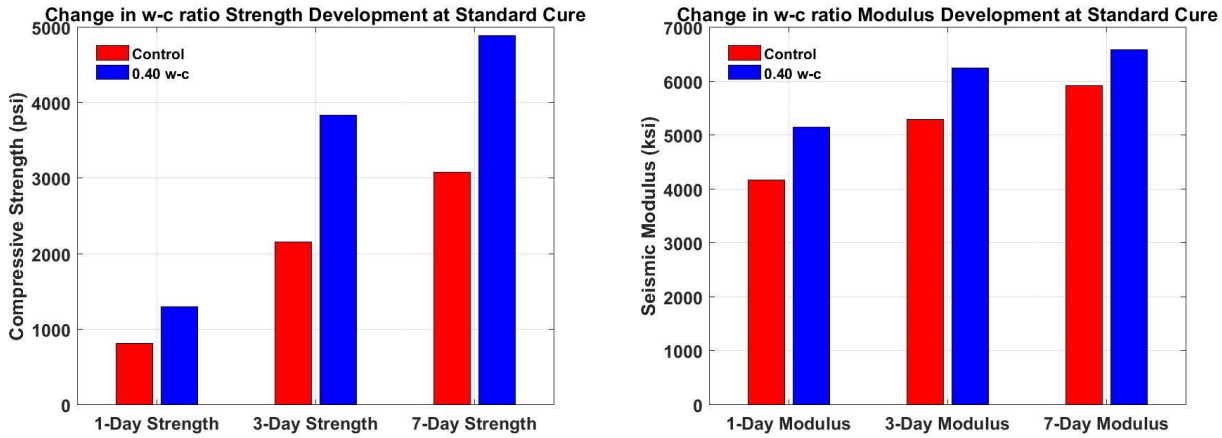

Figure 4.18 Strength and Modulus under Standard Curing with Reduced Water-Cement Ratio

4.5.2 Impact of Accelerating Agent

The impact of an accelerating agent on the early-age behavior of concrete was evaluated with the use of Accelguard ACN 200. The effect of this admixture was studied by preparing and testing specimens near the recommended low dosage (15 fl oz per 100 lbs of cement), and high dosage (45 fl oz per 100 lbs of cement). In addition, another mix with the high dosage of accelerating agent (45 fl oz per 100 lbs of cement) with the reduced water-to-cement ratio of 0.40 was evaluated.

As shown in Figure 4.19, the addition of the accelerating agent resulted in a faster set. However, the amount of accelerating agent used had little impact on the times of set. Using the penetrometer, the initial sets were within six minutes while the final sets were within 30 minutes of one another. Based on these results, the high dosage of accelerating agent in the mix may result in a slightly faster set compared to the low dosage mix.

As shown in Figure 4.20, the strengths and moduli of the mixes with accelerating agent were nearly the same or lower than those of the reference mix at all test periods. The mix with the

high dosage of accelerating agent actually exhibited lower strengths and moduli than the mix with the low dosage of accelerating agent.

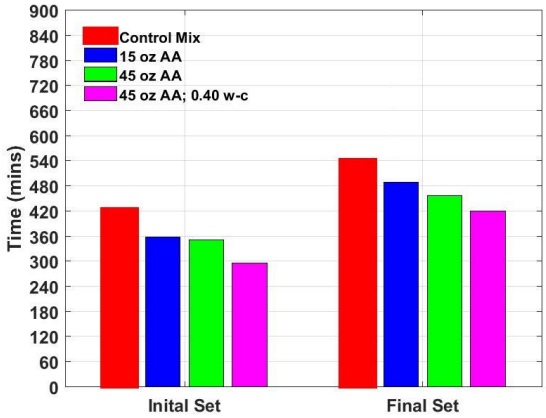

Figure 4.19 Impact of Set Caused by Addition of Accelerating Agent

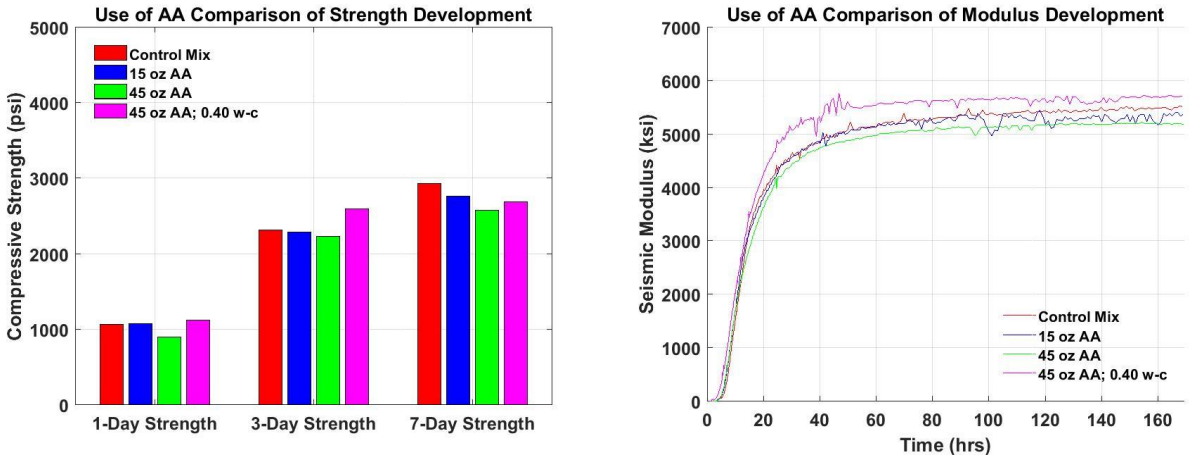

Figure 4.20 Strength and Modulus Development for Addition of Accelerating Agent

The mix with the combination of accelerating agent and lower water-cement ratio further reduced the times to the initial set and final set relative to the mix with just the high dosage of accelerator. That mix exhibited a one hour faster initial set than the mix with the high dose of accelerating agent and two hours faster than the reference mix. The mix with the reduced water-cement ratio also achieved a faster set and higher one- and three-day strengths than just the mix with the high dose of accelerating agent. However, when compared to the mix with the low dose of accelerating agent, the one-day strengths were within 50 psi of each other. The variations in

the modulus with time exhibit the same pattern as strength, i.e., higher moduli throughout the seven-day testing for the mix with the high dose of accelerating agent and reduced water mix.

Figure 4.21 contains the variations of strength and modulus with time for the specimens that were cured under the standard curing conditions. Under standard curing, all three mixes with the accelerating agent achieved higher strengths than the reference mix. Similar to the specimens cured at the humidity of 40% (shown in Figure 4.19), the two mixes with the low and high dose of the accelerating agent exhibited similar strengths. The moduli of the three mixes were essentially the same for all three mixes with the accelerating agent which were typically marginally or significantly greater than the corresponding moduli from the reference mix.

Strengths recorded under standard curing were 500 psi higher than the low humidity curing at one-day and over 1,000 psi greater at seven days. This was observed regardless of mix. Similarly, results were observed for the seismic modulus. This shows the advantage of adding accelerating agent are more apparent under standard curing than at 40% humidity, but regardless of curing conditions, the change in quantity of admixture used yields limited benefit.

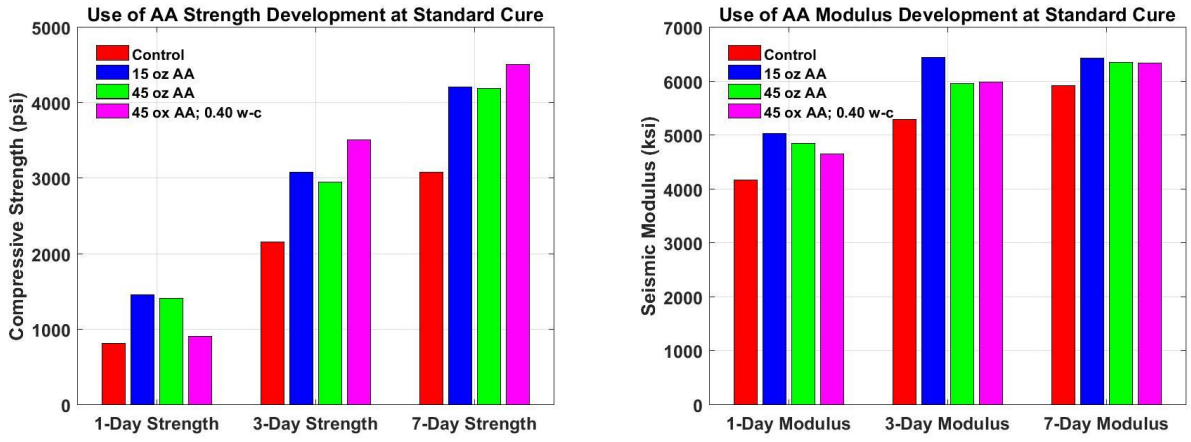

Figure 4.21 Strength and Modulus under Standard Curing with Accelerating Agent

4.5.3 Impact of High Range Water Reducer

A high-range water reducer (HRWR), Eucon SP, was used to evaluate its impact on the early-age characteristics of concrete. Two mixes near the recommended low dosage (10 fl oz per 100 lbs of cement) and high dosage (15 fl oz per 100 lbs of cement) were used for this purpose. Once again, a third mix with the low dosage of HRWR (10 fl oz per 100 lbs of cement) with the water-to-cement ratio with of 0.40 was also evaluated.

For all three mixes the times of set were slower than the reference mix, as depicted in Figure 4.22. The mix with the low dose of HRWR exhibited an initial and final set that was about 2 hrs later than the reference mix and one hr earlier than the mix with the high dose of HRWR. The mix with the low dose of HRWR and reduced water-cement ratio reached initial set about 30 minutes after the reference mix. Considering that the purpose of HRWR is to increase the workability with less water, it makes sense that the sets were slower in the mixes with this admixture than the sets of the reference mix.

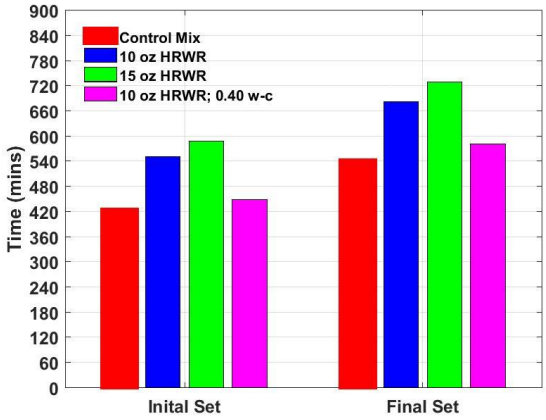

Figure 4.22 Impact of Set Caused by Addition of High-Range Water Reducer

The variations in the strength and modulus with time for the three mixes with HRWR are depicted in Figure 4.23. The mix with the low dose of HRWR achieved greater strength than the mix with high dose of HRWR at each day of testing and was greater than the corresponding

strengths for the reference mix at all but the one-day test. On the other hand, the mix with the high dose of HRWR recorded lower strengths than the reference mix during all three days of testing. This pattern for the most part is evident in the variations in the modulus with time as well. Modulus development began slightly sooner than the mixes with HRWR, but also approached the long-term modulus sooner. The mix with the high dosage of HRWR had a similar long-term modulus but went through a faster initial growth due to the delayed start. A similar initial growth was seen by the low dose mix, but this mix saw a longer growth which resulted in a nearly 500 ksi higher modulus than the high dose mix at seven days.

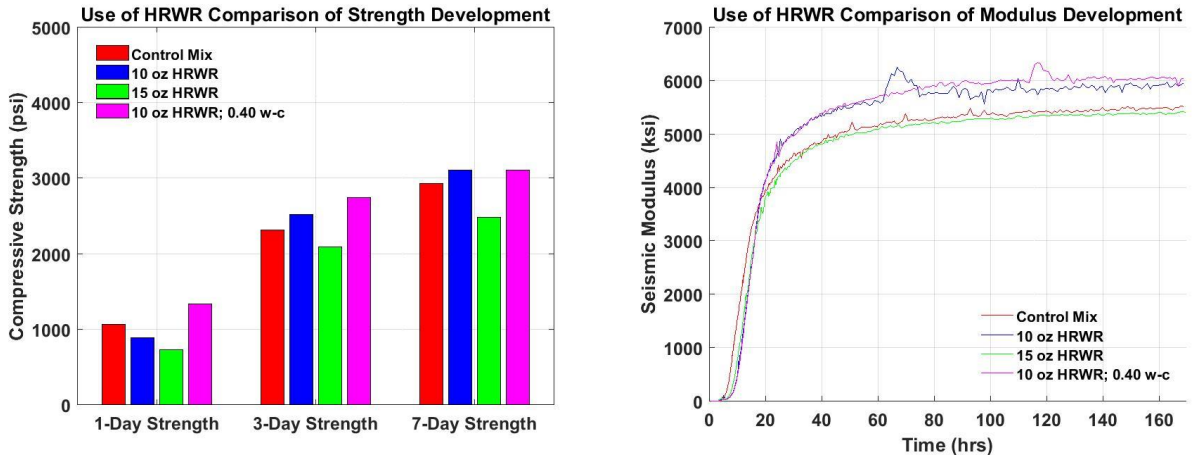

Figure 4.23 Strength and Modulus Development for Addition of HRWR

Comparing the characteristics of the mix with the low dose of HRWR with the mix with the low dose of HRWR and reduced water-cement ratio mix shows the advantage of reducing water as the strengths were consistently higher in the latter mix. The variations in the modulus with time for the first 40 hours are similar until the mix with the reduced water exhibits a slightly higher modulus than the mix with just HRWR.

Similar to the use of the accelerating agent, the mixes containing HRWR cured under standard curing showed greater strengths as seen in Figure 4.24. Under these conditions, the mix with the low dose of HRWR exhibited a similar strength to the standard mix after 1 day and nearly

1,000 psi higher strength at three- and seven-days. The mix with the low dose of HRWR and reduced water experienced a further 1,000 psi strength than the mix with the low dose of HRWR at three and seven-days. The mix with the high dose of HRWR achieved a lower strength than the mix with the low dose of HRWR, but higher strength than the reference mix. The moduli measured after standard curing were more consistent between the mixes with the low and high dose of HRWR. The mix with the low dose of HRWR and reduced water-cement ratio exhibited the highest strengths among the four mixes. The differences in the moduli among the mixes diminishes as the specimens cure longer.

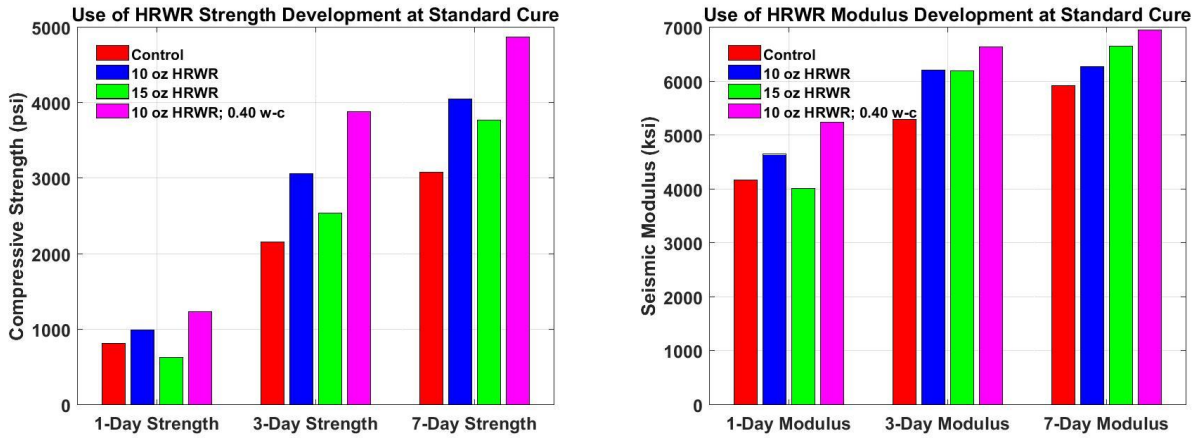

Figure 4.24 Strength and Modulus under Standard Curing with HRWR

4.5.4 Impact of Air Entraining Agent

The impact of an air entraining agent (AEA) on early-age behavior was evaluated using Eucon AEA-92. The impact of the dosage of this admixture was carried out at two levels of the recommended low dosage (0.5 fl oz per 100 lbs of cement) and high dosage (4 fl oz per 100 lbs of cement). Again the effect of the combination of adding a low dosage of AEA (0.5 fl oz per 100 lbs of cement with the reduced water-cement ratio of 0.40 was studied.

Figure 4.25 provides a comparison of times of set among the mixes. The mix with the low dose of AEA achieved times of initial and final set nearly the same as the reference mix while the

mix with the high dose of AEA was close to an hour slower at reaching the set. The initial set of the mix with the low dose of AEA and reduced water was reached about 30 minutes faster than the mix with the low dose of AEA, but final set was closer to that of the mix with the high dose of AEA.

As shown in Figure 4.26, the strengths and moduli for the mixes with the high and low doses of AEA are very different. The mix with the low dose of AEA yielded strengths that were comparable to the strengths from the reference mix after 3 days of low-humidity curing. The variations in the modulus with time are even more similar for these two mixes (especially after 24 hours).

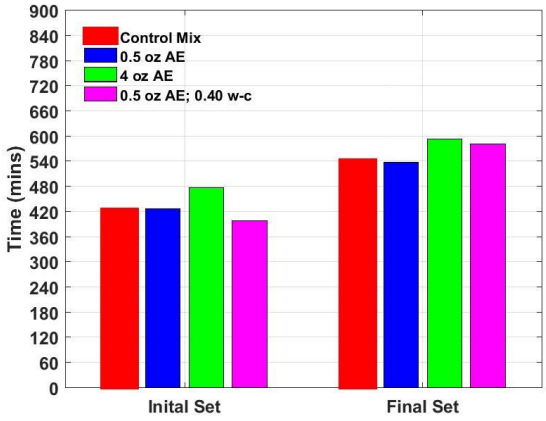

Figure 4.25 Impact of Set Caused by Addition of an Air Entraining Agent

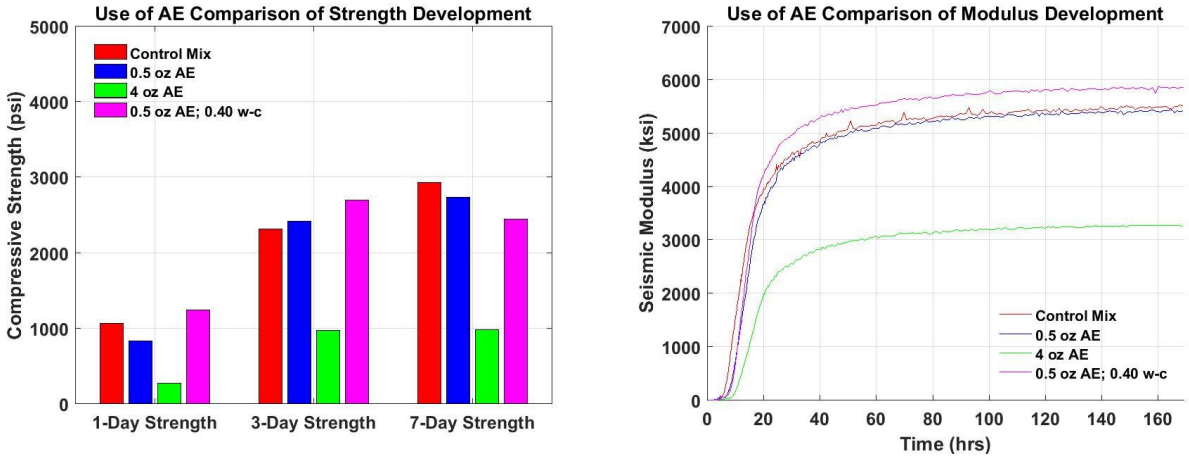

Figure 4.26 Strength and Modulus Development for Addition of Air Entraining Agent

Using the high dosage of air entraining agent had a negative impact on both the strength and modulus of the mix. At that dosage, the strengths of specimens remained less 1,000 psi even after seven days. Similarly, the modulus development for that mix was severely impaired.

Even under standard curing conditions, the mix with the high dose of AEA was negatively impacted with a seven-day strength of about 1,000 psi and modulus of about 4000 ksi. The mix with the low dose of AEA showed a strength advantage under these conditions, with a slightly lower modulus advantage as compared to the reference mix as seen in Figure 4.27.

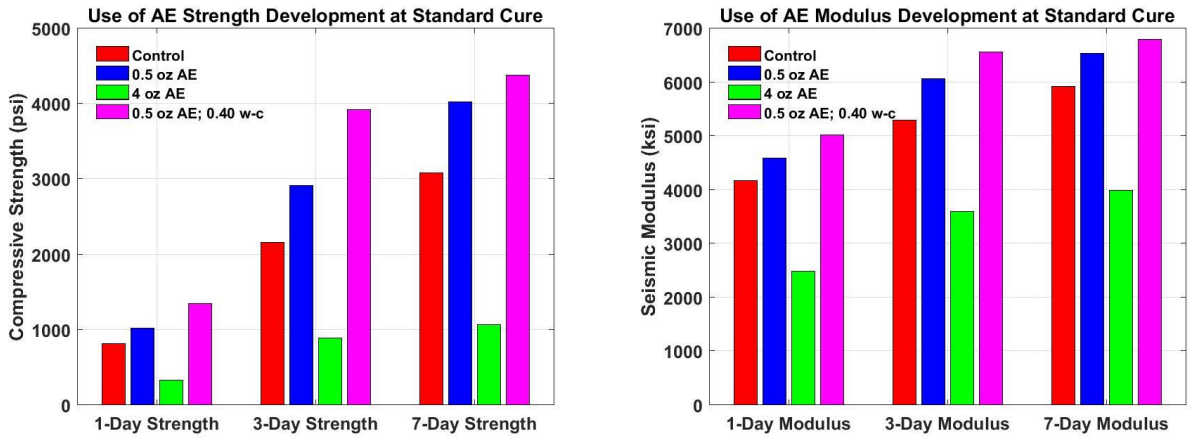

Figure 4.27 Strength and Modulus under Standard Curing with Air Entraining Agent

Similar to the other admixtures used, reducing the water-cement ratio was advantageous. The mix with the high dose of AEA and reduced water-cement ratio yielded higher strengths than both the reference mix and the mix with the low dose of AEA after one-and three-days of curing the specimens at 70°F and 40% humidity, and higher at all three testing days under standard curing. Under the low humidity curing, that mix showed a higher modulus that was greater than the mix with the low dose of AEA after 24 hours of curing. Under standard curing conditions, the mix with the high dose of AEA and reduced water-cement ratio exhibited nearly 1,000 ksi higher modulus than the reference mix.

4.5.5 Impact Coarse Aggregate Size and Gradation

To gain an understanding on the impact of the aggregate gradation, two mixes were tested that used just one coarse aggregate in a 60:40 ratio of coarse to fine aggregate. Figure 3.6 depicted the change in coarse aggregate gradation of the reference mix and the two single coarse aggregate mixes. Using just the largest coarse aggregate, resulted in a mix with the crushed stone being larger than 0.5 in. The intermediate aggregate contained crushed stone that was between 0.5 and 0.05 in.

As shown in Figure 4.28 and as expected, no significant impacts on the times of initial or final set due to changes in coarse aggregates were observed. The reason for this is that the mortar mixes used for checking the set using the penetrometer were similar.

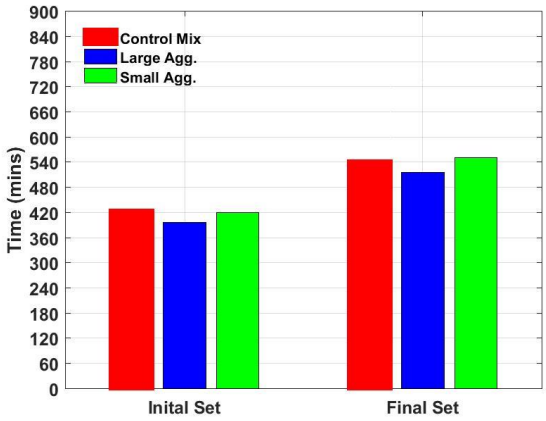

Figure 4.28 Impact of Set Caused by Change in Coarse Aggregate

Despite a minimal impact on the measured sets, the strengths and moduli were significantly impacted as depicted in Figure 4.29 for low humidity curing. The mix with the smaller coarse aggregates generally exhibited a higher strength, while the mix with the coarser large aggregates exhibited a higher modulus. The one-day strengths for specimens were very similar for the three mixes. At three and seven days the reference mix had recorded strengths greater than the large aggregate mix. Modulus development of the three mixes began at approximately the same time,

but the large aggregate mix had a longer period of development resulting an over 500 ksi higher modulus at seven days. Results of higher strengths from the small aggregate is the result of fewer voids remaining, thus allowing greater bonding with the cement and increases interaction amongst aggregates.

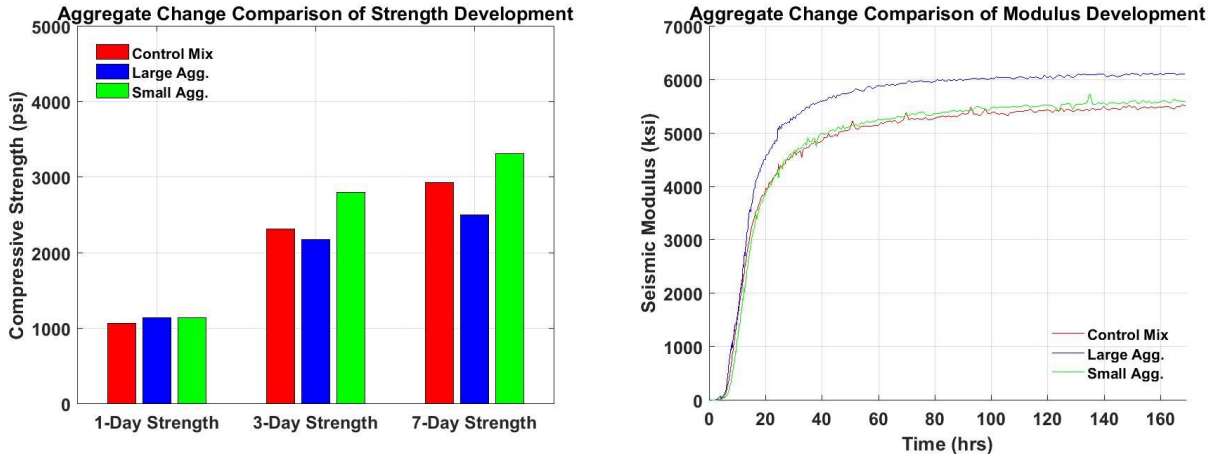

Figure 4.29 Strength and Modulus Development for Change in Coarse Aggregate

When cured under standard curing conditions similar results were observed as seen in Figure 4.30. However, under standard curing the large aggregate mix achieved a higher seven-day strength than both the reference and small aggregate mix. Also observed is the similarity in three-day strengths of the large and small aggregated mixes, which were within 100 psi of each other versus nearly 1,000 psi as seen under low humidity curing. Modulus development occurred in much the same manner as seen at low humidity curing. The large aggregate mix was over 500 ksi higher than the small aggregate mix at all three testing days. One difference in modulus development was that the small aggregate mix showed a slightly higher modulus development than seen at low humidity curing. Lower confidence occurs in these observations since only single cylinders were tested under standard curing.

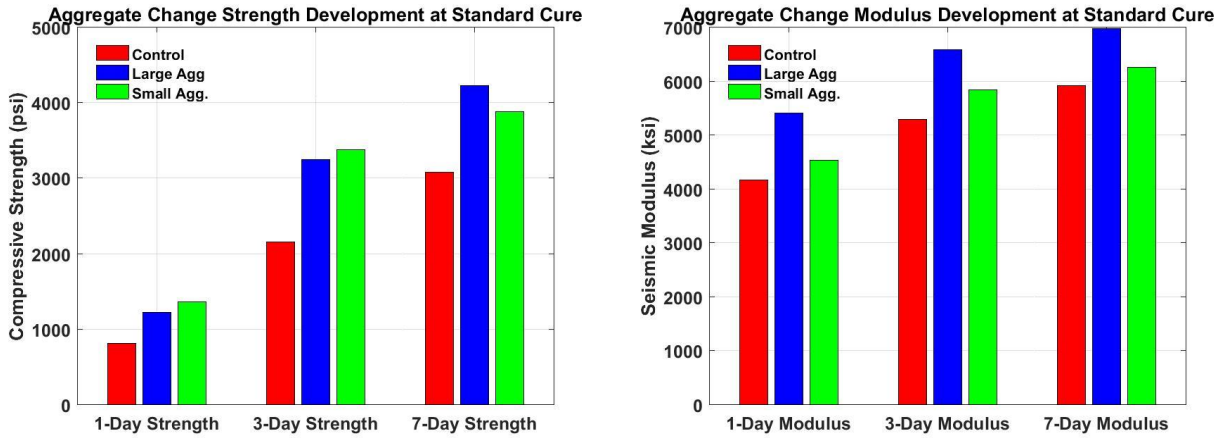

Figure 4.30 Strength and Modulus under Standard Curing with Aggregate Change

4.6 Comments and Conclusions

Use of the testing apparatus yielded reliable modulus readings which were within 11% of the modulus reading obtained using the traditional FFRC method. In addition to this, the modulus-strength relationships for all mixes had similar k-coefficient values. The standard maturity-strength relationship on the other hand, showed m-coefficients within a certain range based on the curing temperature.

Results obtained from the environmental testing confirmed that curing temperature has a larger impact on times of set and one-day strength than humidity. As expected the higher temperatures caused faster times of initial and final set and higher strength. Regardless of curing temperature, the seismic modulus was shown to approach a similar seven-day value with higher temperatures having a faster development. The impact of humidity was most evident in the low temperature curing. At this temperature the penetration resistance showed a greater difference in times of set, with higher humidity taking longer to achieve both initial and final set. Conversely, the lower humidity had strengths consistently lower by several hundred pounds per square inch.

Mix parameter changes showed that a reduction in water-cement ratio was the only consistent parameter that provided benefits in terms of faster sets as well as higher strengths and

moduli. This was seen when the ratio was reduced by itself and when reducing in combination with a chemical admixture. Addition of an accelerating agent only improved the time of set, with little or no benefit to strength or modulus under the low humidity curing regardless of the dosage used. Only at standard curing was there a benefit in three- and seven-day strengths, with the greatest occurring when the low dosage was used. Similarly, the greatest benefit on set, strength, and modulus was achieved when the low dosage of HRWR was added under both the standard curing and low-humidity curing. Addition of an air-entraining agent had essentially no impact on set, strength or modulus when used at low dosage, but a severe negative impact on modulus and strength when used at the recommended high dose. Low dosage of this chemical admixture was beneficial to strength under standard curing, but still greatly detrimental at high dosage. In general, the low quantity of the tested chemical admixtures were more beneficial than the high dosage with the benefits being greater under standard curing.

A change in the aggregate gradation and size showed a greater modulus growth when a larger aggregate was used. A higher strength was seen with the small aggregate at low humidity while similar strengths were seen at standard curing. The small aggregate saw very similar modulus development as the reference mix. Smaller aggregates allowed for increased bonding with the cement paste as well as increased interaction with each other because of smaller voids.

Chapter 5: Developed Methods

5.1 Introduction

This chapter highlights the results of three developed methods used during this research. The first topic discussed deals with set determination with a predictive method based on standard penetration in addition to two methods to define set based on the modulus development. The second method discussed is a detailed look at an alternative maturity method which provides a unique trend for each mix. Lastly, the thermal profiles created by using a thermal camera are discussed.

5.2 Set Determination

The primary approach to determine times of set of concrete is based on standard penetration resistance method as explained in ASTM C403. Although that method has served the engineering community well, it has some drawbacks. For example, that method determines the set based on using only the mortar mix rather than the actual concrete mix. Aside from being tedious and time consuming, the impact of coarse aggregates on the workability of concrete is neglected. An alternative method for the determination of times of set more objectively was described in Chapter 3. The method is based on the continuous monitoring of the modulus of a specimen from the time of pouring up to 3 days. The proposed methodology is evaluated in this chapter.

5.2.1 Prediction from Penetration Resistance

Determination of set using the penetration resistance method occurred on every mix. Since this method requires a mortar mix, all six environmental test as well as the large and small aggregate mixes utilized the same mortar mix. Figure 5.1 depicts the times of initial and final set of the reference mix checked three times, large aggregate mix, and small aggregate mix cured at 70°F and 40% humidity. The initial sets for all five tests were within one hour while the final sets

were within 75 minutes of each other. The variability in the sets demonstrates the uncertainty associated with using the penetration method since all mortar mixes were essentially the same.

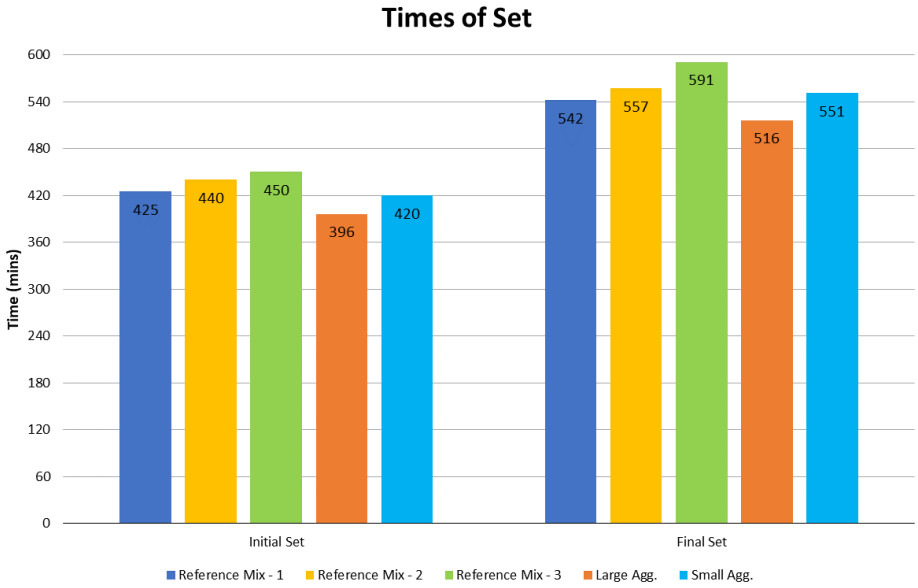

Figure 5.1 Ranges of Sets based on Penetration Resistance on Similar Mortar Mix

Referring back to Figure 4.7, which depicted the times of set of the six environmental test as well as standard curing, a nearly proportional change was noticed based on changes in temperature and humidity. Using the 70°F curing as the reference, it took about 50% longer for the specimens cured in 50°F temperature to reach their initial and final sets, while it took around 25% less for the specimens in 90°F temperature to achieve these sets. Similarly, slight reduction of times of set were noticed as the humidity decreased being cured at the standard 70°F temperature. These observations led to the parameters indicated in Table 5.1. These parameters can be multiplied by the initial or final set measured at standard curing condition of 70°F and100% humidity to predict the set under other curing conditions as seen in equation 5.1.

$$set_{exp} = set_{SC} * t * h \qquad \text{EQN 5.1}$$

where set_{SC} is the penetration resistance determined time of either initial or final set and set_{exp}.is the time of set under the expected curing temperature and humidity. Parameter t, is the value used

based on the expected curing temperature while parameter h is used to adjust for the expected humidity conditions.

Table 5.1 Penetration Resistance Adjustment Factors to Predict Set

Temperature (°F)	Parameter *t*		Humidity	Parameter *h*
90	0.75		100%	1
70	1		80%	0.98
50	1.5		40%	0.94

Figures 5.2 provides a comparison of the predicted and measured initial sets while Figure 5.3 compares the final sets. Overall this approach resulted in predicted sets within 4% of the measured for both environmental changes and mix changes. The greatest differences occurred at 50°F curing followed by mixes with high-range water reducer added. The use of accelerating agent decreased the times of set while the high-range water reducer increased the set to times closer to that of the low temperature curing test. The use of an air entraining agent also increased the time of set from the reference mix, but to a lesser degree. Regardless of the type of chemical admixture added, a reduction in the water-cement ratio generally reduced the times of set as compared to the same mix with the higher water content.

Although this predictive approach looks promising a few shortfalls are still present. Aside from neglecting the impact of the coarse aggregates and the level of uncertainty of the measurements, these factors were only verified at curing conditions of 70°F and 40% humidity.

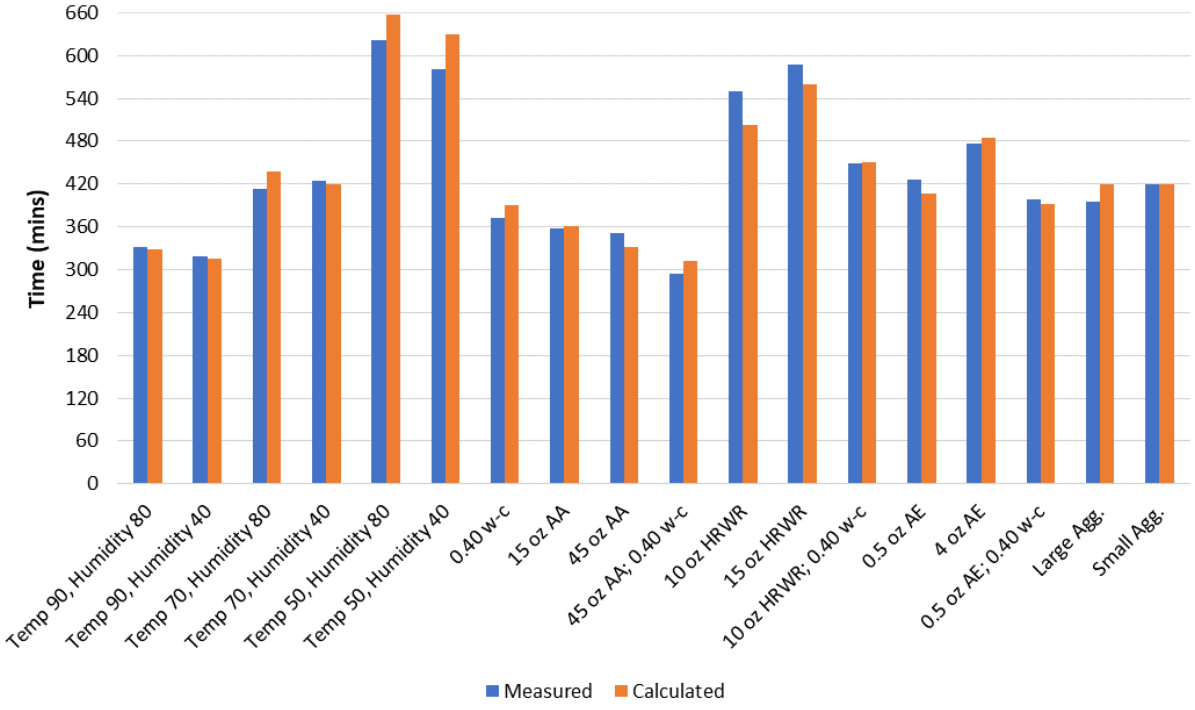

Figure 5.2 Comparison of Penetration Resistance Predicted Initial Set

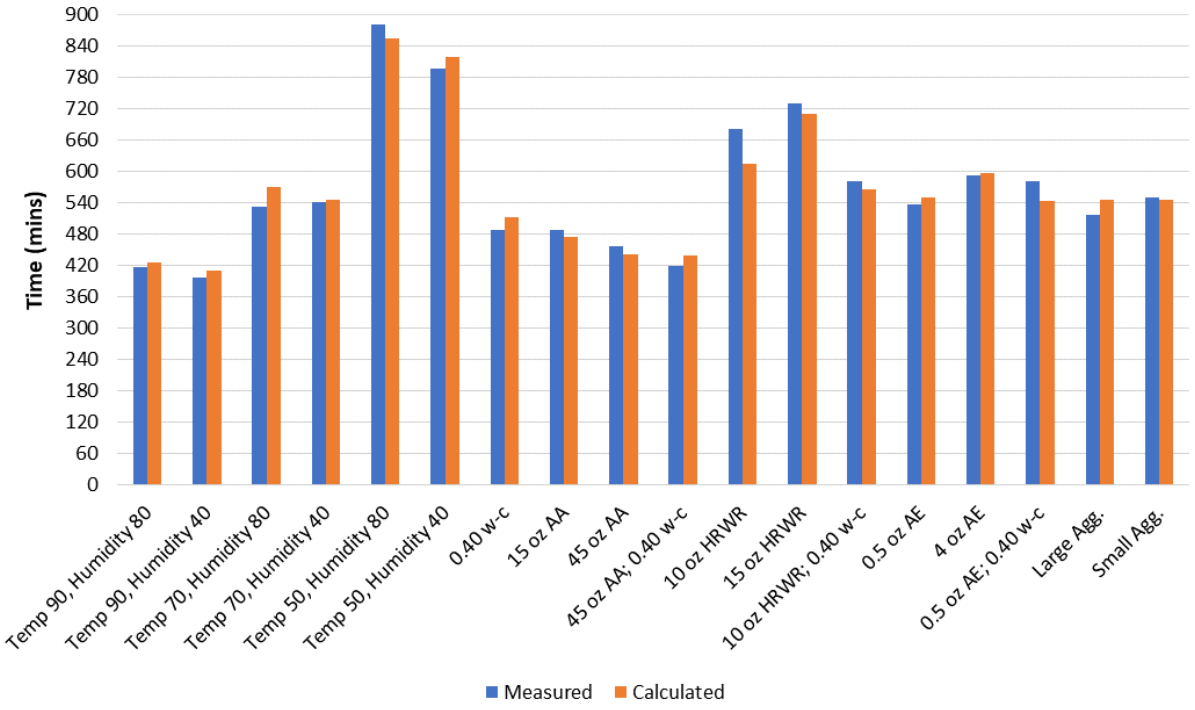

Figure 5.3 Comparison of Penetration Resistance Predicted Final Set

Figure 5.4 shows the calculated strengths of the reference mix cured at 70°F and 40% humidity using both the modulus-strength relationship and standard maturity-strength relationship over time as discussed in Chapter 4. The times of initial and final sets based on penetration resistance are also marked in the figure. The strength calculated from the modulus strength-relationship just begins a period of rapid growth around the final set, while the strength calculated from the standard maturity-strength relationship just begins to have a calculated strength greater than zero at final set. This period of rapid growth using the modulus-strength relationship occurred at or after final set for every mix, while a positive strength at the same time using the standard maturity-strength relationship was observed in over half of the mixes tested. The mixes that did not follow that trend included the mixes subjected to the high temperature curing, three of the four mixes with reduced water-cement ratio, and the mix that used just the large aggregate. Based on these results, the definition of the final set being the point that the concrete can sustain a load is questionable as the calculated strengths from both relationships are under 90 psi at the final set as determined from the penetration resistance.

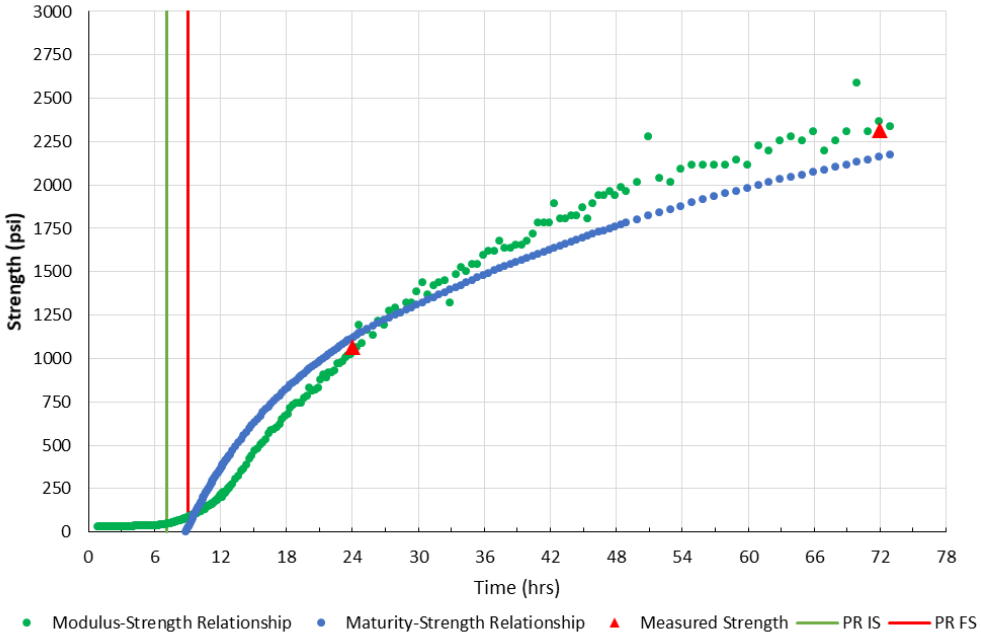

Figure 5.4 Calculated Strength Compared to Penetration Determined Set

5.2.2 Modulus Approach

The process of estimating the times of initial and final set based on the modulus vs. time curve that was discussed in Section 3.6.1 were found for each mix. The modulus curve can be broken into three segments corresponding to the dormant, setting, and hardening of the specimen.

Table 5.2 provides the coefficients of equation 3.1 used to model the recorded data for each mix. The corresponding R^2 value is also listed to show the level of confidence in the modeled equation.

Table 5.2 Coefficients and R^2 Values from Modulus over Time Equation

Mix	*a*	*b*	R^2
Temp 50 Humidity 40	8.54	257.41	1.00
Temp 50 Humidity 80	8.48	228.64	1.00
Temp 70 Humidity 40	8.58	123.51	1.00
Temp 70 Humidity 80	8.64	139.09	1.00
Temp 90 Humidity 40	8.61	65.07	1.00
Temp 90 Humidity 80	8.64	87.82	0.99
0.40 w-c	8.65	109.77	1.00
15 oz. AA	8.56	111.27	1.00
45 oz. AA	8.52	113.11	1.00
45 oz. AA; 0.40 w-c	8.63	93.37	0.99
10 oz. HRWR	8.73	197.59	0.99
15 oz. HRWR	8.60	173.03	1.00
10 oz. HRWR; 0.40 w-c	8.73	199.21	0.99
0.5 oz. AE	8.60	177.97	1.00
4 oz. AE	8.11	239.71	1.00
0.5 oz. AE; 0.40 w-c	8.70	173.56	0.99
Large Agg.	8.71	121.85	1.00
Small Agg.	8.61	150.68	1.00

Looking at all of the *a*- and *b*-coefficients shown above, little variation in parameter *a*, which corresponds to the long-term modulus of the mixes was observed. Parameter *a* was replaced by the average value of 8.6 as shown in Eq. 5.1

$$modulus = e^{\left(8.6-\left(\frac{b}{(time)^2}\right)\right)} \qquad \text{EQN 5.2}$$

In this case, parameter *b* controls the rate of change of modulus due to changes in the environmental and mix parameters. The resulting parameter *b* for the same mix subjected to different curing conditions are listed in Table 5.3. As the curing temperature increases parameter *b* decreases, translating to the shorter time to reach the long-term modulus. The impact of temperature was minimal relative to the temperature and as such not included in the table.

Table 5.3 Primary *b*-Coefficients for Modulus Approach

Temperature (°F)	*b*-Coefficient
50	243
70	131
90	76

Table 5.4 contains relative changes in parameter *b* due to changes in the mix parameters, where the relative change is defined as the parameter *b* for a given mix divided by coefficient *b* from the standard mix. Since a number less than unity indicates a faster gain in modulus, reducing water-cement ratio, adding accelerating agent will result in a faster set. On the other hand, adding HRWR or air entraining agent retards the set.

Table 5.4 Parameter *b* and Relative Change due to Mix Changes for Modulus Approach

Mix change	Parameter *b*	Relative Change
Control Mix at 70°F	131	1.00
Reduce w-c ratio from 0.45 to 0.40	110.04	0.84
Add low dosage Accelerating Agent	111.35	0.85
Add high dosage Accelerating Agent	112.66	0.86
Add accelerating agent and reduce w-c ratio	93.01	0.71
Add low dosage of HRWR	197.81	1.51
Add high dosage of HRWR	172.92	1.32
Add low dosage of HRWR and reduce w-c ratio	199.12	1.52
Add low dosage of air entraining agent	176.85	1.35
Add high dosage of air entraining agent	239.73	1.83
Add low dosage of air entrain agent and reduce w-c ratio	172.92	1.32
Use large aggregate	121.83	0.93
Use small aggregate	150.65	1.15

5.2.3 Hybrid Maturity-Modulus Approach

Using the equation discussed in section 3.6.2 and a similar methodology as the time-based modulus approach, sets were determined using the standard maturity-based modulus. However, this approach provided points of initial and final set as the standard time-temperature factor. By reviewing the collected raw data for these points the approximate time of sets could be determined.

Table 5.5 contains the three coefficients needed to model the recorded data using equation 3.2 based on environmental and mix changes. The associated R^2 for mix is also include to show the level of confidence in modeling the recorded data.

Table 5.5 Coefficients and R^2 Values from Modulus over Standard Maturity Equation

Mix	*c*	*d*	*f*	R^2
Temp 50 Humidity 40	5002.39	421.97	3.12	1.00
Temp 50 Humidity 80	4856.59	391.74	2.86	1.00
Temp 70 Humidity 40	5135.38	492.11	2.76	1.00
Temp 70 Humidity 80	5365.61	500.87	2.94	0.99
Temp 90 Humidity 40	5330.41	450.89	2.39	0.99
Temp 90 Humidity 80	5377.71	491.42	2.60	1.00
0.40 w-c	5425.56	450.17	2.84	1.00
15 oz. AA	5134.93	473.59	2.54	1.00
45 oz. AA	5091.94	529.98	2.43	1.00
45 oz. AA; 0.40 w-c	5769.15	449.13	2.14	1.00
10 oz. HRWR	5608.22	565.80	3.83	1.00
15 oz. HRWR	5023.15	521.43	3.31	1.00
10 oz. HRWR; 0.40 w-c	5565.65	538.66	3.82	1.00
0.5 oz. AE	5047.52	563.17	3.29	1.00
4 oz. AE	3012.00	641.07	3.75	1.00
0.5 oz. AE; 0.40 w-c	5425.13	503.52	3.63	1.00
Large Agg.	5867.83	474.28	2.76	1.00
Small Agg.	5188.18	524.38	3.06	1.00

Using the standard maturity-based modulus approach as a predictive model to determine set required a similar approach as the time-based method. The original equation used to model the recorded data had three unique coefficients for each mix. However, the *f* coefficient turned out to be within a narrow range of values enabling its replacement with a constant of 3.1, providing the new equation;

$$modulus = \frac{c}{1+\left(d/_{TTF}\right)^{3.1}} \qquad \text{EQN 5.3}$$

Like above, the primary *c*- and *d*-coefficients were based on curing temperature and are shown in Table 5.6. As temperature increased the value of each coefficient increased, but not in proportional increments. Larger increases occurred from 50°F to 70°F than from 70°F to 90°F. A unique

adjustment factor was needed for each coefficient to obtain values similar to the recorded coefficients. This factors were not consistently increasing or decreasing the values of the primary coefficients as can be seen in Table 5.7.

Table 5.6 Primary *c*- and *d*-Coefficients for Hybrid Maturity-Modulus Approach

Temperature (°F)	*c*-Coefficient	*d*-Coefficient
50	4930	405
70	5250	495
90	5350	500

Table 5.7 contains relative changes in both the *c* and *d* parameters due to changes in the mix parameters with the relative change defined in the same manner as the modulus approach. A relative change of the *c* parameter indicates a higher modulus. This is verified when reviewing results from the previous chapter where it was observed that every mix that had a lower water-cement ratio had a higher modulus. Though not as definitive as the modulus approach, a relative change in *d* parameter less than unity generally indicates a faster gain in modulus and therefore a faster set. Reducing water-cement ratio, adding accelerating agent, and the large aggregate mix showed faster initial sets in this scenario. However, final set of these same mixes was not always faster. The reason for less definitive conclusions concerning the unity of the *d* parameter is the result of reducing the two coefficients affecting the modulus growth to a constant and a parameter.

Table 5.7 Parameters and Relative Change due to Mix Changes for Hybrid Maturity-Modulus Approach

Mix change	Parameter *c*	Relative Change	Parameter *d*	Relative Change
Control Mix at 70°F	5250	1.00	495	1.00
Reduce w-c ratio from 0.45 to 0.40	5407.5	1.03	450.45	0.91
Add low dosage Accelerating Agent	5145.0	0.98	475.20	0.96
Add high dosage Accelerating Agent	5092.5	0.97	534.6	1.08
Add accelerating agent and reduce w-c ratio	5775.0	1.1	450.45	0.91
Add low dosage of HRWR	5617.5	1.07	564.30	1.14
Add high dosage of HRWR	5040.0	0.96	5193.75	1.05
Add low dosage of HRWR and reduce w-c ratio	5565.0	1.06	539.55	1.09
Add low dosage of air entraining agent	5040.0	0.96	564.30	1.14
Add high dosage of air entraining agent	2992.5	0.57	643.50	1.3
Add low dosage of air entrain agent and reduce w-c ratio	5407.5	1.03	504.90	1.02
Use large aggregate	5880.0	1.12	475.20	0.96
Use small aggregate	5197.5	0.99	527.70	1.06

By defining the hybrid maturity-modulus sets as time instead of standard TTF a comparison can be made with the modulus method.

5.2.4 Comparison of Approaches

The times of initial set found from the standard method, time-based method, and hybrid method are compared in Figure 5.8 for environmental changes and Figure 5.9 for mix changes. The variance was generally within 3 hours depending on the method and mix being tested. Low temperature testing, mixes with high-range water reducer, and the high quantity of air entraining agent showed the greatest variance. A large variance in the mix with the high dose of air entraining agent was expected because of the significantly lower modulus achieved. Comparing just the modulus defined approaches showed even greater similarity with the time-based approach indicating a slower initial set. The standard maturity method generally indicated quicker times of initial set while the penetration resistance method was the slowest. Mixes with air entraining agent

added and the mix with HRWR and a reduced water-cement ratio where the only mixes that the standard method indicated a faster initial set than both modulus-based methods.

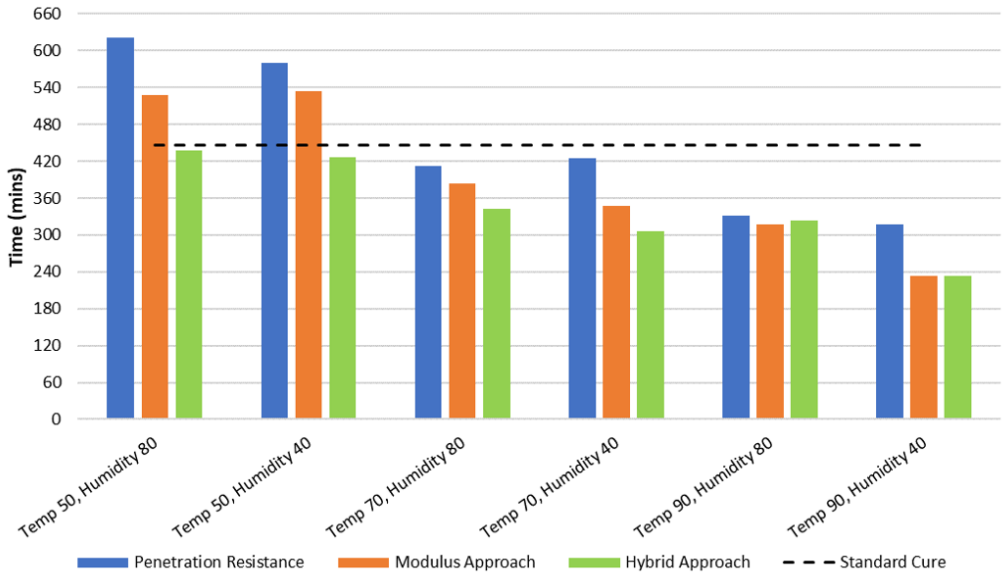

Figure 5.8 Comparison of Initial Set across Environmental Changes

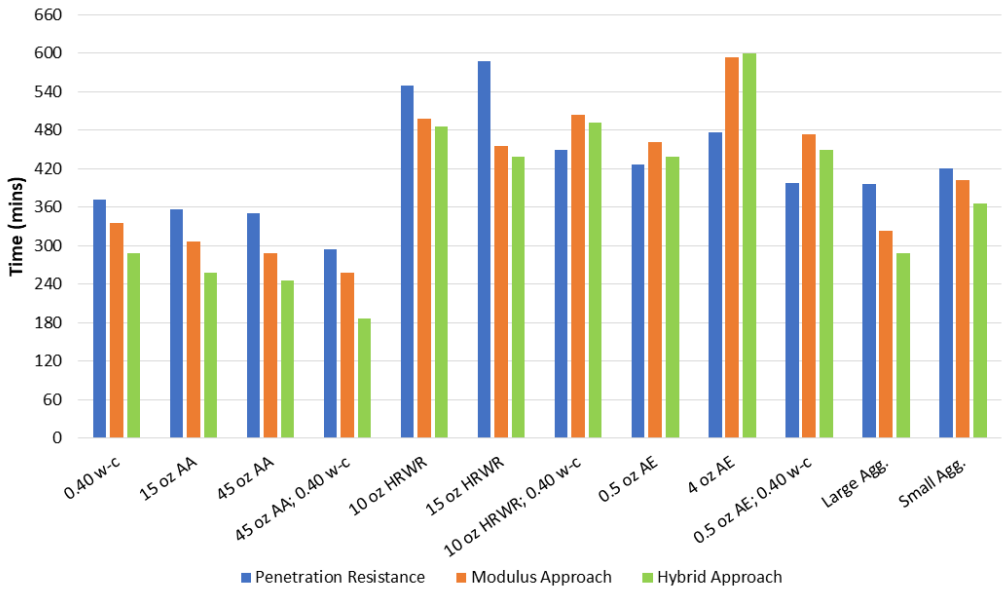

Figure 5.9 Comparison of Initial Set across Mix Changes

Comparison of final set across the three methods are shown in Figure 5.10 across environmental changes while Figure 5.11 depicts comparisons across mix changes. Final set

between the two modulus defined methods, though significantly different from the standard method yielded times within two-hours of each other except for the low temperature testing for the recorded data. The penetration resistance method times of final set generally occurred in half the time as the two modulus-based methods. The modulus method showed final set was attained faster than the hybrid method for every mix except those cured at 90°F. The similarity in the determined initial set as well as final set using the two modulus-based methods provides further evidence that defining set based on the modulus of concrete is a feasible non-destructive method.

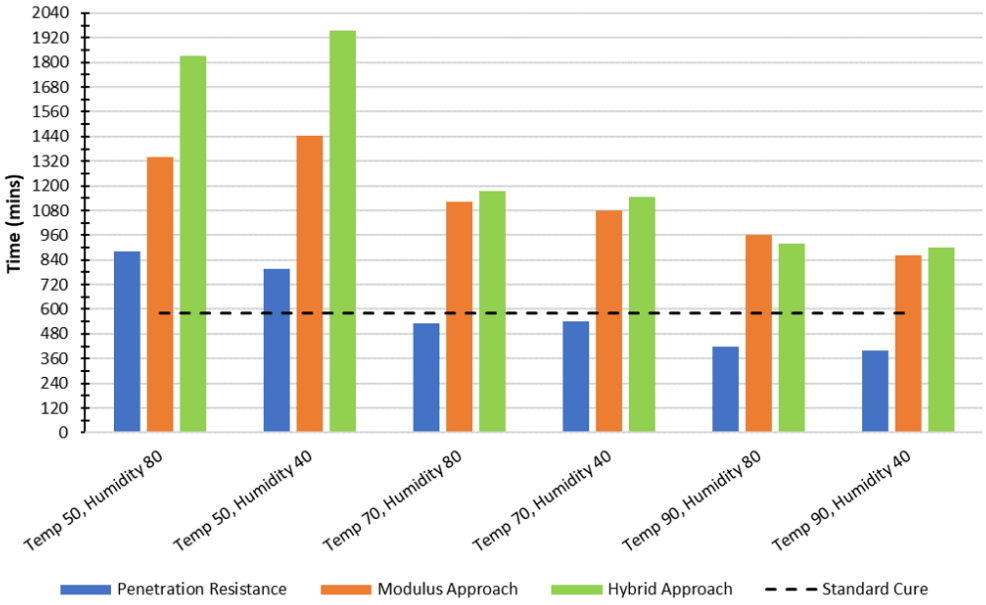

Figure 5.10 Comparison of Final Set across Environmental Changes

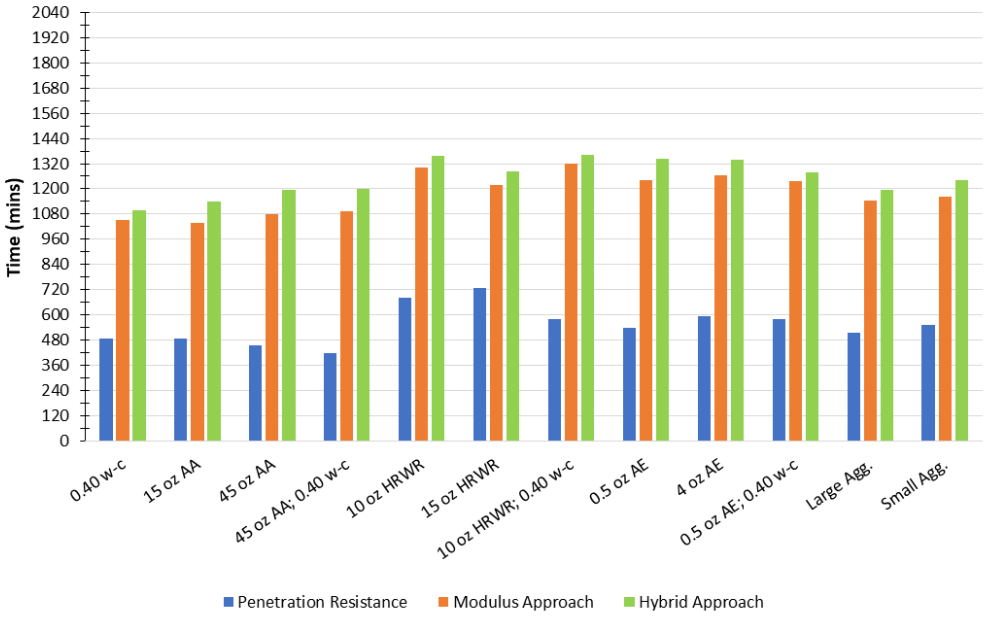

Figure 5.11 Comparison of Final Set across Mix Changes

The extrapolated strengths at time of final set using the modulus and hybrid method are shown in Figure 5.12. Strengths calculated from the recorded data, using the modulus-strength and standard maturity-strength relationships are shown like in Figure 5.4 above. In this figure, both methods show calculated strengths closer to 750 psi, compared to less than 100 psi seen in Figure 5.4, which is a more reasonable strength for final set as per definition. Because of the much greater strengths calculated at final set using these methods, there is a need to redefine final set.

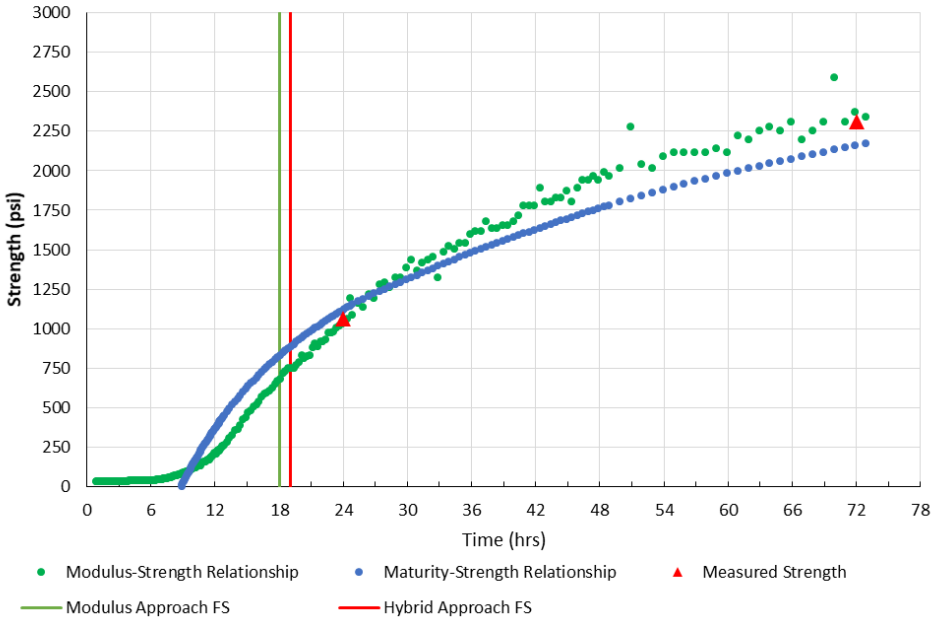

Figure 5.12 Calculated Strength Compared to Modulus Determined Set

This supports the need to define initial set as the point of rapid modulus development corresponding to stiffening of the cement paste and loss of workability. Whereas the definition of final set could be, the point of cessation of modulus growth caused by culmination of primary hydration.

5.3 Alternative Maturity

The concept of alternative maturity was introduced in Section 3.3.2. In that concept, the arbitrary datum of 32°F was replaced with the instantaneous ambient temperature. Appendix B contains the alternative maturity time histories for all eighteen mixes tested. Typical alternative maturity curves for the same mix cured at three different temperatures are shown in Figure 5.13. An alternative TTF curve with a positive slope indicates that the specimen is warmer than the ambient temperature while a negative slope indicates the opposite. Beyond an age of 60 hrs, a linear trend is observed partially due to perhaps systematic differences in temperature of the middle of the specimen relative to the ambient temperature. Also, every mix exhibits a sharp drop in the

alternative maturity after the peak at around 24 hours that was attributed to the removal of the mold and rapid evaporation of the moisture trapped by the mold (see Section 4.4.3).

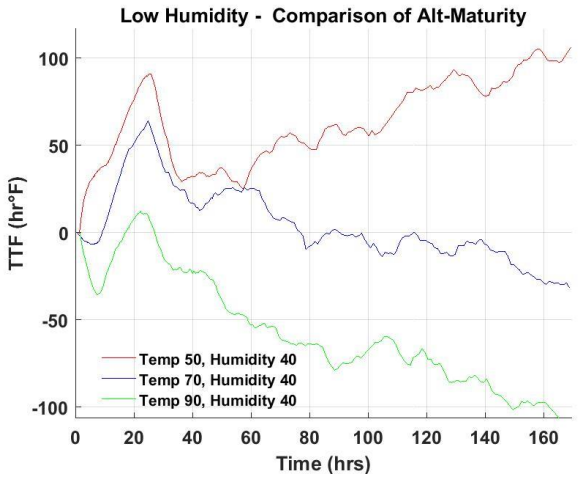

Figure 5.13 Typical Variations of Alternative TTF with Temperature

As indicated in Chapter 3, the patterns observed in the figure are impacted by two phenomena of the generation of heat of hydration and the heat transfer between the specimen and the environment. The specimen cured at 70°F in Figure 5.13 exhibits a small dip for the first 10 hrs primarily due to heat transfer. As observed in Figure 5.12, the specimen does not gain any stiffness at all. The rapid rise in alternative TTF between 10 to 24 hrs is primarily due to the generation of heat of hydration since during this time period the specimen gains significant stiffness (see Figure 5.12). The significant decrease in the alternative TTF starting from 24 hrs, which coincides with the time the mold was removed, and perhaps up to 40 hrs is on one hand due to the cooling affect associated with the removal of the mold and on the other hand due to the generation of the heat of hydration to facilitate further gain in stiffness. Past 60 hrs, the alternative TTF is more or less constant for that specimen indicating significant deceleration in gain in stiffness. Some of the fluctuations in the results can be attributed to the accumulation of residual errors due to the prolonged integration of the area between the specimen and ambient temperatures.

To expand the discussion to the temperatures significantly warmer or cooler than 70°F, the alternative TTF curves from these two temperatures are expanded up to a time of 60 hours in Figure 5.14. The corresponding times of initial and final sets as determined using the modulus approach are also included in the figure. For the specimen cured in a higher ambient temperature, the time of initial set is about 3 hrs before the minima of the alternative TTF curve while the final set is roughly half way to the maxima of the alternative TTF curve. The initial set for the specimen cured at a cooler ambient temperature occurs around the transition point of the alternative TTF curve. This trend also shows the final set occurring closer to the maximum peak. Since by definition, the modulus-based initial set corresponds to the time when the specimen starts to transition from liquid to solid, the arrows associated with the initial sets may point to the time when the generation of the heat of hydration becomes significant. Before the modulus-based initial set, the alternative TTF is primarily dominated by the heat transfer between the specimen and ambient temperatures.

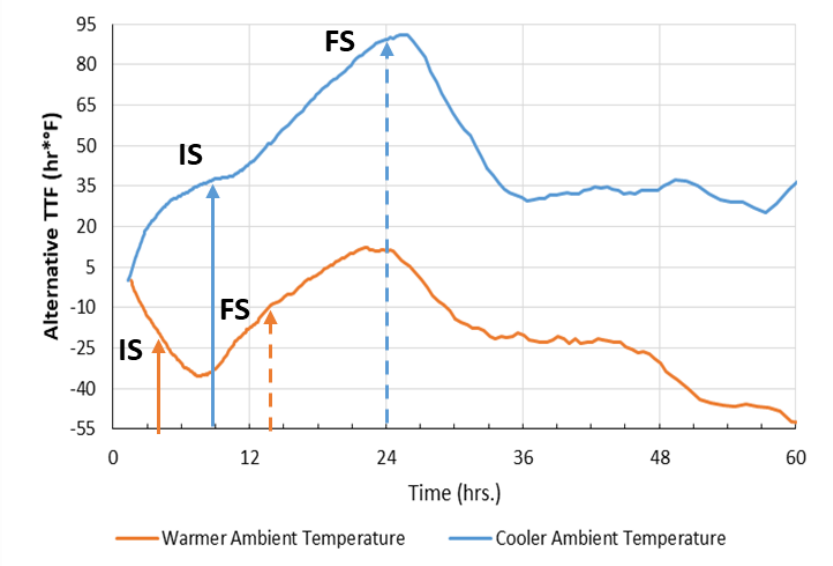

Figure 5.14 Alternative TTF Trends and Times of Set

Based on the discussion above, it would be desirable to subtract the heat transfer between the specimen and ambient condition, to better relate the gain in strength to the heat of hydration.

From Figure 5.14, the specimen cured in the warmer ambient temperature was cured at 90°F. Not only there was a temperature difference between the mixing and curing, there was also an approximate 1.5 hr gap from start of mixing until start of testing, which recorded the specimen temperature at about 79°F. Likewise, the specimen cured in the cooler ambient temperature was cured at 50°F, but prepared at 70°F and had a 1.3 hr gap until the first specimen temperature reading of 69°F. By removing the heat transfer between the specimen and curing environment, the heat of hydration, can be isolated and will theoretically indicate time of initial set.

Previous studies on early-age heat in concrete either focused on the heat evolution with regard to cracking or as a way to model heat of hydration based on equivalent age maturity (Ballim and Graham 2004; Schindler and Folliard 2005). Schindler and Folliard (2005) determined that the heat of hydration is affected by the composition of cement, amount of cement, and water to cement ratio and that the specific heat capacity of the concrete changes over time. Further, Khan (2002), showed the difference in thermal conductivity of the aggregates based on type and moisture content. Other studies (e.g., Bentz 2008; Lee et al. 2009; Guo et al. 2011) have found that thermal conductivity and heat transfer coefficients change throughout the hydration process and are affected by wind velocity, curing conditions, and evaporation. Generally, thermal conductivity is affected to a greater extent by concrete constituent properties while heat transfer variations primarily occurred due to the environmental curing conditions. As such, the precise determination of heat transfer becomes more difficult, since these parameters are not normally measured. Despite these complications, a simple heat transfer model was developed assuming representative values for the thermal conductivity, k, and heat transfer coefficient, h of the concrete mix.

A simple steady-state heat transfer model was developed to determine the heat energy usage, s_{rxn}, at each time step. Expressed as BTU/hr, the heat energy use per hour was found using;

$$s_{rxn} = \frac{T_{cyl} - T_{amb}}{\frac{r^2}{4k} + \frac{r}{2h}} * V_{cyl} \qquad \text{EQN 4.5}$$

where T_{cyl} = temperature of cylinder in °F, T_{amb} = ambient temperature in °F, V_{cyl} =volume of the cylinder and r = radius of the specimen. A value of 0.35 BTU/hr/(ft*°F) was used for the thermal conductivity, ("Thermal Conductivity of Common Materials and Gases" 2003), while 3.5 BTU/hr/(ft^2*°F) was used for the heat transfer coefficient (Lee et al. 2009). Since both properties vary based on numerous factors, the selected values were selected based on conditions that closely represented the testing process used in this research

The heat energy time history was estimated by calculating the heat energy usage at each time step, as depicted in Figure 5.15. The heat energy and internal temperature trends shown in Figure 4.2 are similar. For the specimen cured in a warmer ambient temperature, the local minima corresponds closely to a neutral heat energy as seen in Figure 5.15. This neutral heat energy also corresponds to the transitions point of the specimen cured at a cooler ambient temperature.

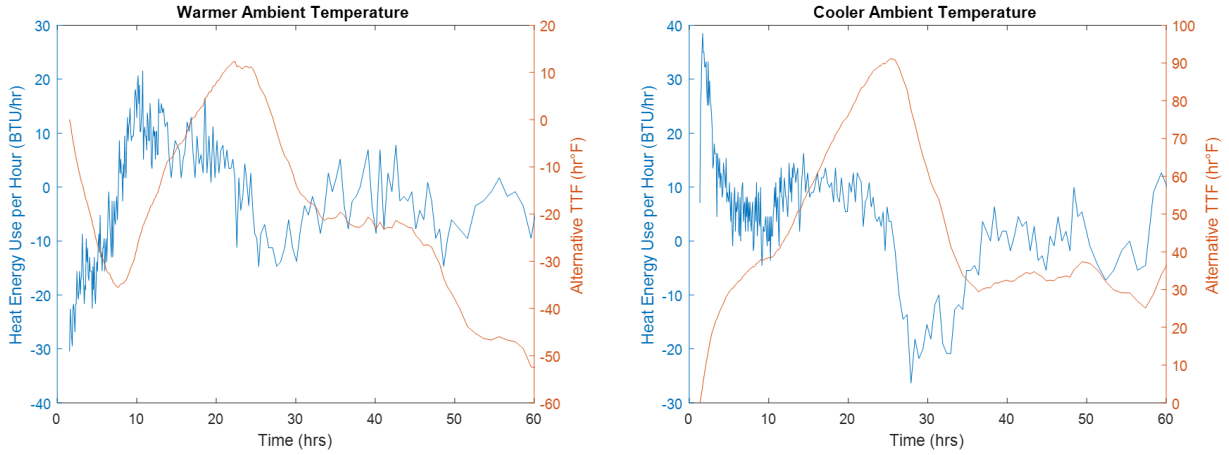

Figure 5.15 Heat Energy Use and Alternative TTF Trends

The numerical integration of the heat energy time histories in Figure 5.15 are compared with the corresponding alternative TTF curves in Figure 5.16. The two curves follow similar trends but shifted by a factor of approximately two for the specimen subjected to the warmer curing and approximately 2.5 for the specimen subjected to cooler curing. This similarity indicates that

the alternative TTF is the equivalent of a quasi-steady state heat transfer analysis, assuming the rate of heat production is constant.

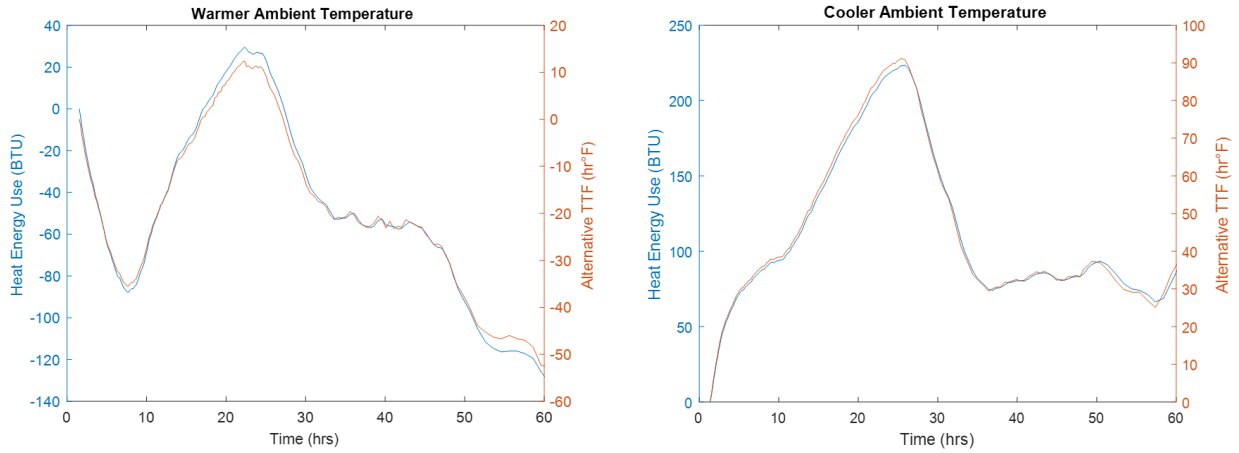

Figure 5.16 Heat Energy Use and Alternative TTF Trends

Figure 5.17 depicts a theorized alternative TTF for the two ambient temperatures based on two assumptions. First, it assumes that no heat transfer occurs and a temperature difference only begins once hydration starts. This assumption is based on the corresponding times of neutral heat energy usage corresponding to the transition point and local minima indicted in Figure 5.15. No heat production occurring past 36 hours, resulting in the specimen having the same temperature as the ambient, is the second assumption made. As depicted, the alternative TTF for both curing conditions become normalized with the growth indicating the start of hydration and initial set. The positive slope would indicate the rate of hydration while the negative slope would indicate the rate of equilibrating to the ambient temperature once hydration ceases. Additionally, the similarity in maximum alternative TTF is expected in this normalized model since maximum internal temperatures were consistently around 110% of the curing temperature as noted in Section 4.1.

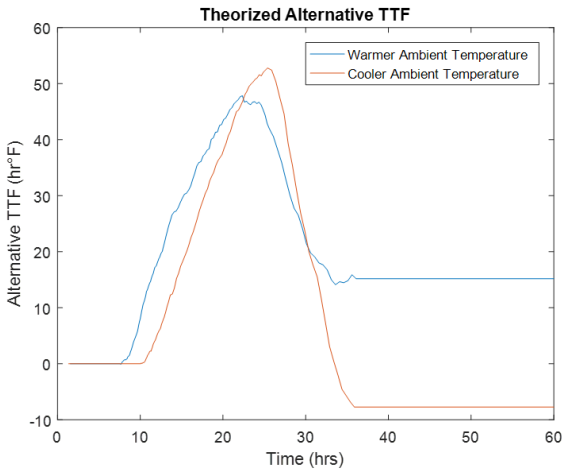

Figure 5.17 Theorized Alternative TTF Trends

The use of this alternative TTF provides the potential to monitor hydration of concrete regardless of curing temperature and determine the time of initial set using minimal equipment. It can also be used as a method to conduct a rudimentary heat transfer analysis. A more precise model would be possible if heat transfer and heat of hydration can be isolated.

5.4 Thermal Profile

As discussed in Section 3.4, a thermal camera was used to obtain simultaneous images of the triplicate specimens undergoing maturity and seismic monitoring from each mix at set times. For the most part, the full area of each cylinder was imaged, except in some occasions when small parts of the outer cylinders were cut off. Similar to the seismic and maturity methods, all three cylinders yielded similar profiles as seen in Figure 5.18, using the color codes discussed in section 3.4.

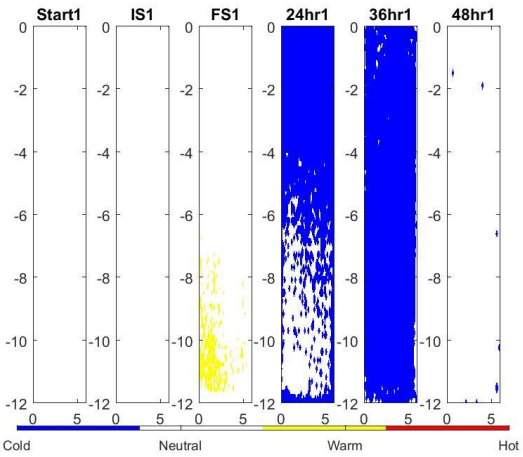

(a) Cylinder 1

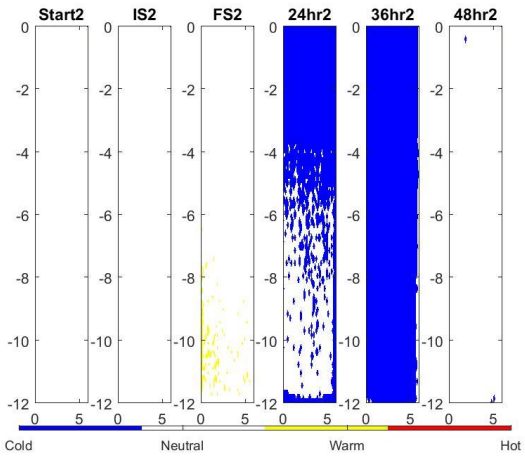

(b) Cylinder 2

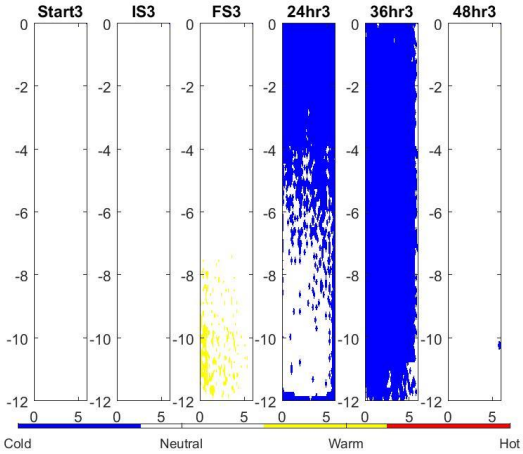

(c) Cylinder 3

Figure 5.18 Thermal Profile for Reference Mix at 70°F and 40% Humidity

The header above each profile indicates the time when the image was captured. Start corresponds to the first image captured, IS corresponds to the image at the initial set while FS corresponds to the image at the final set using the traditional method. The last three images correspond to the temperature profile at 24 hrs, 36 hrs, and 48 hrs from the initial water-cement contact. The images from the center cylinder for each mix are shown in Appendix C. Generally, the modulus approach yielded warmer images at IS and FS as compared to the standard approach. The hybrid approach profiles are not shown because of the similarities with the modulus-based results. Generally, the images at 36 hrs and 48 hrs ages are close to or cooler than the ambient temperature.

Figure 5.19 compares the variations in the internal temperature recorded with the thermocouple with the minimum, maximum, and average temperature of the surface of the specimen captured with the thermal camera of a specimen cured at 70°F and 40% humidity without the mold removed. The internal temperatures are typically within 3°F of the average temperature recorded by the camera with both having the same general trend. From approximately 9 hrs to 18 hrs age, the average surface temperature readings show the greatest difference from the internal temperatures. This time period corresponds with the time that the specimen is in the setting phase and indicates that heat generation is more prominent at the center.

Referring back to Figure 4.14, a temperature drop commonly seen around 24 hrs was not as large in the specimen that did not have the mold removed. A similar effect is seen in Figures 5.20 and 5.21 which depict the thermal profiles of the reference mix cured at 70°F and 40% humidity with the mold removed after one day and without the mold removal. The specimen retained in the mold has a consistent profile at 24 hrs, 36 hrs, and 48 hrs. The temperature profiles of the specimen demolded undergoes a drop in temperature at 24 hrs and 36-hrs. Review of the

raw data recorded by the thermal camera showed that the average temperature of the demolded specimen is about 65°F at 24 hrs and 36 hrs, while the average temperature of the specimen retained in the mold are around 68°F at 24 hrs and close to 72°F at 36 hrs. Comparison of these profiles, internal temperature readings, and alternative maturity indicate that the mold acts as a barrier that holds heat and moisture within the system. Maintaining the heat and moisture in the system encourages accelerated hydration that results in higher strength and modulus as discussed in Section 4.4.3. Once the mold was removed, the evaporation of moisture causes a reduction in the internal and surface temperatures of the specimen, resulting in a reduced rate of hydration.

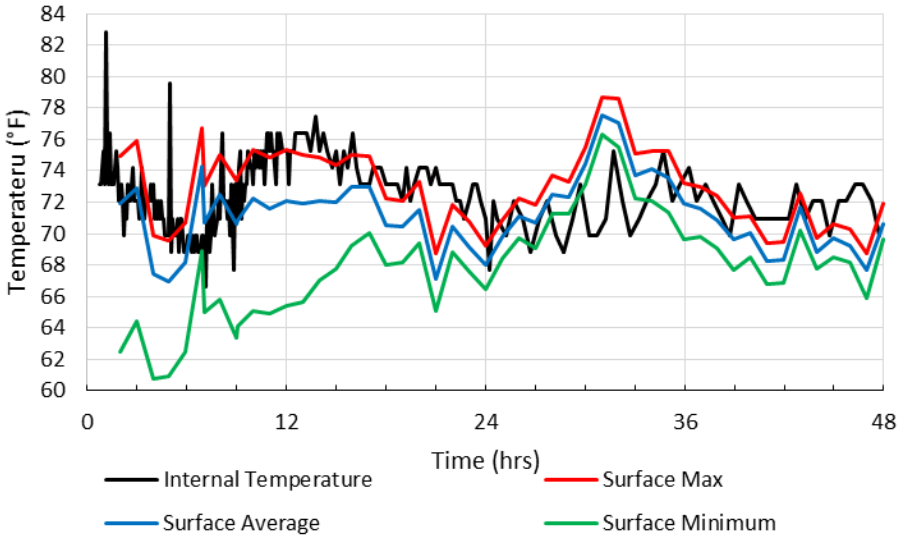

Figure 5.19 Comparison of Internal and Surface Temperatures of Specimen without the Mold Removed

The infrared camera showed that specimens from the same mix and under the same curing conditions undergo similar heat dissipation. Additionally, the surface temperatures recorded by the camera were similar to the internal temperature recorded by the thermocouple. The temperature profiles indicate that initially the bottom of the specimen is warmer and that heat dissipates. Additionally, the Start, IS, and FS profiles generally appear cooler at the top. This is expected since the mold does not cover the top, thus allowing unimpeded heat transfer out of the

system. From all of the mixes monitored, there was no noticeable profile or behavior indicating initial or final set.

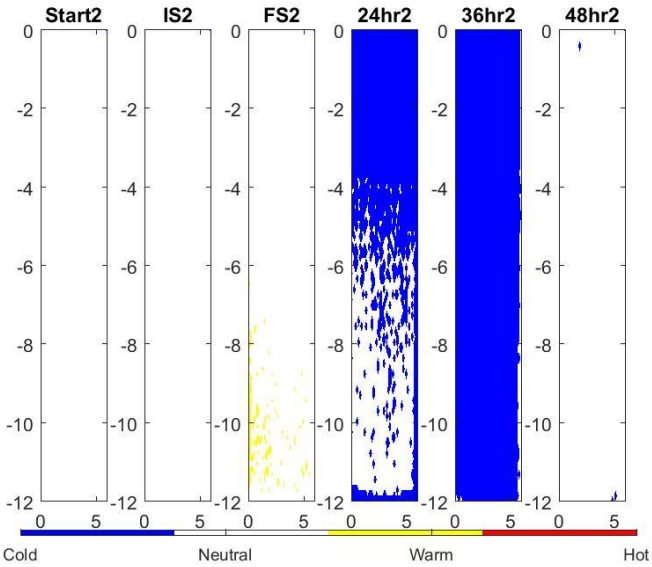

Figure 5.20 Thermal Profile with Mold Removed After 24 Hours

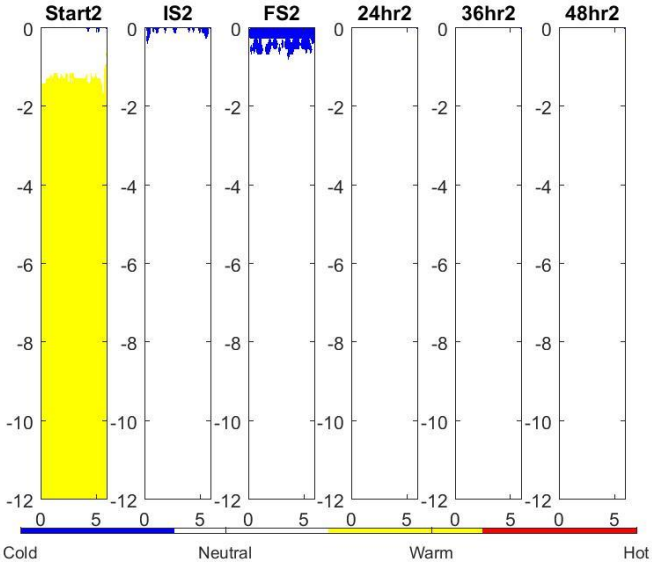

Figure 5.21 Thermal Profile without the Mold Removed

5.5 Comments and Conclusions

Applying some adjustment factors to the set measured at standard cure, times of set of the same mix were predicted under other curing conditions. Good confidence was seen across the six environmental conditions as well as the 12 mix changes. Although this is method provided

predictions of set with good confidence, it still has the shortfalls of only using a mortar mix to determine set, completely ignoring the coarse aggregates.

Dividing the modulus growth into dormant, setting, and hardening segments provided a method to determine set in terms of either time or standard TTF based off the entire concrete mix. The first approach used the modulus growth over time while the hybrid method used the modulus over standard maturity to determine the standard TTF at times of initial and final set. Results from both approaches showed similar times of initial set compared to the standard method. The hybrid method generally determined an earlier initial set and later final set compared to the modulus approach. The difference between the methods was generally within two hours. When extrapolating the specimen strengths using the determined strength relationships these approaches indicated strengths at final set of over 600 psi versus the penetration resistance method which indicated strengths of under 100 psi, indicating the need for redefinition of set.

The introduction of an alternative method to measure maturity in terms of a time-temperature factor provided a unique trend when plotted over time versus a linear trend seen with the standard TTF over time. This approach changed the datum temperature from a constant temperature to the instantaneous ambient temperature to provide an indication of the effect of ambient temperature on the maturity of the concrete. Continued focus on this method may provide another method to determine set based on curve changes identified in the plots. This method may also provide a way to track the heat transfer in the cylinder to pin-point the time that hydration begins to generate heat.

Thermal imaging provided a means to create a thermal profile of a concrete specimen at distinct times during curing. Results indicated essentially no heat generation beyond 36 hours as well as similar trends between internal and surface temperatures. Although it was thought that a

unique profile would be evident at time of initial or final set no such indication was seen. Even when using the modulus approach determined set, a repeated unique feature was not seen at initial or final set. But it did show a profile at final set that was generally warmer compared to the penetration method defined final set.

Chapter 6: Conclusions and Recommendations

6.1 Review of Testing Approach

The goals of this study consist of modelling the early age strength and modulus development of concrete more accurately and determining the initial and final setting times more systematically. There are some shortfalls associated with using the traditional penetration resistance for defining the set. For example, that approach does not account for the coarse aggregate effect on the set. On the other hand, set defined based on modulus provides several advantages. First, it takes into account the inclusion of large aggregates. Another advantage is the ability to not only develop a systematic process to predict times of set, but also to develop a relationship between the strength and modulus for more mechanistic approach to estimating the time for saw cutting and premature cracking of the concrete.

The free-free resonant column (FFRC) tests provides a convenient way to monitor nondestructively the increase in the modulus of the concrete that can potentially lead to a more objective way of determining the initial and final set. Thermocouples embedded in the same specimens monitored for modulus can be used to estimate the maturity of the concrete as a complementary approach for the determination of set and strength with time. Once the specimens were monitored for seven days, their compressive strength can be determined for relating modulus and maturity to strength.

A thermal camera was also used to model the dissipation of heat from the concrete specimens over the course of the first 48 hours as they cured to understand better the impact of the ambient temperature and humidity on the curing of the concrete.

6.2 Limitations of Research

Although a robust number of cylinders were tested during this research, several limitations related to this study should be enumerated. Most limitations dealt with the limited number of perturbations of the parameters due to the time limitations. The continuous monitoring of the reference mix under standard curing (100% humidity and 70°F) as a "true reference" was not possible because of the prototype nature of the system developed. Further, no monitoring of internal humidity occurred, which could potentially further model the termination of hydration.

Since concrete mixes are usually designed based on compressive strength, neither the tensile strength nor flexural strength of the concrete was studied due to time constraints and limited space in the temperature control chamber. Another limitation in the process is that direct correlation to standard maturity and seismic modulus to strength development were only obtained for the specimens tested after seven days of curing.

6.3 Recommendations for Future Research

Of the limitations just discussed, there is great potential for future research to fill the gaps. Areas of focus would be a reference mix comprised of only Portland cement with no SCMs or admixtures and a single coarse aggregate. From this mix add different chemical admixtures in five quantities to provide an increased understanding of the effects. This will also identify a point of diminishing returns for the ideal amount of chemical admixture to use for the desired results. Additionally, changes in the aggregate types and gradation will verify if similar trends continue to appear and allow identification of any potential correlations.

To obtain better direct correlation, consider monitoring the one and three-day specimens in addition to the seven-day specimens to fully see the strength development of early age concrete. Additionally, expand to 28-day test to see the effect on the correlation and to provide a more

practicable means to accurately predict strength. Based on initial observations of the modulus-strength and standard maturity-strength relationships the potential exist to determine base coefficients and adjustment factors to apply based on mix and environmental changes.

Another area of focus would be to expand the environmental testing to increase the temperature ranges and humidity levels to verify if the trends identified in this research hold true. In addition to this testing of set, using the penetration method, will confirm its viability as a predictive approach until the two modulus-based methods are further refined. Refinement of these methods could include refinement of coefficients treated as a constant or refinement of adjustment factors. Minor adjustments could be made to the selection of where to split the curve into segments, but the slope values used in this research created linear models that could be consistently created to match the recorded data regardless of mix or environmental changes.

The alternative TTF approach provides a unique plot for each mix with several phenomenon to explore. This would require a controlled environment for all steps upon completion of oven drying aggregates. By doing this, the initial phase of the plot would be essentially zero until the initiation of hydration since all materials would start at the set ambient temperature. Initial temperature difference would most likely be caused by frictional forces during mixing and cylinder preparation. From this a better understanding of heat transfer can be modeled to separate hydration heat from environmental heat. Additionally, since this research found that the maximum internal temperature was 110% of the ambient temperature, a controlled environment would show if the same trend occurs at curing with mix changes causing the only changes in trends.

Other future research can utilize this test procedure and apply the process to field testing. Results from the field testing can confirm that the effects of admixtures fall within the range

determined in lab testing and provide better understanding to contractors and agencies. Additionally, it can provide a more precise test method for the field when determining when to make saw cuts and remove formwork.

References

Alexander, K. M. (1972). “The Relationship Between Strength and the Composition and Fineness of Cement.” *Cement and Concrete Research*, 2, 663–680.

ASTM C1074. (2011). “Estimating Concrete Strength by the Maturity Method.” *American Society for Testing and Materials*.

ASTM C125. (2015). “Standard Terminology Relating to Concrete and Concrete Aggregates.” *American Society for Testing and Materials*.

ASTM C215. (2014). “Standard Test Method for Fundamental Transverse , Longitudinal , and Torsional Resonant Frequencies of Concrete Specimens.” *American Society for Testing and Materials*.

ASTM C403. (2016). “Standard Test Method for Time of Setting of Concrete Mixtures by Penetration Resistance.” *American Society for Testing and Materials*.

Azari, H., and Nazarian, S. (2015). *Exploratory Study of Use of Surface Waves to Determine Defects in Concrete*.

Azenha, M., Faria, R., and Figueiras, H. (2011). “Thermography as a Technique for Monitoring Early Age Temperatures of Hardening Concrete.” *Construction and Building Materials*, Elsevier Ltd, 25(11), 4232–4240.

Babu, K. G., and Apparao, C. V. (1996). “Strength Behaviour of Concretes Containing Metakaolin.” *Design Quality in Higher Education Buildings*, R. K. Dhir, M. D. Newlands, and L. J. Csetenyi, eds., 231–239.

Badogiannis, E., Tsivilis, S., Papadakis, V. G., and Chaniotakis, E. (2002). “The Effect of Metakaolin on Concrete Properties.” *Innovations and Developments In Concrete Materials And Construction*, R. K. Dhir, P. C. Hewlett, and L. J. Csetenyi, eds., 81–89.

Ballim, Y., and Graham, P. C. (2004). “Early-Age Heat Evolution of Clinker Cements in Relation to Microstructure and Composition: Implications for Temperature Development in Large Concrete Elements.” *Cement and Concrete Composites*, 26(5), 417–426.

Benaicha, M., Burtschell, Y., and Alaoui, A. H. (2016). “Prediction of Compressive Strength at Early Age of Concrete - Application of Maturity.” *Journal of Building Engineering*, 6, 119–125.

Bentz, D. P. (2008). “A Review of Early-Age Properties of Cement-Based Materials.” *Cement and Concrete Research*, 38(2), 196–204.

Bertagnoli, G., Mancini, G., and Tondolo, F. (2009). “Numerical Modelling of Early-Age Concrete Hardening.” *Magazine of Concrete Research*, 61(4), 299–307.

Büyüköztürk, O. (1998). “Imaging of Concrete Structures.” *NDT & E International*, 31(4), 233–243.

Caldarone, M. A. (2009). *High-Strength Concrete: A Practical Guide*. Taylor & Francis.

Clark, M. ., McCann, D. ., and Forde, M. . (2003). “Application of Infrared Thermography to the Non-Destructive Testing of Concrete and Masonry Bridges.” *NDT & E International*, 36(4), 265–275.

Collier, Z., Rupnow, T., and Raghavendra, A. (2017). *Implementation of Maturity for Concrete Strength Measurement and Pay*.

Construction Division - Materials & Pavements, T. (2016). “Chemcial Admixtures for Concrete.” TxDOT.

Dinakar, P., and Ganesh Babu, K. (2006). “Strength Efficiency of Metakaolin in Concrete.” *Structural Concrete*, 7(1), 27–31.

Ding, J. T., and Li, Z. (2002). “Effects of Metakaolin and Silica Fume on Properties of Concrete.” *ACI Materials Journal*, 99(4), 393–398.

Fournier, B., Berube, M.-A., Folliard, K. J., and Thomas, M. (2010). *Report on the Diagnosis, Prognosis, and Mitigation of Alkali-Silica Reaction (ASR) in Transportation Structures*.

Gams, M., and Trtnik, G. (2013). “A New US Procedure to Determine Setting Period of Cement Pastes, Mortars, and Concretes.” *Cement and Concrete Research*, Elsevier Ltd, 53, 9–17.

Giannini, E. R., Folliard, K. J., Zhu, J., Bayrak, O., Kreitman, K., Webb, Z., and Hanson, B. (2013). *Non-Destructive Evaluation of In-Service Concrete Structures Affected by Alkali-Silica Reaction (ASR) or Delayed Ettringite Formation (DEF)—Final Report, Part I*.

Glisic, B., and Simon, N. (2000). “Monitoring of Concrete at Very Early Age Using Stiff SOFO Sensor.” *Cement and Concrete Composites*, 22, 115–119.

Guo, L., Guo, L., Zhong, L., and Zhu, Y. (2011). “Thermal Conductivity and Heat Transfer Coefficient of Concrete.” *Journal of Wuhan University of Technology-Mater. Sci. Ed.*, 26(4), 791–796.

Hiasa, S., Birgul, R., Watase, A., Matsumtot, M., Mitani, K., and Catbas, F. N. (2014). “A Review of Field Implementation of Infrared Thermography as a Non-destructive Evaluation Technology.” *International Conference on Computing in Civil and Building Engineering*, 1715–1722.

Ismael, N. S., and Ghanim, M. N. (2015). “Properties of Blended Cement Using Metakaolin and Hydrated Lime.” *Advances in Cement Research*, 27(6), 1–8.

Khan, M. . (2002). “Factors Affecting the Thermal Properties of Concrete and Applicability of its Prediction Models.” *Building and Environment*, 37(6), 607–614.

Kosmatka, S. H., Kerkhoff, B., and Panarese, W. C. (2002). *Design and Control of Concrete Mixtures*. Portland Cement Association, Skokie, IL.

Kreitman, K. L. (2011). "Nondestructive Evaluation of Reinforced Concrete Structures Affected by Alkali-Silica Reaction and Delayed Ettringite Formation." The University of Texas at Austin.

Langan, B. W., Weng, K., and Ward, M. A. (2002). "Effect of Silica Fume and Fly Ash on Heat of Hydration of Portland Cement." *Cement and Concrete Research*, 32(7), 1045–1051.

Lara, G. W. (2008). "Quality Evaluation of Portland Cement Concrete at Early Age with Free-Free Resonant Column." The University of Texas at El Paso.

Lee, Y., Choi, M. S., Yi, S. T., and Kim, J. K. (2009). "Experimental Study on The Convective Heat Transfer Coefficient of Early-Age Concrete." *Cement and Concrete Composites*, Elsevier Ltd, 31(1), 60–71.

Lin, F., and Meyer, C. (2009). "Hydration Kinetics Modeling of Portland Cement Considering the Effects of Curing Temperature and Applied Pressure." *Cement and Concrete Research*, Elsevier Ltd, 39(4), 255–265.

Maser, K. R., and Roddis, W. M. K. (1990). "Principles of Thermography and Radar for Bridge Deck Assessment." *Journal of Transportaion Engineering*, 116(5), 583–601.

Medichetti, A. (2002). "A Methodology for Optimizing Opening of Traffic to PCC Pavements." The University of Texas at El Paso.

Mehta, P. K., and Monteiro, P. J. M. (2006). *Concrete: Microsturcture, Properties, and Materials*. McGraw-Hill.

Mindess, S., Young, J. F., and Darwin, D. (2003). *Concrete*. Prentice Hall.

Nazarian, S., Yuan, D., Smith, K., Ansari, F., and Gonzalez, C. (2006). *Acceptance Criteria of Airfield Concrete Pavement Using Seismic and Maturity Concepts*.

Nazarian, S., Yuan, D., Weissinger, E., and McDaniel, M. (1997). "Comprehensive Quality Control of Portland Cement Concrete With Seismic Methods." *Transportation Research Record*, 1575(1), 102–111.

Neville, A. M. (1996). *Properties of Concrete*. John Wiley & Sons.

Newman, J., and Choo, B. S. (Eds.). (2003a). *Advanced Concrete Technology: Constituent Materials*. Elsevier.

Newman, J., and Choo, B. S. (Eds.). (2003b). *Advanced Concrete Technology: Concrete Properites*. Elsevier.

Newman, J., and Choo, B. S. (Eds.). (2003c). *Advanced Concrete Technology: Processes*. Elsevier.

Nixon, P., Fournier, B., and Thomas, M. (2016). "Options for Minimising the Risk of Alkali – Aggregate Reactions." *Proceedings*, 169(CM4).

Papadakis, V. G., and Tsimas, S. (2002). "Supplementary Cementing Materials in Concrete. Part I: Efficiency and Design." *Cement and Concrete Research*, 32(10), 1525–1532.

Parande, A. K., Chitradevi, R. H., Thangavel, K., Kartikeyan, M. S., Ganesh, B., and Palaniswamy, N. (2009). "Metakaolin: A Versatile Material to Enhance the Durability of Concrete – An Overview." *Structural Concrete*, 10(3), 125–138.

Payá, J., Monzó, J., Peris-Mora, E., Borrachero, M. V., Tercero, R., and Pinillos, C. (1995). "Early-Strength Development of Portland Cement Mortars Containing Air Classified Fly Ashes." *Cement and Concrete Research*, 25(2), 449–456.

Pla-Rucki, G. F., and Eberhard, M. O. (1995). “Imaging of Reinforced Concrete: State-of-the-Art Review.” *Journal of Infrastructure Systems*, 1(2), 134–141.

Popovics, S. (1982). *Fundamentals of Portland Cement Concrete: A Quantitaive Approach Volume 1: Fresh Concrete*. John Wiley & Sons.

Schindler, A. K., and Folliard, K. J. (2005). “Heat of Hydration Models for Cementitious Materials.” *ACI Materials Journal*, 102(1), 24–33.

Swaddiwudhipong, S., Chen, D., and Zhang, M. H. (2002). “Simulation of the Exothermic Hydration Process of Portland Cement.” *Advances in Cement Research*, 14(2), 61–69.

Targan, C. ¸, Olgun, A., Erdogan, Y., and Sevinc, V. (2002). “Effects of Supplementary Cementing Materials on the Properties of Cement and Concrete.” *Cement and Concrete Research*, 32(10), 1551–1558.

“Thermal Conductivity of Common Materials and Gases.” (2003). *Engineering ToolBox*, <https://www.engineeringtoolbox.com/thermal-conductivity-d_429.html> (Mar. 23, 2018).

Thomas, M. D. A., Fournier, B., and Folliard, K. J. (2012). *Selecting Measures to Prevent Deleterious Alkali-Silica Reaction in Concrete: Rationale for the AASHTO PP65 Prescriptive Approach*.

Thomas, M. D. A., Fournier, B., and Folliard, K. J. (2013). *Alkali-Aggregate Reactivity (AAR) Facts Book*.

TxDOT. (2014). “Standard Specifications for Construction and Maintenance of Highways, Streets, and Bridges.” *TxDOT*.

TxDOT Designation: Tex-426-A. (2010). *Estimating Concrete Strength by the Maturity Method*. *TxDOT*.

Weil, G. J. (1991). “Infrared Thermographic Techniques.” *CRC Handbook on Nondestructive Testing of Concrete,* V. M. Malhotra and N. J. Carino, eds., CRC Press.

Yi, S. T., Moon, Y. H., and Kim, J. K. (2005). “Long-term strength prediction of concrete with curing temperature.” *Cement and Concrete Research*, 35(10), 1961–1969.

Yikici, T. A., and Chen, H. L. (2015). “Use of Maturity Method to Estimate Compressive Strength of Mass Concrete.” *Construction and Building Materials*, Elsevier Ltd, 95, 802–812.

Yuan, D., Nazarian, S., and Medichetti, A. (2003). *A Methodology for Optimizing Opening of PCC Pavements to Traffic*.

Yuan, D., Nazarian, S., Perea, A., and Zhang, D. (2005). *Relating Seismic Modulus to Strength Parameters of Portland Cement Concrete*.

Appendix A: Internal Temperature Trends Based on Mix Changes

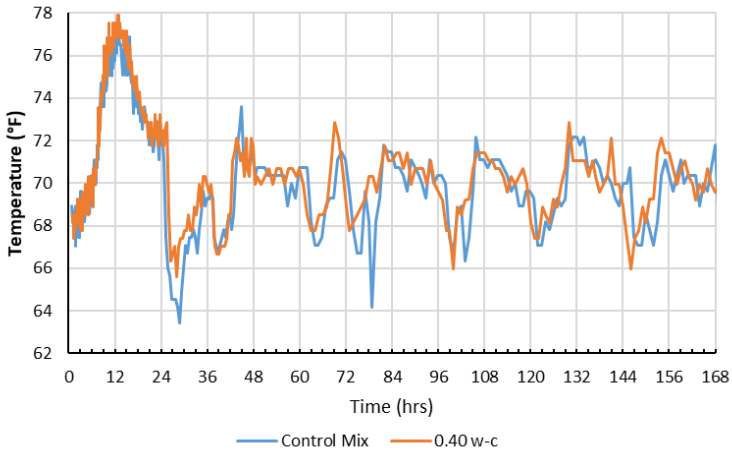

Figure A.1 Internal Temperature Trends from Change in Water-Cement Ratio

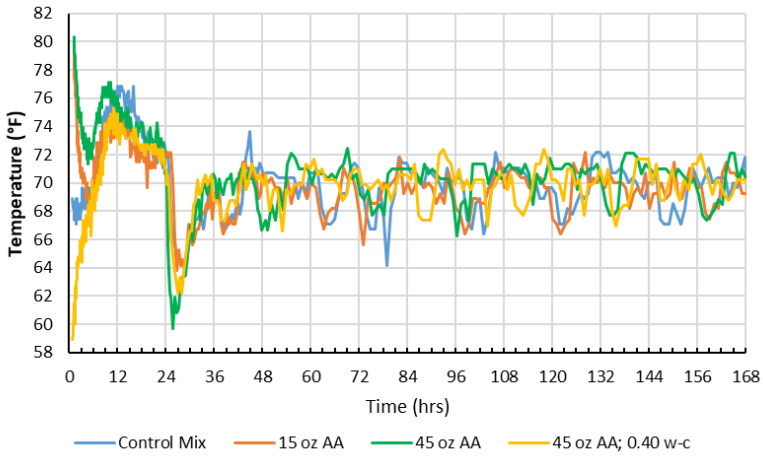

Figure A.2 Internal Temperature Trends from Addition of Accelerating Agent

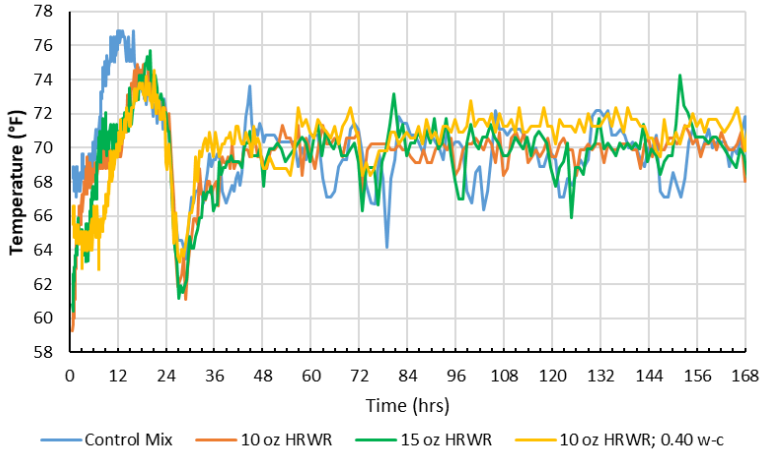

Figure A.3 Internal Temperature Trends from Addition of HRWR

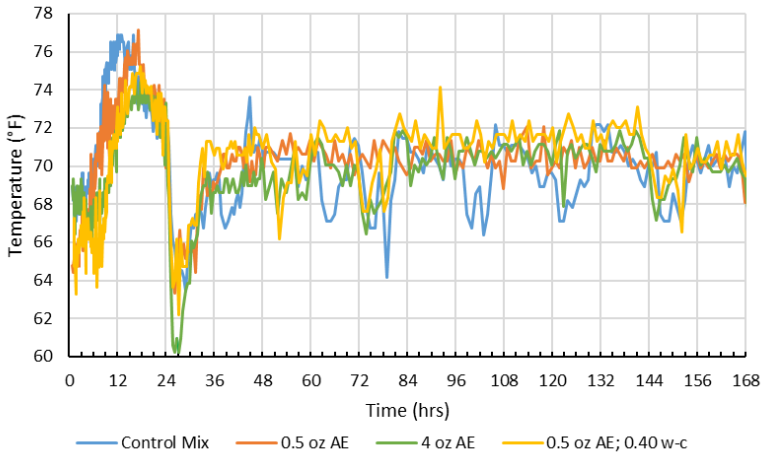

Figure A.4 Internal Temperature Trends from Addition of AEA

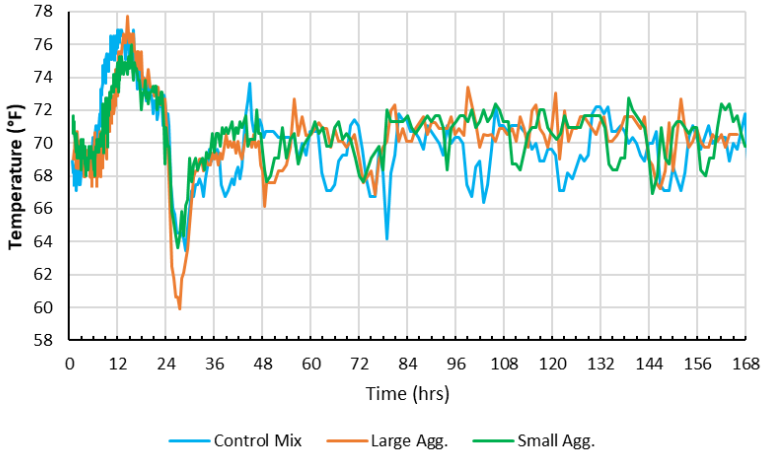

Figure A.5 Internal Temperature Trends from Change in Coarse Aggregate

Appendix B: Alternative TTF Trends

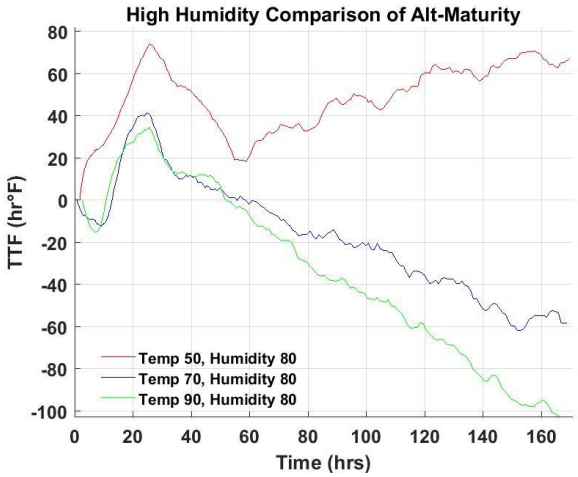

Figure B.1 Alternative TTF at High Humidity

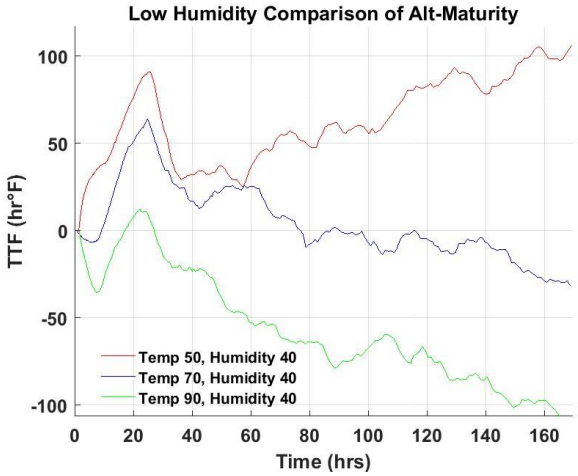

Figure B.2 Alternative TTF at Low Humidity

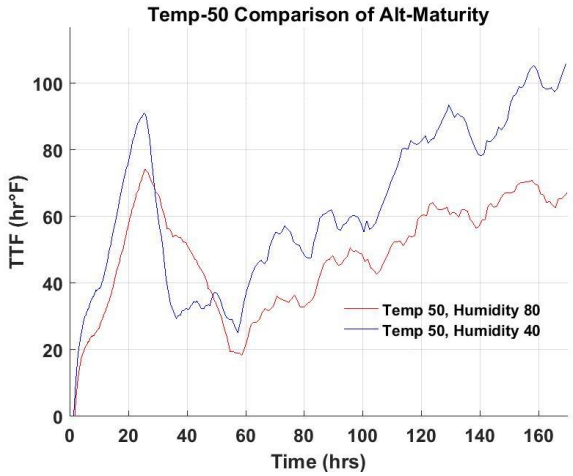

Figure B.3 Alternative TTF at 50°F Curing

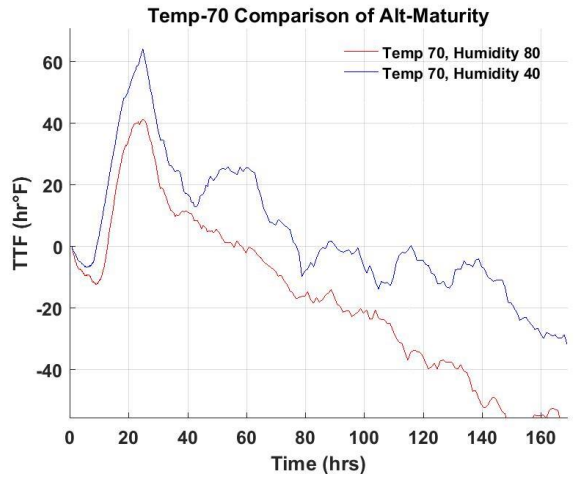

Figure B.4 Alternative TTF at 70°F Curing

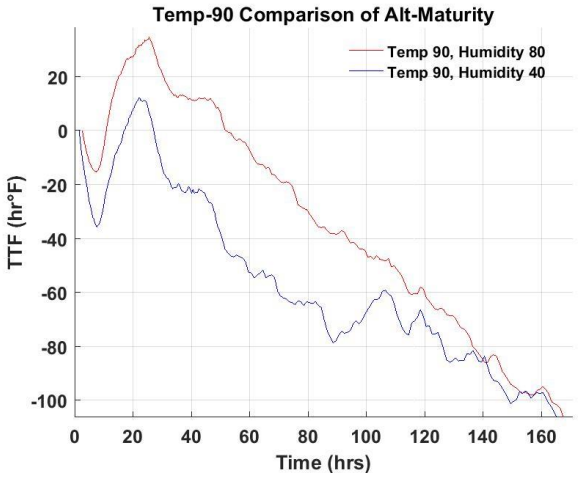

Figure B.5 Alternative TTF at 90°F Curing

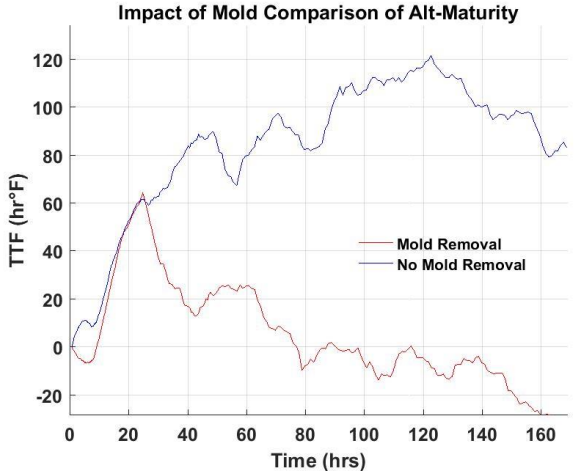

Figure B.6 Alternative Maturity Impacts from Mold of Specimens Cured at 70°F and 40% Humidity

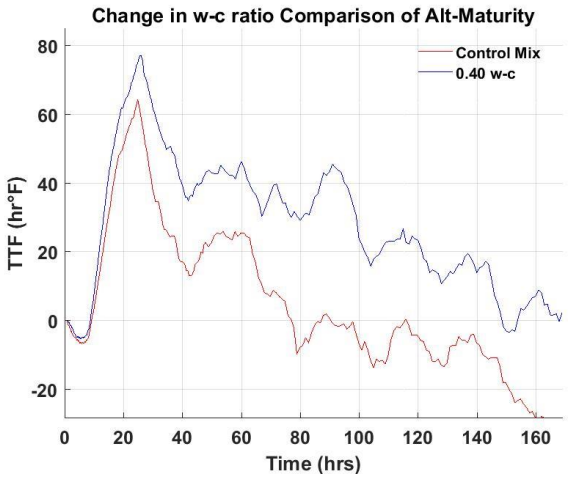

Figure B.7 Alternative Maturity Impacts from Change in Water-Cement Ratio

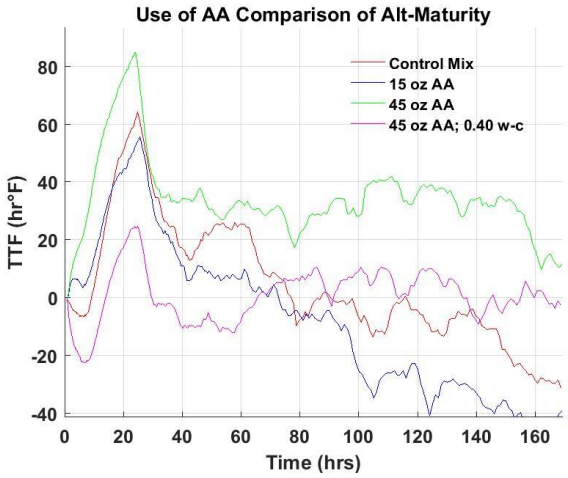

Figure B.8 Alternative Maturity Impacts from Addition of Accelerating Agent

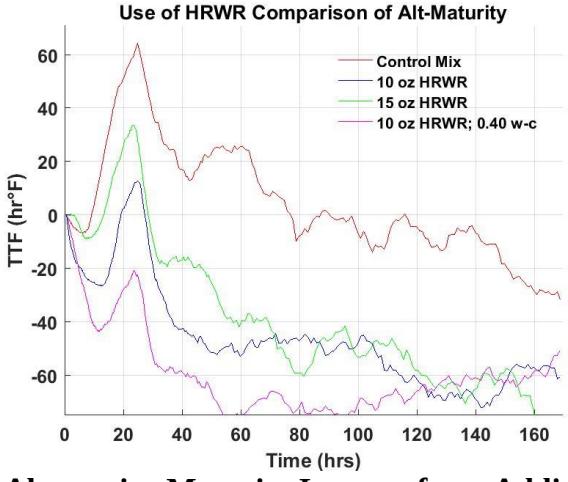

Figure B.9 Alternative Maturity Impacts from Addition of HRWR

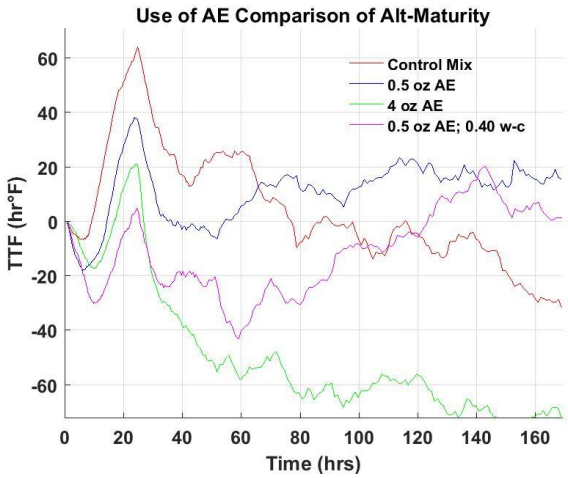

Figure B.10 Alternative Maturity Impacts from Addition of AEA

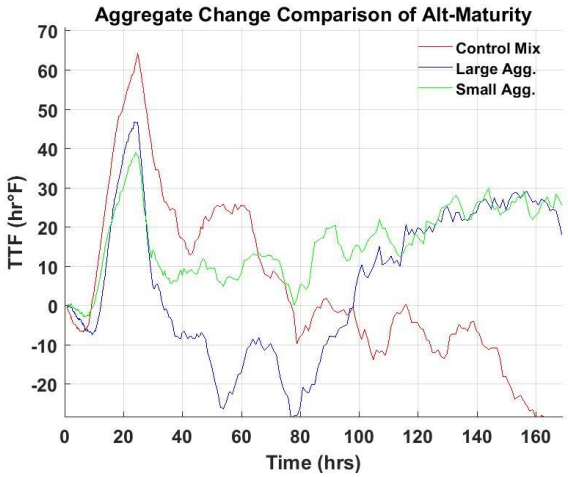

Figure B.11 Alternative Maturity Impacts from Change in Coarse Aggregate Gradation

Appendix C: Thermal Profiles

Images on the left use penetration determined times of initial and final set while images on the right use the time based modulus approach to determine times of set

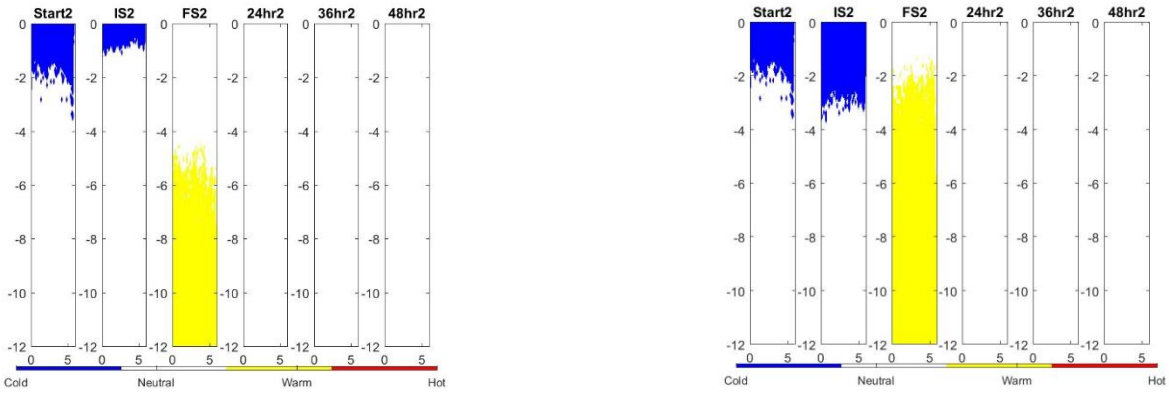

Figure C.1 Thermal Profile of Reference Mix at 90°F and 40% RH

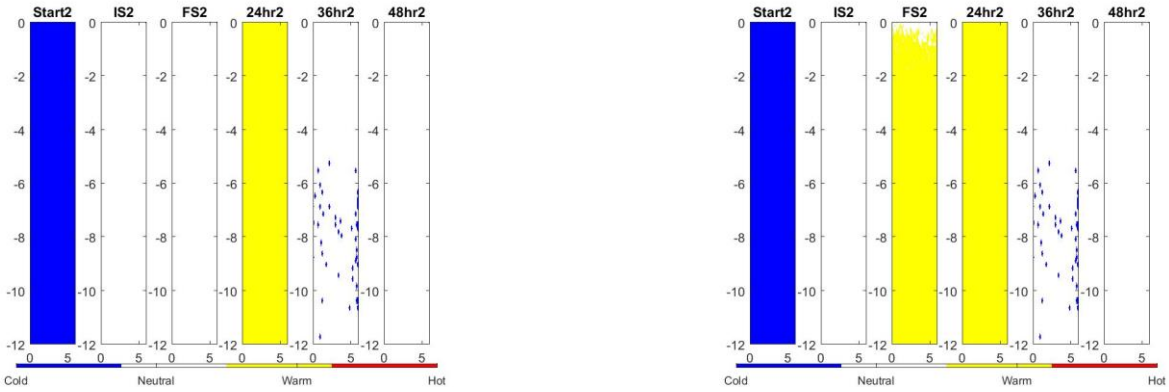

Figure C.2 Thermal Profile of Reference Mix at 90°F and 80% RH

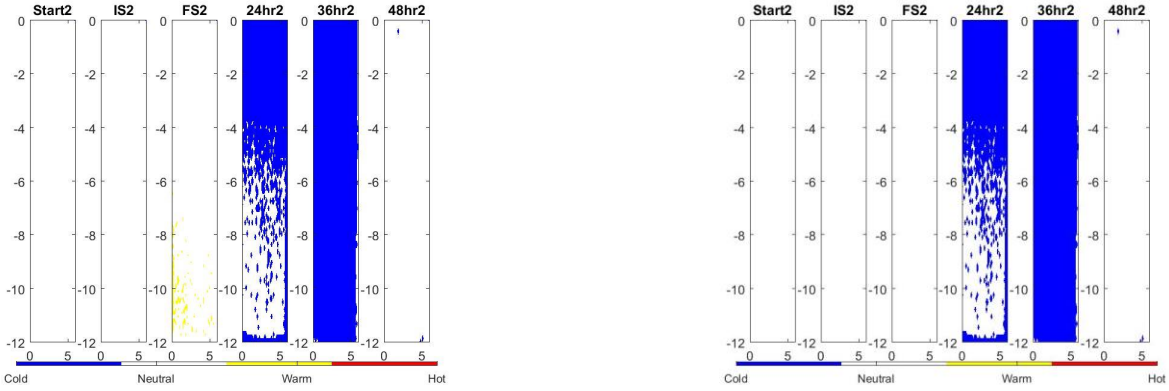

Figure C.3 Thermal Profile of Reference Mix at 70°F and 40% RH

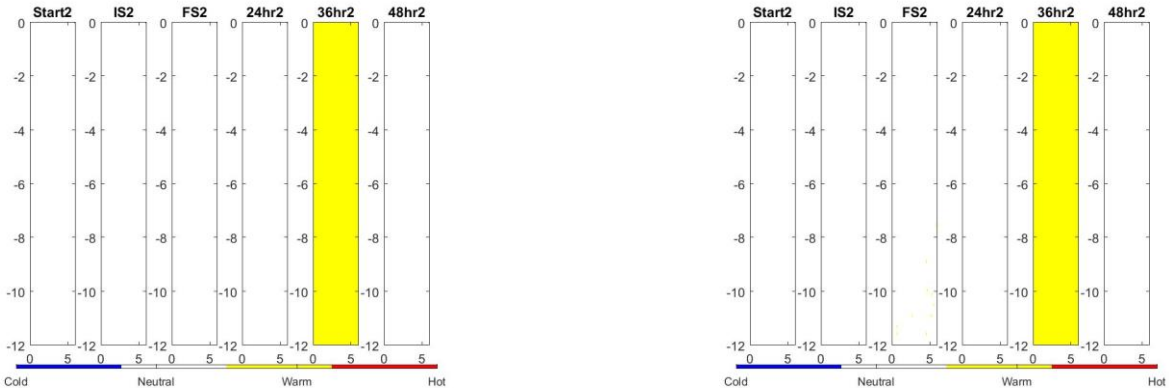

Figure C.4 Thermal Profile of Reference Mix at 70°F and 80% RH

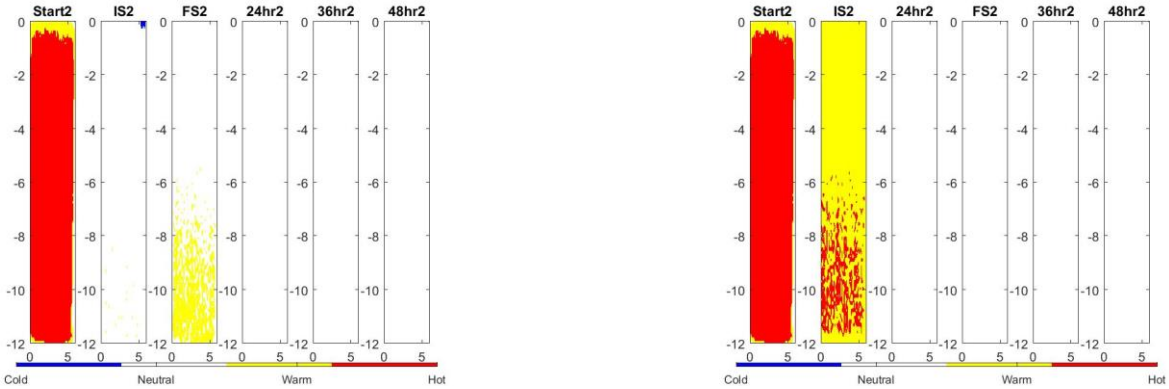

Figure C.5 Thermal Profile of Reference Mix at 50°F and 40% RH

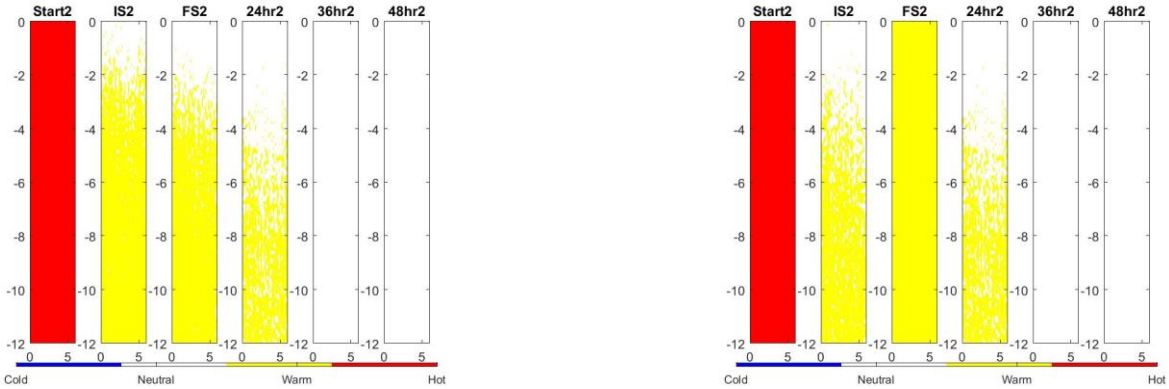

Figure C.6 Thermal Profile of Reference Mix at 50°F and 80% RH

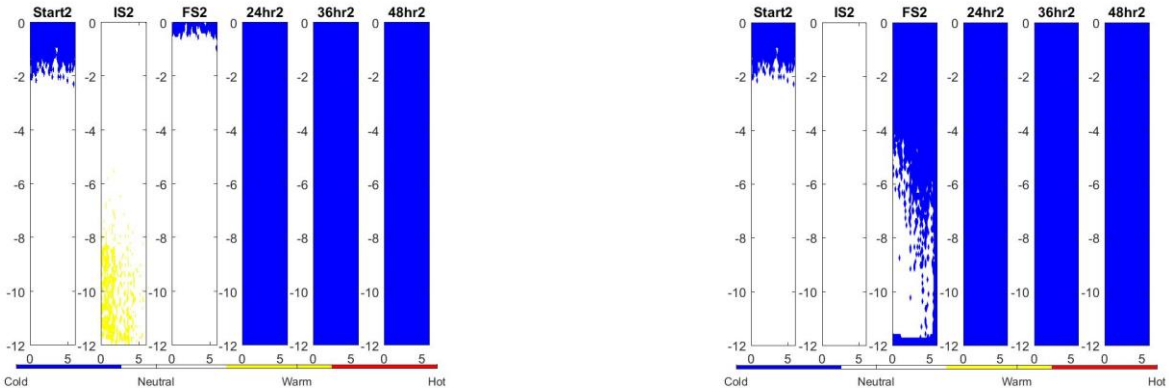

Figure C.7 Thermal Profile of Mix with Water-Cement Ratio of 0.40

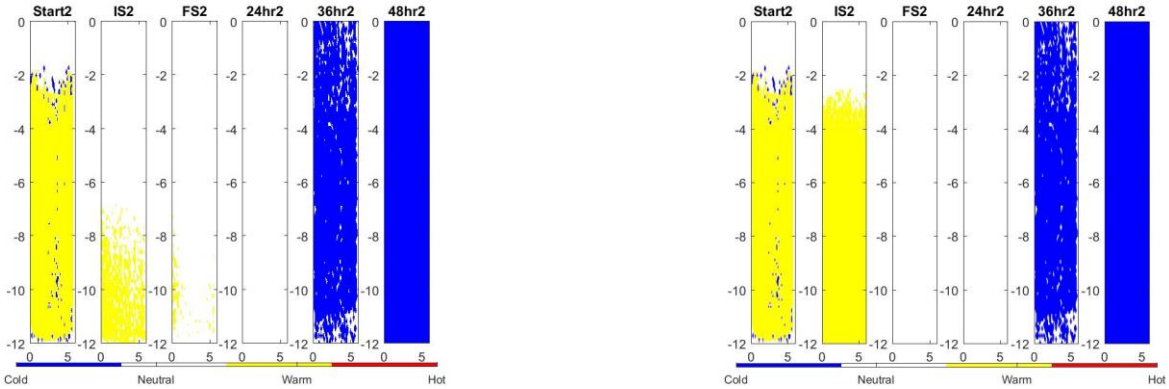

Figure C.8 Thermal Profile of Mix with 15 oz of Accelerating Agent

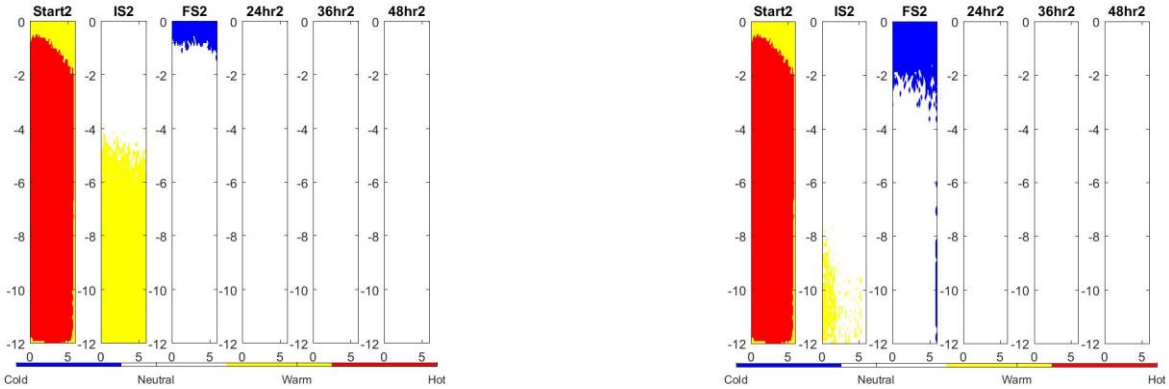

Figure C.9 Thermal Profile of Mix with 45 oz of Accelerating Agent

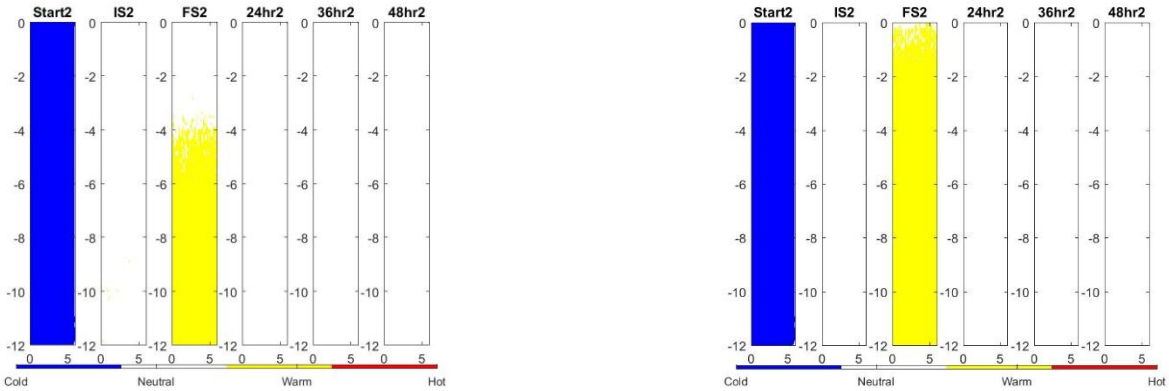

Figure C.10 Thermal Profile of Mix with 45 oz of Accelerating Agent and Water-Cement Ratio of 0.40

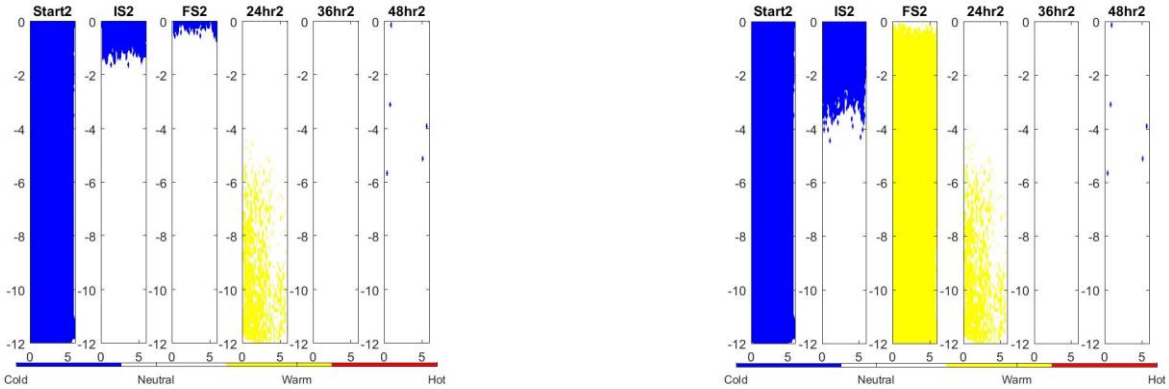

Figure C.11 Thermal Profile of Mix with 10 oz of HRWR

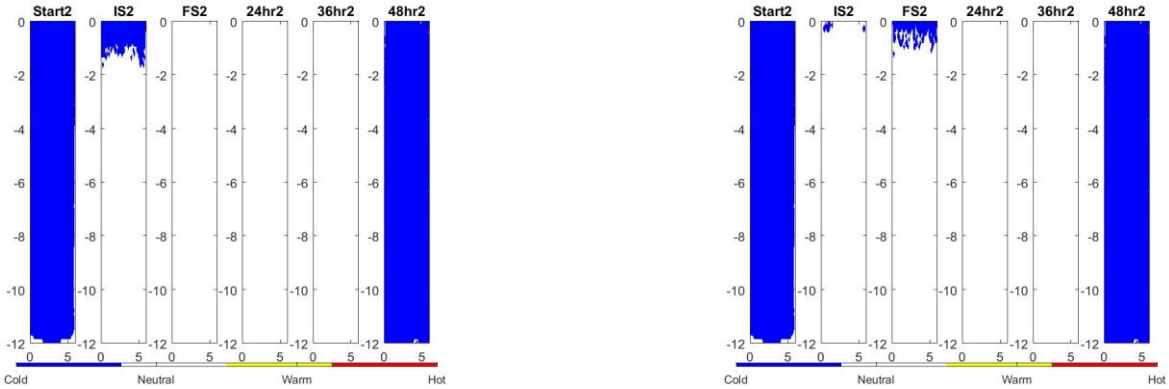

Figure C.12 Thermal Profile of Mix with 15 oz of HRWR

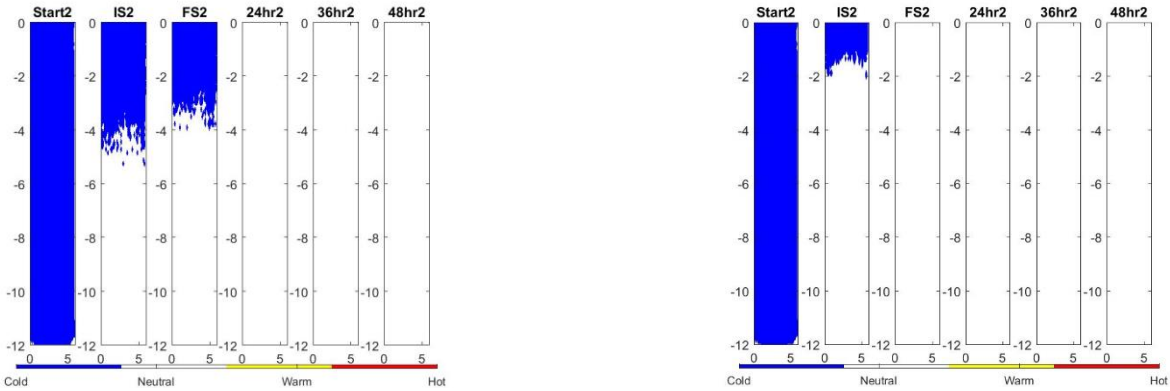

Figure C.13 Thermal Profile of Mix with 10 oz of HRWR and Water-Cement Ratio of 0.40

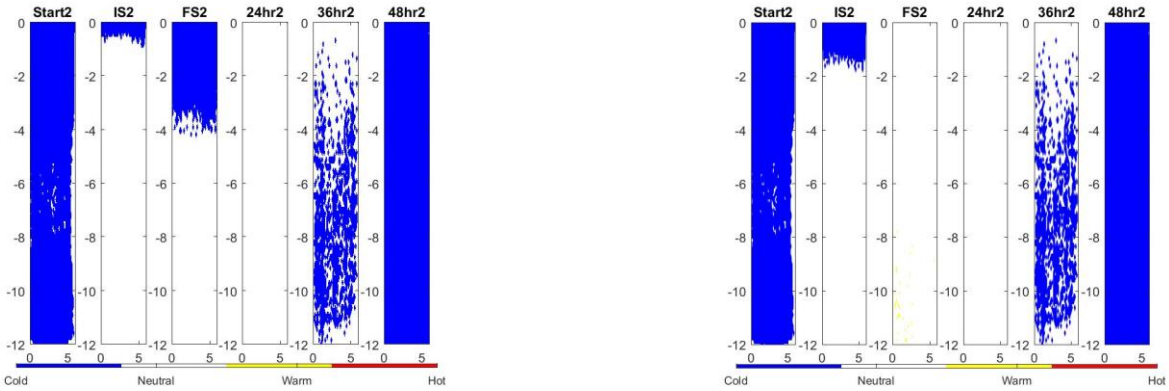

Figure C.14 Thermal Profile of Mix with 0.5 oz of AEA

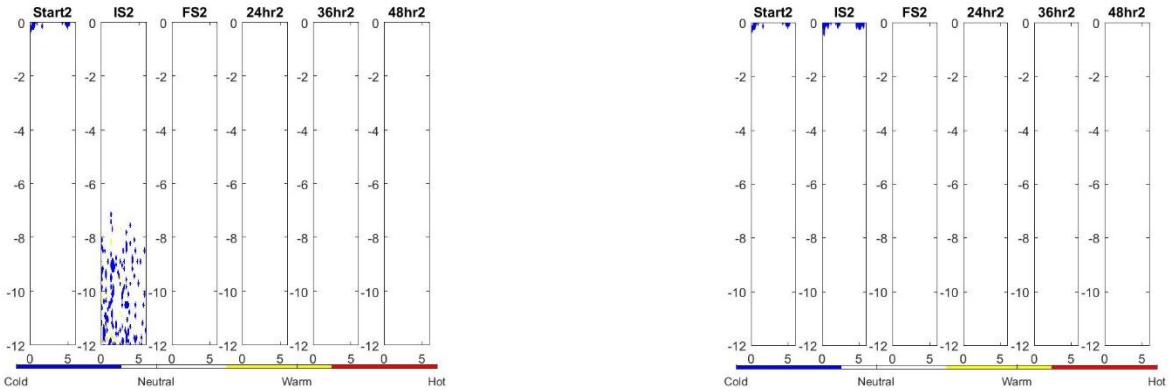

Figure C.15 Thermal Profile of Mix with 4 oz of AEA

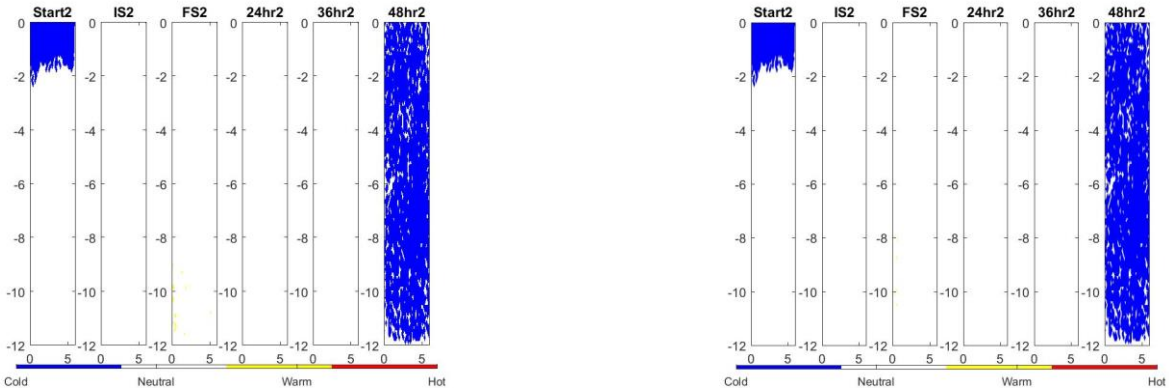

Figure C.16 Thermal Profile of Mix with 0.5 oz of AEA and Water-Cement Ratio of 0.40

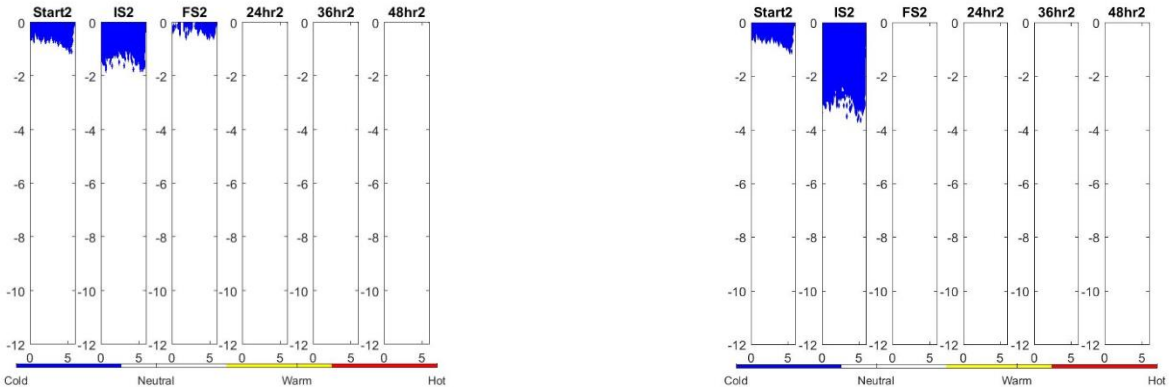

Figure C.17 Thermal Profile of Mix with Large Aggregate

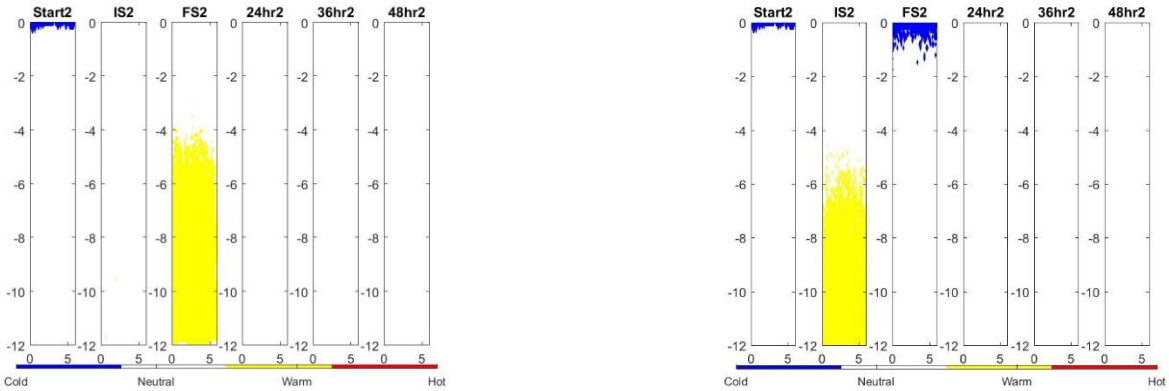

Figure C.18 Thermal Profile of Mix with Small Aggregate

Vita

Evan Lee Wolf was born in Cozad, Nebraska, USA, on May 30, 1983. The third son of Scott and Yvonne Wolf, he graduated from Cozad High School, Cozad, Nebraska in 2002. He then entered the United States Military Academy at West Point where he received a B.S. in Civil Engineering in 2006 and commissioned as an Engineer officer in the United States Army. He received a Master's degree in Engineering Management from the Missouri University of Science and Technology in Missouri in 2011. In August 2013, he began part-time work in the doctoral program in Civil Engineering at The University of Texas El Paso with full-time work starting in August 2016.

This dissertation was typed by Evan Wolf